Les stratégies de coopération inter-cellules pour l'atténuation des interférences dans les systèmes OFDMA

Reben Kurda

UNIVERSITÉ PARIS-SUD

ÉCOLE DOCTORLE 427:
INFORMATIQUE PARIS SUD
LABORATOIRE DE RECHERCHE EN INFORMATIQUE

THÈSE DE DOCTORAT

INFORMATIQUE

Par

Reben KURDA

Cooperation strategies for inter-cell interference mitigation in OFDMA systems

Date de soutenance : 18/03/2015

Directeur de thèse :	Dr. Lila Boukhatem	Université Paris-Sud
Co-directeur de thèse :	Dr. Tara Ali Yahiya	Université Paris-Sud

Composition du jury:

Rapporteurs :	Prof. Anne Wei	CNAM-CEDRIC
	Dr. Thi-Mai-Trang Nguyen	Université Paris 6
Examinateurs :		
	Prof. André-Luc Beylot	IRIT/ENSEEIHT
	Prof. Véronique Vèque	L2S-Supelec
	Prof. Jean-Louis Rougier	Télécom ParisTech
	Dr. Megumi Kaneko	Graduate School of Informatics, Kyoto University

Abstract

Recently the use of modern cellular networks has drastically changed with the emerging Long Term Evolution Advanced (LTE-A) technology. Homogeneous networks which were initially designed for voice-centric and low data rates face unprecedented challenges for meeting the increasing traffic demands of high data-driven applications and their important quality of service requirements. Therefore, these networks are moving towards the so called Heterogeneous Networks (HetNets).

HetNets represent a new paradigm for cellular networks as their nodes have different characteristics such as transmission power and radio frequency coverage area. Consequently, a HetNet shows completely different interference characteristics compared to homogeneous deployment and attention must be paid to these disparities when different tiers are collocated together. This is mostly due to the potential spectrum frequency reuse by the involved tiers in the HetNets. Hence, efficient inter-cell interference mitigation solutions in co-channel deployments of HetNets remain a challenge for both industry and academic researchers.

This thesis focuses on LTE-A HetNet systems which are based on Orthogonal Frequency Division Multiplexing Access (OFDMA) modulation. Our aim is to investigate the aggressive interference issue that appears when different types of base stations are jointly deployed together and especially in two cases, namely Macro-Femtocells and Macro-Picocells co-existence. We propose new practical power adjustment solutions for managing inter-cell interference dynamically for both cases.

In the first part dedicated to Femtocells and Macrocell coexistence, we design a MBS-assisted femtocell power adjustment strategy which takes into account femtocells users performance while mitigating the inter-cell interference on victim macrocell users. Further, we propose a new cooperative and context-aware interference mitigation method which is derived for realistic scenarios involving mobility of users and their varying locations. We proved numerically that the Femtocells are able to maintain their interference under a desirable threshold by adjusting their transmission power. Our strategies provide an efficient means for achieving the desired level of macrocell/femtocell throughput trade-off.

In the second part of the studies where Picocells are deployed under the umbrella of the Macrocell, we paid a special attention and efforts to the interference management in the situation where Picocells are configured to set up a cell range expansion. We suggest a MBS-assisted collaborative scheme powered by an analytical model to predict the mobility of Macrocell users passing through the cell range expansion area of the picocell. Our goal is to adapt the muting ratio ruling the frequency resource partitioning between both tiers according to the mobility behavior of the range-expanded users, thereby providing an efficient trade-off between Macrocell

and Picocell achievable throughputs.

Simulation results obtained for both HetNets scenarios; i.e. Macro-Femtocells and Macro-Picocells illustrated significant gain in the cell-edge throughput, a better guaranteed quality of service for the different ongoing applications in the different adjacent tiers, and finally a gain in the capacity of the whole system.

Keywords: LTE-A, HetNet, power adjustment, mobility prediction, Quality of Service, Interference Mitigation.

Resume

Récemment, l'utilisation des réseaux cellulaires a radicalement changé avec l'émergence de la quatrième génération (4G) de systèmes de télécommunications mobiles LTE/LTE-A (Long Term Evolution-Advanced). Les réseaux de générations précédentes (3G), initialement conçus pour le transport de la voix et les données à faible et moyen débits, ont du mal à faire face à l'augmentation accrue du trafic de données multimédia tout en répondant à leurs fortes exigences et contraintes en termes de qualité de service (QdS). Pour mieux répondre à ces besoins, les réseaux 4G ont introduit le paradigme des Réseaux Hétérogènes (HetNet).

Les réseaux HetNet introduisent une nouvelle notion d'hétérogénéité pour les réseaux cellulaires en introduisant le concept des smalls cells (petites cellules) qui met en place des antennes à faible puissance d'émission. Ainsi, le réseau est composé de plusieurs couches (tiers) qui se chevauchent incluant la couverture traditionnelle macro-cellulaire, les pico-cellules, les femto-cellules, et les relais. Outre les améliorations des couvertures radio en environnements intérieurs, les smalls cells permettent d'augmenter la capacité du système par une meilleure utilisation du spectre et en rapprochant l'utilisateur de son point d'accès au réseau. Une des conséquences directes de cette densification cellulaire est l'interférence générée entre les différentes cellules des diverses couches quand ces dernières réutilisent les mêmes fréquences. Aussi, la définition de solutions efficaces de gestion des interférences dans ce type de systèmes constitue un de leurs défis majeurs.

Cette thèse s'intéresse au problème de gestion des interférences dans les systèmes hétérogènes LTE-A. Notre objectif est d'apporter des solutions efficaces et originales au problème d'interférence dans ce contexte via des mécanismes d'ajustement de puissance des petites cellules. Nous avons pour cela distingués deux cas d'étude à savoir un déploiement à deux couches macro-femtocellules et macro-picocellules.

Dans la première partie dédiée à un déploiement femtocellule et macrocellule, nous concevons une stratégie d'ajustement de puissance des femtocellules assisté par la macrocellule et qui prend en compte les performances des utilisateurs des femtocells tout en atténuant l'interférence causée aux utilisateurs des macrocellules sur leurs liens montants. Cette solution offre l'avantage de la prise en compte de paramètres contextuels locaux aux femtocellules (tels que le nombre d'utilisateurs en situation de *outage*) tout en considérant des scénarios de mobilité réalistes. Nous avons montré par simulation que les interférences sur les utilisateurs des macrocellules sont sensiblement réduites et que les femtocellules sont en mesure de dynamiquement ajuster leur puissance d'émission pour atteindre les objectifs fixés en termes d'équilibre entre performance des utilisateurs des macrocellules et celle de leurs propres utilisateurs.

Dans la seconde partie de la thèse, nous considérons le déploiement de picocellules sous l'égide de la macrocellule. Nous nous sommes intéressés ici aux solutions d'extension de l'aire picocellulaire qui permettent une meilleure association utilisateur/cellule réduisant ainsi l'interférence et augmentant en conséquence l'efficacité efficacité spectrale. Nous proposons donc une approche basée sur un modèle de prédiction de la mobilité des utilisateurs qui permet de mieux ajuster la proportion de bande passante à partager entre la macrocellule et la picocellule en fonction de la durée de séjour estimée de ces utilisateurs ainsi que de leurs demandes en bande passante. Notre solution a permis d'offrir un bon compromis entre les débits réalisables de la Macro et des picocellules.

Keywords: Macrocelly, Femtocells, Picocells, Mobility, Optimization, Power.

Acknowledgment

It is a pleasure to express my gratitude to many people who directly and indirectly helped and made this thesis possible.

First and foremost, I am greatly indebted to my supervisor Lila Boukhatem, for her guidance and support with her knowledge and patience. She was always willing to give very generously her time for my research, and her doors were always open. Her wisdom, academic insight, sharp focus, and on-going belief were constant sources of motivation for me to achieve the outcome included in this thesis. I am truly privileged to have had her as mentors. Without her it would not have been possible for me to write my thesis on-time.

I convey my acknowledgment to my second supervisor Tara Ali Yahiya, for her support, help and kindness in the difficult times by many interesting ideas in my research area. She also helped me to significantly improve my writing skills, and she provides me her student's experience to improve and develop my open source framework. She is one of the persons I came to admire the most.

I express my gratitude to the committee member Dr. Megumi Kaneko for the interest. She showed in my thesis proposals and her very by valuable comments, suggestions, and insights which have enriched the content of this thesis.

I wish to thank all my friends and colleagues at LRI, all the networking group members for their encouragement and who made my working here enjoyable.

Finally, I would like to thank my parents, brothers and my sister who always stood by me with great patience and good wishes. I thank my wife for her support and encouragement.

I dedicate this thesis to my late parents to whom this thesis would have matters the most.

Acronyms

1G First Generation

2G Second Generation

3GPP 3rd Generation Partnership Project

ABS Almost Blank Sub-frame

AS Access Stratum

CN Core Network

CP Cyclic Prefix

CQI Channel quality Indicator

CRE Cell Range Expansion

CSG Closed Subscriber Group

CSI Channel State Indicator

CSO Cell Selection Offset

DeNB Donor eNB

DSL Digital Subscriber Line

e-ICIC enhanced Inter-Cell Interference Coordination

E-UTRAN Evolved UMTS Terrestrial Radio Access Network

eNBs evolved NodeBs

EPC Evolved Packet Core

EPS Evolved Packet System

EXP-PF Exponential Proportional Fair

FDD Frequency Division Duplex

FFR Fractional Frequency Reuse

FR Frequency Reuse

FRS Frequency Reuse Schemes

GPA Global Power Adjustment

GSM Global System for Mobile communication

GT Game Theory

HeNodeB Home eNodeB

HetNets Heterogeneous Networks

HSS Home Subscriber Server

IC Interference Cancellation

IHO Intra-cell Handove

IM Interference Mitigation

IoT Internet of Things

IP Internet Protocol

ISI Inter-Symbol Interference

LPNs Low Power Nodes

LTE Long Term Evolution

MBS Macrocell Base Stations

MCS Modulation and Coding Scheme

MGR Minimum Guaranteed Bit Rate

MLWDF Modified Largest Weighted Delay First

MME Mobility Management Entity

NAS Non-Access Stratum

NB Normal Band

NL Network Listen

PAMF Power Adjustment scheme in Macro-Femtocell

PAMF Power Adjustment scheme in Macro-Femtocell

PB Platinum Band

PBS Picocell Base Station

PDA Personal Digital Assistant

PFR Partial Frequency Reuse

QoS Quality of Service

RANs Radio Access Networks

RB Resource Block

REMs Radio Environment Maps

RL Reinforcement Learning

RMM Realistic Mobility Model

RN Relay Nodes

RPUEs Range expanded PUEs

RRC Radio Resource Control

RSRP Reference Signal Received Power

RSRQ Reference Signal Received Quality

RSS Received Signal Strength

S-GW Serving Gateway

SAE System Architecture Evolution

SFR Soft Frequency Reuse

SINR Signal to Interference Noise Ratio

SPA Selective Power Adjustment

TDD Time Division Duplex

TTI Transmission Time Interval

UMTS Universal Mobile Telecommunications System

WLANs Wireless Local Area Networks

List of Symbols

M	A macrocell
F_l	A femtocell l
P_l	A picocell l
L	Set of femtocells or picocells
I	Set of MUEs
J	Set of FUEs or PUEs
K	Set of RBs
k	A RB k
MUE_i	A macrocell user i
FUE_j	A femtocell user j
$SINR^k_{M,MUE_i}$	SINR of a given MUE_i associated with MBS M on RB k
p^k_M	Transmit power allocated on RB k by the serving cell M
$\lvert G^k_{M,MUE_i}\rvert$	Channel fast fading gain between M and MUE_i on RB k
$p^k_{F_l}$	Transmit power of neighboring femtocell F_l on RB k
$\mathcal{Z}_{i,k}$	Set of all interfering FBSs on user MUE_i on RB k
$\lvert G^k_{F_l,MUE_i}\rvert$	Channel fast fading gain between MUE_i and the neighboring F_l on RB k
PL_{M,MUE_i}	Pathloss between MUE_i and its serving cell MBS M
PL_{F_l,MUE_i}	Pathloss between MUE_i and neighboring F_l
$SINR^k_{F_l,FUE_j}$	SINR of a given FUE_j associated with a femtocell F_l on RB k
$p^k_{F_l}$	Transmit power allocated on RB k by the serving femtocell F_l
$\lvert G^k_{F_l,FUE_j}\rvert$	Channel fast fading gain between FUE_j and its serving femtocell F_l
$p^k_{F_m}$	Transmit power of a neighboring FBS F_m
$\mathcal{V}_{j,k}$	Set of all interfering FBSs on user FUE_j on RB k
$\lvert G^k_{F_m,FUE_j}\rvert$	Channel fast fading gain between FUE_j and its neighboring FBS F_m
PL_{F_l,FUE_j}	Pathloss between FUE_j and FBS F_l

A_j^k	Interference generated by MBS M on resource block k
$SINR_{MUE}^{target}$	Predefined SINR requirement threshold of MUEs
$SINR_{FUE}^{target}$	Predefined SINR requirement threshold for FUEs
RSS_{M,MUE_i}^k	Received signal strength by MUE_i from MBS M on RB k
RSS_{F_l,MUE_i}^k	Received signal strength by MUE_i from FBS F_l on RB k
$\Delta SINR$	A positive SINR protection margin, measured in dBs
ΔP	A positive power protection margin, measured in dBs
$\mathcal{K}_i$	Set of RBs allocated to MUE_i
$\mathcal{K}_j$	Set of RBs allocated to FUE_j
$P_{F_l}^{Max}$	Maximum transmit power of femtocell F_l
$f(F_l)$	Score Function
$\mathcal{R}_{F_l}$	Set of MUEs impacted by femtocell F_l
R_{F_l}	Cardinality of $\mathcal{R}_{F_l}$
$\mathcal{N}_{F_l}$	Set of MUEs located in the overlapping areas between F_l and any neighboring F_m
N_{F_l}	Cardinality of $\mathcal{N}_{F_l}$
$\mathcal{Q}_{F_l}$	Set of FUEs observing an outage after decreasing the power of their serving cell F_l
Q_{F_l}	Cardinality of $\mathcal{Q}_{F_l}$
$MI_{MUE_i}^k$	Maximum interference allowed by a victim MUE_i on RB k
$p_{F_l}^{'k}$	New value of transmission power of femtocell F_l on RB k
$\alpha_{F_l}^k$	Proportional value to $f(F_l)$ score
θ_i	Weighting factor reflecting the priorities of the context parameters.
$\beta_{F_l}^k$	Allowed per-femtocell interference level
$p_{P_l}^k$	Transmit power of neighboring picocell P_l on RB k
$\mathcal{U}_{i,k}$	Set of all interfering PBSs on user MUE_i on RB k
$\lvert G_{P_l,MUE_i}^k \rvert$	Multipath channel fading gain between MUE_i and the neighboring P_l on RB k
PL_{P_l,MUE_i}^k	Pathloss between MUE_i and PBS P_l on RB k
$SINR_{P_l,PUE_j}^k$	A PUE_j associated with a given picocell P_l on resource block k

$\lvert G^k_{P_l,PUE_j}\rvert$	Multipath channel fading gain between PUE_j and its serving picocell P_l
$p^k_{P_m}$	Transmit power of a neighboring PBS P_m
$\mathcal{V}_{j,k}$	Set of all interfering PBSs on user PUE_j on RB k
$\lvert G^k_{P_m,PUE_j}\rvert$	Multipath channel fading gain between PUE_j and its neighboring P_m
$PL^k_{P_l,PUE_j}$	Pathloss between PUE_j and PBS P_l
$S_{\max}$	The cell having the strongest DL-RSS
α	A bias value
β	Muting Ratio
RPUE_j	A picocell user j within the CRE region
T_j	The traveling time of each RPUE_j within the CRE area
ϕ_1 and ϕ_2	The successive positions of RPUE_j at two different times t_1 and t_2
D_j	The travelled distance beween points ϕ_1 and ϕ_2
τ	Travelling time threshold
M_j and M_k	Are the amounts of RB units required by RPUE_j and MUE_k users
N^{TARGET}	Predefined number of affected FUEs (i.e. $SINR^k_{F_l,FUE_j} < SINR^{target}_{FUE}$)
N_0	Power of the additive White Gaussian noise
$\mathcal{N}_l$	Set of PUEs in the CRE region of picocell l
N_I	Set of MUEs served by a macrocell l
$\mathfrak{N}_l$	Set of all PUEs in P_l including $\mathcal{N}_l$
N_{total}	Set of $N_I \cup \mathfrak{N}_l$

Contents

List of Figures

List of Tables

Chapter 1

Introduction

1.1 Background

Wireless communication networks have become an ubiquitous part of modern life, transforming the way we live, conduct business and interact. Since the inception of cellular concept in the 1960s, the communications industry has witnessed tremendous growth of new technologies being developed and brought to market on an almost daily basis. The history of mobile telephony can be traced back to the early eighties, when the frequency division multiplexing networks appeared to embody First Generation (1G) systems in order to satisfy users' demands by carrying voice services through analog signals [1].

Then, the Second Generation (2G) of mobile systems such as GSM, IS-95, IS-136 and PDC (Personal Digital Assistant) appeared in the early 1990's to provide reliable narrowband communication links mostly for voice and text services with high mobility [2]. These networks were supported by the local area networks such as Wi-Fi to offer broadband multimedia with limited mobility. 3G networks such as (Universal Mobile Telecommunications System) in Europe emerged in the beginning of the millenary to improve users' throughput and connectivity and to face the growth of mobile data demand due to the advent of intelligent mobile devices such as smartphones and tablets [3] [4] [5].

Recently, the 3rd Generation Partnership Project (3GPP) standardization body has developed the EPS (Evolved Packet System) which consists of the 4G Long Term Evolution (LTE) wireless mobile broadband technology for radio access and the System Architecture Evolution (SAE), as part of LTE release 8 [6]. LTE moved cellular systems for a transition to an all-IP flat core network with a simplified architecture and open interfaces. It allows to meet the requirements for increased data rate capacity, reduced latency, and improved spectral efficiency. However, experts' forecasts have shown that the resources offered by this latest generation will not be enough to sustain the wireless data explosion ((see Figure 1.1) [7]. This increase in data demand is mainly driven by the recent changes in communications usage. The introduction of high capacity devices such as smartphones and tablets as well as the intense video consumption have drastically changed the way data is been consumed. Along with this tendency, the new introduced wearable devices (such as smartwatches) or the connected cars materializing the concept of Internet of Things

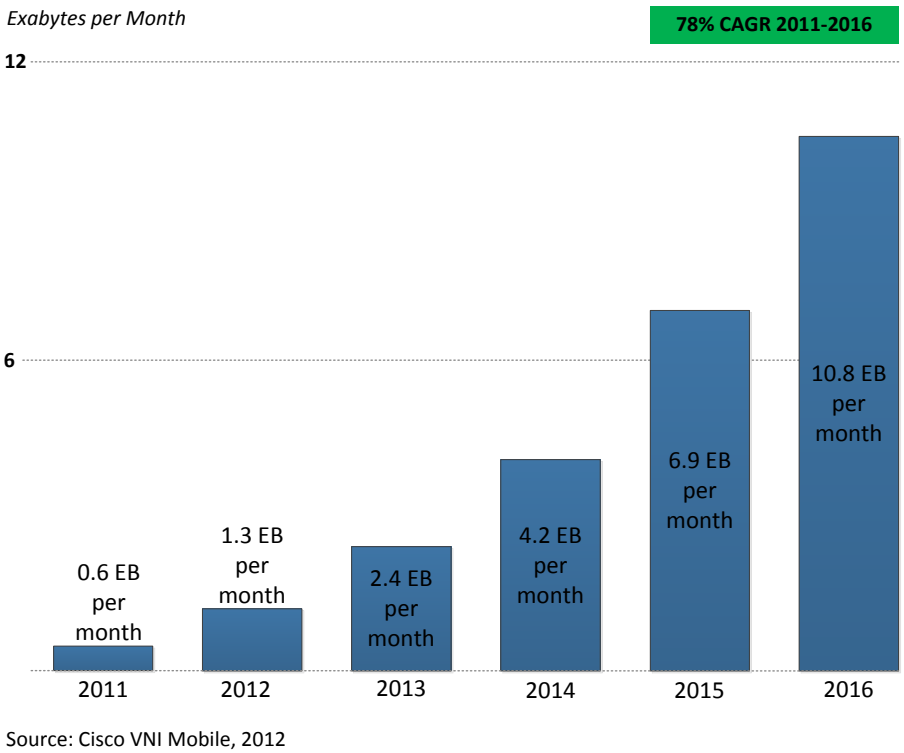

Figure 1.1: Cisco forecast for growth of global mobile traffic by 2017

(IoT) where billions of small devices are always connected will highly participate to this deluge of data.

To meet these requirements in a cost effective way, LTE-Advanced system, also known as LTE release 10/11, is designed. It is intended to support further evolution of LTE and to establish E-UTRAN as an IMT-Advanced technology through higher capacity, increased peak data rate, improved performance, higher spectral efficiency, and inter-working with other radio access technologies [8]. Achieving these goals involves several upgrading components that have to be considered. Apart from physical layer and radio link enhancements, the next leap in mobile and wireless networks will come from evolved network organization, the ultimate aim being the improvement of the spectral efficiency per unit area. LTE-A system proposed overlaying smaller transmission Low Power Nodes (LPNs) (also known as small cells) on top of existing MBSs (Macrocell Base Stations). The concept of small cells consists in decreasing cells' radius to cover a smaller geographical area (compared to macrocell) with higher capacity gains, as a result of a more efficient frequency reuse deployment [9]. Moreover, end users, including those on the cell-edge, benefit from higher channel experience due to their proximity to the LPNs transmitters.

In general, the deployments of LPNs under the umbrella of macrocells is 4G systems is usually defined as Heterogeneous Networks (HetNets) [10] [11][12]. The term HetNets most often refers to a two-tiered network architecture including a combination of MBSs and LPNs which can be either operator or consumer deployed such as picocells, relays and femtocells. Other definitions of HetNets consider the

integration of (Wireless Local Area Networks) as another underlying network. This would also enable data offloading from heavily loaded cellular tiers.

Due to limited spectrum resources and to achieve maximum capacity for the system, frequency resources may be shared by the different tiers. In other words, the frequency channels in one cell are the same used in an adjacent cell making the emitted signals interfere with each other. The generated cross-tier and inter-cell interference affects the quality of data transmission and impairs user throughput and experience. This makes the interference one of the major and challenging issues in HetNets. Many other aspects add more complexity to this problem such as the random femtocell deployment (as they are installed by users without network planning) as well as the unpredictable and changing relative location between victim and aggressor users.

Under the effect of interference, some advanced techniques and methods need to be developed to mitigate its impact. The standardization bodies as well as the research community suggested different approaches for inter-cell interference handling. This thesis aims at proposing new interference mitigation techniques which offer a better quality of experience for users. We will mainly focus on two-tier HetNets embedding femtocells and picocells as an underlying layer.

1.2 Thesis Contributions

Many research works have been proposed to investigate the interference mitigation problem in HetNets, and create new models and optimization techniques that help enhancing the network performance. In this thesis, we propose new interference mitigation strategies which rely on the Base-Station-assistance to adaptively adjust the small cells transmit power or turn-off some of its resources relieving the interfering users.

Following the above mentioned challenges, the contributions of the present thesis can be summarized as follows:

- We propose PAMF, a power control mechanism for interference mitigation in a mobility environment where macrocells and femtocells are co-located together. The key benefits of this scheme is to achieve higher performance for non-closed subscriber users, as well as avoiding potential service degradation of femtocell users by taking into account mobile users locations and SINR at both macro and femtocell sides.

- We propose SORA, a simple algorithm implemented at the network side to decrease the signaling overload caused by the proposed MBS-assisted power control scheme.

- We develop dynamic simulations in a realistic residential femtocell scenario, where different application types were considered. They allowed us to evaluate the performance of the proposed scheme under realistic assumptions. These analyses came to conclusions and perspectives that draw out the way towards proposing more enhancements for improved system performance.

- We propose a coordinated and context-aware MBS-assisted femtocell power control approach for mitigating the interference experienced by macrocell users while preventing the femtocell throughput degradation. In particular, we developed two power adjustment strategies called respectively GPA and SPA which implement two degrees of awareness of femtocells users throughput. Our strategies make use of femto and macro users' context information in terms of positioning, for setting the appropriate prioritization weights based on the current victim macro users and the femto users in outage. System-level simulations show that the proposed prioritization weights allow to achieve the required level of macrocell/femtocell throughput trade-off.

- We propose a mobility-aware e-ICIC scheme for collocated macro-picocells with cell range expansion. Our scheme turns-off some of the resource blocks in the macrocell in function of the mobility behavior of the range-expanded picocell users, thereby providing an efficient trade-off between macrocell and picocell achievable throughputs.

1.3 Organization of the Thesis

The remainder of this thesis is organized as follows.

- **Chapter 2,** presents an overview of HetNets architecture for LTE-advanced system. At first, we introduce the small cells concepts and give the different characteristics of typical deployable cells. Then, we introduce some LTE PHY layer characteristics such as the multicarrier OFDMA technology, CQI basics and the main feedback measurement reports generated by the users equipments. Finally, we show the radio resource functionalities on the MAC layer that are related to the concepts dealt with in this thesis.

- **Chapter 3**, presents the interference issue that arises in macro-femtocells and macro-picocells deployments. Then, we review the state of the art related to the interference avoidance. Our analysis distinguishes the approaches according to the type of networks (OFDMA and non-OFDMA) as well as the centralized or distributed feature of their rationale. We proposed a classification and discussion of some reference schemes in each category.

- **Chapter 4**, presents PAMF, a new MBS-assisted power adjustment scheme which aims at increasing the throughput of macro-users suffering from interference while being aware of femtocell users performance. At first, we introduce the system model we used in the macrocell femtocell scenario. Then, we detail the proposed power allocation strategy with its three different decision steps. In order to reduce the signaling overhead, we propose SORA algorithm which reduces the reports exchanged between the macrocell and femtocells. Finally, the simulation results demonstrate the gain in network capacity when using the proposed scheme under service differentiation assumptions.

- **Chapter 5**, enhances the proposal presented in chapter 4 by developing an approach which involves coordination between macrocell and femtocell for an

Table 1.1: Major publications constituting the core chapters

Article Conference/Journal	Publication
Chapter 4	IEEE WCNC2014
Chapter 5	IEEE ISCC 2014
Chapter 5	EURASIP Journal on wireless communication and networking (Submitted)
Chapter 6	IEEE PIMRC2014
Chapter 5	IEEE communication Magazine (Submitted)

efficient power adjustment based on users context information. We first describe the core idea of the cooperation strategy by presenting the main context parameters as well as the adjustment steps. Then we detail the GPA and SPA strategies and argue about their performance trade-off objectives. We show and discuss the effect of the weighting parameters defined by our approaches and prove the effectiveness of our proposals compared to reference schemes.

- **Chapter 6**, deals with the interference mitigation issue in two-tier macro-picocells systems. We first introduce the system model and then describe the basics of our mobility-aware e-ICIC scheme. Hence, we detail our assumptions about the mobility of users which allows us to derive the expected travelling times of Cell Range Expanded users within the picocell. Based on this estimation, we define the dynamic muting ratio which rules the frequency resource partitioning between the macrocell and picocell. We show that our approach provides an excellent trade-off between macro and picocells throughput.

- **Chapter 7**, concludes the documents and summarizes the basic insights. Finally, it proposes suggestions for the future research investigations.

The developed contributions were published in different international conferences. The following table summarizes the concerned communications.

Chapter 2

An Overview on HetNets

2.1 Introduction

Digital mobile data is generating very heavy traffic that represents a challenging issue to be addressed by telecommunication companies while providing their services anytime and anywhere. 4G LTE and LTE-A systems are considered as the technology of choice as they provide cost effective methods for an efficient use of the radio spectrum. With the introduction of the new radio access E-UTRAN (Evolved UMTS Terrestrial Radio Access Network), LTE has significantly improved end-user quality of service in terms of throughput, capacity offering, reduced user plane latency, and brought important enhancement for user experience with the support of full mobility. LTE/LTE-A also deliver and support an all-IP (Internet Protocol) based traffic with end-to-end QoS. Introducing different types of access networks in LTE is essential to cope with the increasing number of mobile broadband data subscribers and bandwidth-consuming services competing for the limited radio resources. Since the sole macrocells cannot meet the requirements of mobile users in terms of QoS, LTE-A specifications introduced small cells concepts through the addition of low-power base stations to existing eNBs (evolved NodeBs). These small cells namely picocells, femtocells as well as Wi-Fi hotspots can offload traffic from highly loaded macrocells. Furthermore, LTE-A also introduced the use of relay nodes in order to expand the coverage area of the macrocells and offer cell-edge users a better signal quality and avoid them to be penalized by the poor interference and the transmitted signal from the eNB [11][13].

In this chapter, we introduce the different characteristics of heterogeneous networks covered by LTE-A specifications and we focus on the HetNets scenarios that are considered in this dissertation. Then, we provide an executive summary for the most important features of physical and MAC layers in LTE-A which are closely related to our models. This constitutes an important step towards a better understanding of our contributions in the subsequent chapters.

2.2 HetNets Architecture in LTE-A

A generic LTE-A HetNet architecture consists of different types of Radio Access Networks (RANs) or cells: picocells, femtocells and relay nodes underlying a collocated

macrocell (eNBs or MBS) as shown in Figure 2.1. The eNBs are inter-connected with each other via the X2-interface while they are connected through the S1-interface to the operator's Core Network (CN), also referred to as Evolved Packet Core (EPC). The main difference between RAN and CN is the split of functionality, as the EPC is part of the non-radio evolution called SAE. Together the LTE-A RAN and SAE comprise EPS.

EPC supports access to the packet-switched domain only, with no access to the circuit switched domain and it consists of several different types of nodes, some of which are briefly described below:

- **Mobility Management Entity** (**MME**); is the control-plane node of the EPC. Its responsibilities include connection/release of bearers to a mobile user, handling of IDLE to ACTIVE transitions, handling of security keys, and it is also responsible for authenticating the user by interacting with the Home Subscriber Server (HSS). The functionality operating between the EPC and the mobile user is also referred to as the Non-Access Stratum (NAS), in order to separate the EPC from the Access Stratum (AS) which supports the functionalities between the terminal and the RAN. The MME is also responsible for the generation and allocation of temporary identities to mobile users.

- **Serving Gateway** (**S-GW**); is the user-plane node connecting the EPC to the LTE RAN. The S-GW acts as a mobility anchor when mobile users travel between eNodeBs, and a mobility anchor for other 3GPP technologies. it is also responsible to route and forward user data packets [14].

- **HeNodeB GW**; is the control-plane node of the EPC, connecting the femtocells to the EPC through Internet. The main functionality of the HeNodeB GW is to allocate the IP address to the femtocell [15].

The LTE-A RAN uses a flat architecture with a single type of nodes in its HetNets deployment macrocell is considered as an umbrella for the different types of small cells (picocells or femtocells) and can provide the connection to farther users through the deployed relay nodes. The RAN is responsible for all radio-related functionalities of the overall network including for example, scheduling, radio-resource handling, retransmission protocols, coding and various multi-antenna schemes.

2.2.1 Small cells concepts

According to the Small Cell Forum [16]. "Small cells is an umbrella term for operator-controlled, low-powered radio access nodes, including those that operate in licensed spectrum and unlicensed carrier-grade Wi-Fi. Small cells typically have a range from 10 meters to several hundred meters". Small cells are definitely the key technology in HetNets which will bring higher capacity where it is needed the most by getting the access network closer to users, and only a high densification of these low power nodes in the indoors and outdoors (homes, offices, shopping malls, and other venues) can achieve the targeted multiplication in capacity. Small cell nodes can operate either on the licensed or unlicensed spectrum and rely on various technologies such

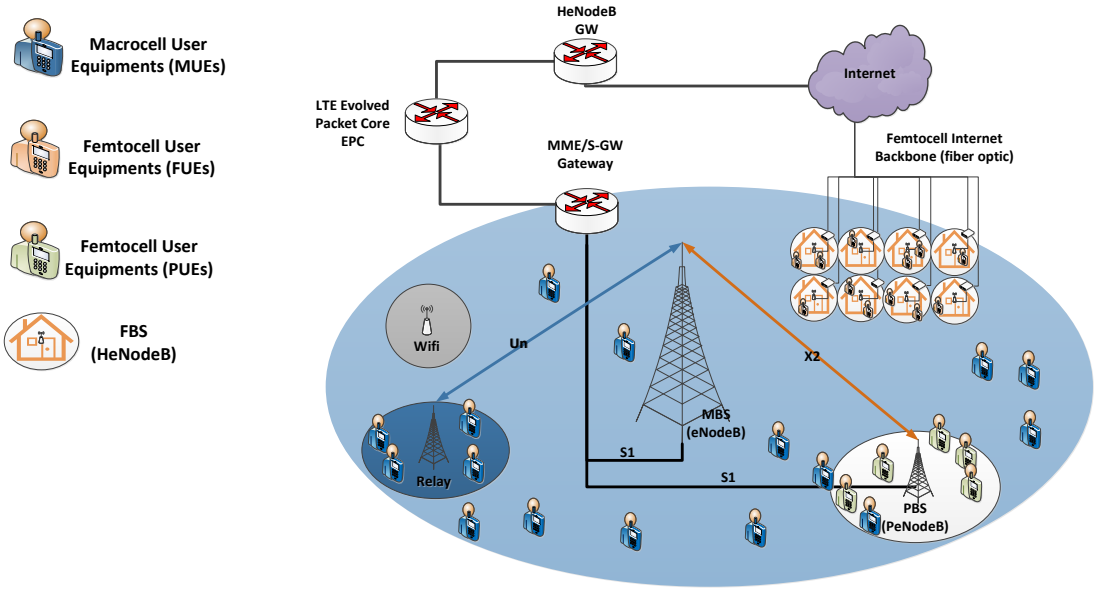

Figure 2.1: Heterogeneous wireless network architecture

as 3G, LTE, Wi-Fi. It is worth to notice that the unlicensed wireless access (such as Wi-Fi) is not considered in this thesis.

There are several and different types of small cells. They vary in their coverage size (radiated power), consumption, number of users they can handle, and their cost. Their main characteristics are summarized in Table 2.1 and more details about their functionalities are given below [14].

2.2.1.1 Picocells

The Picocell coverage is formed through the use of a low power node base station called Picocell Base Station (PBS). It is typically of a smaller order of magnitude compared to eNB, since PBS integrates an antenna radiating a transmit power ranging from 23 to 30 dBm. Note that, the omni-directional antennas installed for picocell are different from the sectorial ones used for MBSs. Moreover, the operator can deploy picocells using backhaul and access features compliant with classical eNBs. Picocells are deployed to fill the macrocell coverage gaps or to improve local cellular service, typically in hotspot areas (for example shopping malls) [17].

2.2.1.2 Femtocells

A femtocell also called Home eNodeB (HeNodeB) is the smallest low power node base station. It is installed by the end-user typically in an indoor installation, and considered as an important part of HetNets. It offers the network operators a means to provide good indoor coverage, for different types of traffic namely voice, video and high data services. FBSs are connected to the network operator's backhaul via a wired internet connection such as Digital Subscriber Line (DSL), fiber optic or cable broadband access. The use of femtocells offers several advantages to both the service operator and the end-user. The most important aspect of femtocells design is

Table 2.1: Major characteristics of different cells in HetNets.

Types	Transmit Power	Coverage	Capacity	Connection to Backhaul
Macrocell BS	46 dBm	Few kms-40 km	<1000 Users	Dedicated wired
Picocell BS	23-30 dBm	< 300 m	10-50 Users	Dedicated wired
Femtocell BS	10-23 dBm	< 50 m	4-8 Users	Wired internet access
Relay	23-30 dBm	< 300 m	10-50 Users	Wireless

the access mode mechanism [18]. Femtocells can be configured with three different types of access modes:

Close access mode also referred to as Closed Subscriber Group (CSG) [19] in which the femtocell allows only its subscriber users to establish connections. The list of authorized users is controlled by the femtocell owner. The CSG mode is usually deployed in residential and professional areas that require a high security access and/or high-quality communications to their users.

Open access mode authorizes UEs of the same FBS' operator to connect to the cell when they are in its vicinity. This mode enables the offloading following concept. It requires that the network operator deploys femtocells in public areas where the macrocell coverage is weak.

Hybrid access mode is a mix of both previously mentioned access modes in which most of the resources are operated in closed access mode, and the remaining resources are used in an open access mode.

2.2.1.3 Relays

Relay nodes represent a low cost solution for extending the macrocell coverage and/or improve the throughput of its cell-edge users. Unlike other HetNets nodes such as picocells or femtocells that are connected to the MBS through X2 or internet backhaul connections, Relay Nodes (RN) use a wireless link to connect to the MBS. Generally, a RN can be considered as an access point that decodes/sends data or forwards/broadcasts information received from a BS, in this case it is called Donor eNB (DeNB) or Type-II RN, as it does not have a cell ID or a Realistic Mobility Model (RMM). While a Type-I RN is considered as a small BS which has its own cell ID, broadcasts system information, and can proceed on RMM functions' based on its own reference signals [20][21].

2.3 Fundamentals of LTE Physical layer

The LTE physical layer is based on OFDMA technology. OFDMA is the multiple-access/multiplexing transmission technique scheme which has proven its high efficiency by providing multiplexing operation of data stream from multiple users to enable high-speed data, and high spectral efficiency. OFDMA relies on OFDM (Frequency Division Multiplex) multiplexing technique which has been adopted by

a variety of commercial broadband systems, including DSL, Wi-Fi, DVB-T (Digital Video Broadcasting-Terrestrial), etc. In this section, we cover the basics of OFDMA and provide an overview of the LTE physical layer.

2.3.1 Slot and Frame Structure in LTE OFDMA

Before detailing the LTE PHY layer generic frame structure, it is worthy to mention that the downlink and uplink transmissions in LTE use one of the two duplexing modes: Time Division Duplex (TDD) or Frequency Division Duplex (FDD) in which the duplex is realized in time and frequency, respectively. TDD and FDD modes are widely deployed in the existing cellular system; they both have their own advantages and disadvantages. The operator usually selects the duplexing format according to the supported applications. However, in practical deployment systems, FDD is the most used mode due to its reduced complexity. *In this thesis, we assumed the use of the FDD mode for the whole contributions.*

OFDMA depends on an OFDM PHY layer. OFDM is a multicarrier transmission technique that divide the available bandwidth into a large number subcarriers which are generated sets, and each set of subcarriers is called sub-channel. However, the resource allocation unit is called Resource Block (RB), which is a grid of rectangular block of resource elements, which consists of 12 consecutive sub-carriers in the frequency domain and 6 or 7 OFDMA symbols in the time domain. Thus, in an OFDMA system, a RB is available in the time domain by means of OFDM symbols and in the frequency domain by means of subcarriers. The total number of available RBs depends on the overall transmission bandwidth of the system. LTE-A specification defines different exploitable bandwidths from 1.4 MHz to 20MHz which corresponds respectively to 6 and 100 RBs [22].

Generally, in LTE-A OFDM PHY system, the input data stream is divided into several parallel sub-streams of reduced data rate and each sub-streams is modulated and transmitted on a separate orthogonal subcarrier. The orthogonality among subcarriers depends on the duration of the Cyclic Prefix (CP) or the increased symbol duration which improves the robustness of OFDM to delay spread. In other words, the CP can completely eliminate Inter-Symbol Interference (ISI) in case of a CP duration longer than the channel delay spread. The minimum allocation bandwidth for a UE is one RB. RB allocation is carried out by the MAC scheme for each sub-frame as it is the sub-layer which is responsible for scheduling the packets to transmit over the LTE air interface in both DL/UL directions. It must be noted that, in all OFDMA systems, the scheduler decides which users are allowed to transmit and which RBs to assign to them. Usually, the RB assignment in LTE is carried out each 1 msec corresponding to the Transmission Time Interval (TTI). The scheduler must also decide the quantity of power to be applied to each RB as well as the suitable Modulation and Coding Scheme (MCS) to be assigned to each user. Figure 2.2 shows the LTE-A radio frame structure of 10msec duration for a given 10 MHz bandwidth system. The frame is divided into 10 sub-frames. Each sub-frame further divided into two slots, each of 0.5 msec duration. A slot consits of 7 ODFM symbols with short cyclic prefix. Thus, the total available resources are 600 Subcarriers (Sc) which corresponds to the 50 RBs in the frequency domain. Each RB within the grid represents 84 (12Sc x 7 Symbols) elements. Note that a

RB is the smallest unit of resource allocation assigned by the base station scheduler.

Due to frequency-selective interference and fading fluctuations along the spectrum, different users could experience diverse channel conditions on a given subcarrier. Note that there are two types of subcarrier permutations for sub-channelization; contiguous and diversity. The contiguous permutation also referred to as band-AMC, groups a block of contiguous subcarriers to form a sub-channel. Contiguous permutation enables multi-user diversity by choosing the sub-channel with the best frequency response. The diversity permutation draws subcarriers pseudo-randomly to form a sub-channel. It provides frequency diversity and inter-cell interference averaging. In order to note that, we have used the diversity subchannelization along the spectrum resources.

In OFDMA systems, the transmitters need the average Channel Quality Indicator (CQI) feedback from the users to apply link adaptation, pre-coding, pre-equalization, and adaptive transmit antenna diversity in order to maximize the spectral efficiency. Table 2.2 describes the different MCSs supported by LTE-A, and indexed according to the CQI. As explained, if the channel experience a poor quality, low order modulation is employed, conversely, if the channel shows a good quality a high data rate can be achieved through request higher order modulation. Similarly, code rate and transmission power can be optimized according to the instantaneous channel conditions impacting consequently the required transmission rate and reliability.

Moreover, when a mobile terminal is assigned a subchannel with diversity subchannelization, it sends back a CQI to its base station, which is the average Signal to Interference Noise Ratio (SINR) level of the allocated subcarriers that are distributed over allowable spectrum range, to remove the effect the of frequency-selective fading. When a UE uses contiguous sub-channelization, it sends the quantized SINR level of each subcarrier for each sub-channel. According to the reported CQI method, the base station can know the SINR, and then determines the appropriate MCS level for each RB. These options enable the system designer to make a trade-off between mobility and throughput [6][12][23].

2.3.2 Downlink reference signals

Usually, to select the best serving cell mobile users are continuously measuring and reporting back to their serving cells the RSSI (Received Signal Strength Indicator) and RSRP (Reference Signal Received Power) of the cell-specific RS (Reference Signals). In general, RSSI is the more traditional metric that has long been used to display signal strength for GSM, CDMA1X, etc, which provides information about total received wide-band power measured in all symbols including interference. In other words, RSSI helps in determining interference and noise information (for LTE-A, including LPNs) and provides information about signal strength. While, RSRP is the LTE specific metric which is defined as the linear average over the power contributions (in [W]) of the resource elements that carry cell-specific RSs within

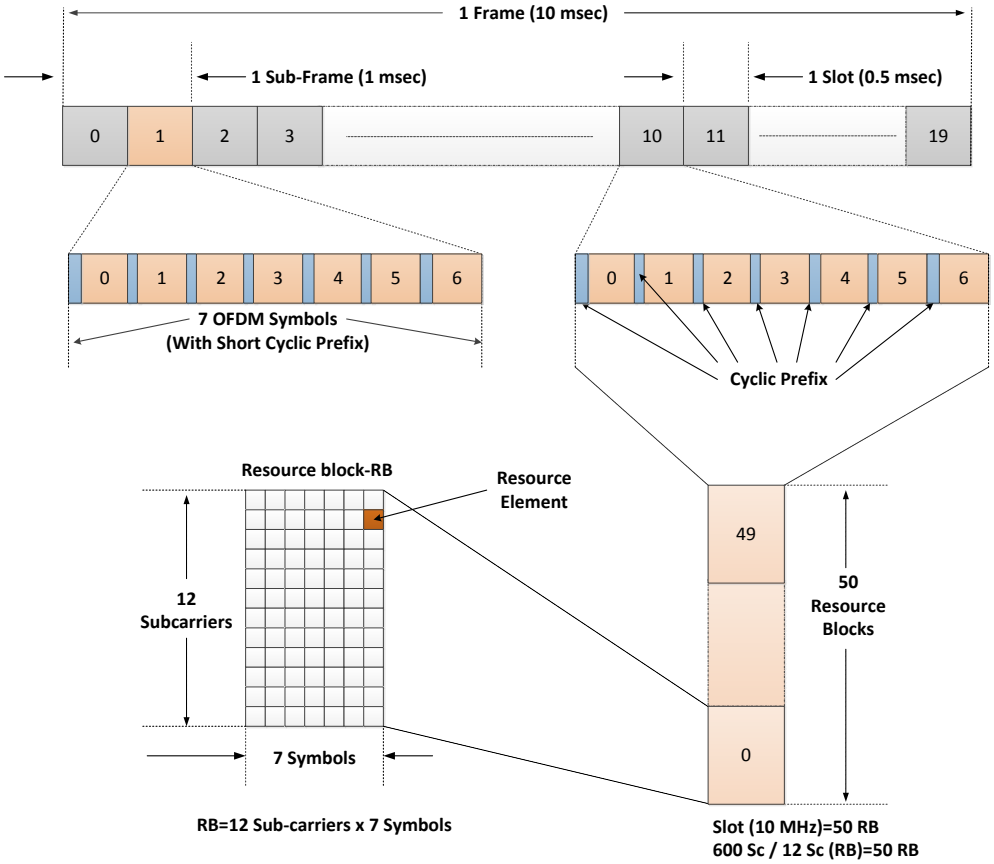

Figure 2.2: Generic frame structure in LTE downlink

Table 2.2: Modulation and coding schemes for LTE (3GPP Release 10)

MCS	Modulation	Code Rate	SINR threshold [dB]	Spectral Efficiency [bits/symbol/Hz]
MCS1	QPSK	1/12	-6.50	0.15
MCS2	QPSK	1/9	-4.00	0.23
MCS3	QPSK	1/6	-2.60	0.38
MCS4	QPSK	1/3	-1.00	0.60
MCS5	QPSK	1/2	1.00	0.88
MCS6	QPSK	3/5	3.00	1.18
MCS7	16QAM	1/3	6.60	1.48
MCS8	16QAM	1/2	10.00	1.91
MCS9	16QAM	3/5	11.40	2.41
MCS10	64QAM	1/2	11.80	2.73
MCS11	64QAM	1/2	13.00	3.32
MCS12	64QAM	3/5	13.80	3.90
MCS13	64QAM	3/4	15.60	4.52
MCS14	64QAM	5/6	16.80	5.12
MCS15	64QAM	11/12	17.60	5.55

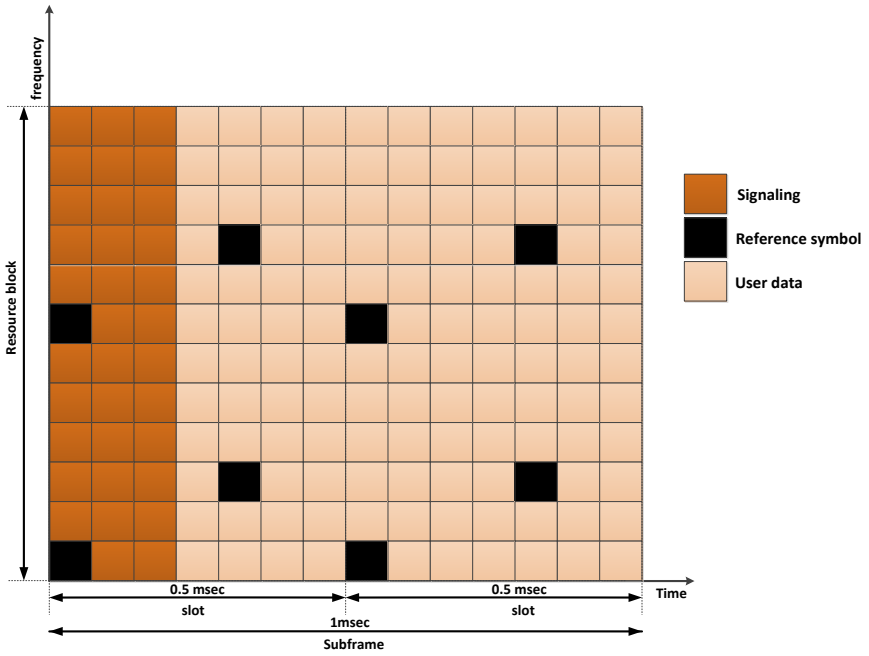

Figure 2.3: Location of reference symbols within a resource block

the considered measurement frequency bandwidth. So, RSRP[1] is only measured in the symbols carrying RS [24].

Finally, RSRQ (Reference Signal Received Quality) measurement and calculation is based on both RSSI and RSRP. Figure 2.3 shows that the mobile terminal can directly estimate the channel condition in both frequency and time domain using the predefined reference symbols (also called pilot symbols) [5]. In LTE specifications, 510 reference signals are used to identify the different cells [25].

2.4 Fundamentals of LTE MAC layer

The most important features of the MAC layer in LTE eNB is to offer Radio Resource Control (RRC) functionalities related to the control and data planes. these functionalities include radio resource management, admission control, scheduling, enforcement of negotiated QoS eNoB connection through HARQ (Hybrid Automatic Repeat Request), and mapping between logical and transport channels. We will focus in the following sections on some MAC features which are closely related to the concerns to our thesis.

2.4.1 Traffic classes and Quality of Service

Managing the quality of experience of users is an issue which is treated carefully by the 3GPP as it introduced in LTE specification some QoS (Quality of Service)

[1]In LTE, users are instructed to perform measurement reports RSRP as regularly as once every 480 ms in order to aid cell selection and handover procedures [24].

mechanisms that allow the operators to mange as the best as possible the different qualities users as regards to the different types of the applications user. Such QoS mechanisms involve both control and user planes. For example, the control plane mechanisms are used to permit the negotiation between the UEs and the network in order to agree on the different QoS requirements identify which UEs and applications are associated to what type of QoS, and enable the network correctly assign resources to each type of service. While, the QoS mechanism in the user plane has the role of agreeing those QoS requirements and controlling the network resource consumed by application/user pairs. As a consequence many applications can be run in a UE and eNB in the same time, each of which has different QoS parameters and requirements. Hence, it is imperative to set up different bearers for supporting those multiple QoS requirements. Each bearer is associated with a QoS support mechanism. Broadly speaking, bearers in LTE are categorized into classes depending on the nature of the QoS they are providing [26][27]: (i) Minimum Guaranteed Bit Rate (GBR) bearers which are used mainly for real-time applications that are requiring guaranteed QoS parameters and (ii) Non-GBR bearers associated with non-real-time applications that do not need a permanent resource allocation guarantee.

2.4.2 Resource Scheduling Algorithms

In LTE, the MAC scheduling is a challenging process which coordinates the access to the shared resources. The objective is to achieve maximum resource optimization while satisfying users' QoS requirements and guaranteeing a good degree of fairness.

Traditional best CQI scheduling algorithm aims to achieve the highest system efficiency by allocating the resources to the user experiencing the best channel quality. Typically, such users are usually located in the cell-center. Cell-edge users which suffer from interference and high path loss fading will starve and will have less opportunity to be served by the scheduler algorithm. selecting UEs with the best CQI for resource scheduling poses an unfairness problem in the resource assignment process. To better take into account both the QoS requirements of users and channel conditions, we adopt in this thesis two opportunistic QoS-aware scheduling algorithms:

- **Exponential Proportional Fair (EXP-PF)**; main purpose is to balance between fairness and throughput among all UEs. The scheduler scheme assigns the resources to UEs by comparing the ratio of current data rate to the average data rate of a particular user. Thus, the fairness can be addressed in this strategy, while maintaining comparable long-term throughput for all users. EXP-PF scheme enhances the basic PF algorithm to enable the support of delay sensitive flows. It adds the EXP rule to consider the packets delay in the priority affected to users.

- **Modified Largest Weighted Delay First (MLWDF)**; is able to handle delay sensitive traffics as well. It schedules the UEs by comparing the combination of packet delay, current data rate and average data rate in an optimal way. MLWDF exploits asynchronous channel variations and allows different mobile terminals to transmit at different data rates, so that higher efficiency

can be achieved. However, it is not providing the explicit QoS guarantees such as delay and data rate to the cell-edge users [10].

2.4.3 Mobility

LTE introduced a hybrid mobile network architecture supporting radio access technologies and several mobility mechanisms. The EPC introduced an important entity for mobility management called MME. This entity is managing the mobility when UEs are handing over from one cell to another in a very transparent way to the end user. Moreover, LTE defined procedures and the protocols to enable mobility and handover between 3GPP and non 3GPP technologies. In this thesis, we mainly interested in handover scenarios between macro/femtocell and macro/picocells within an LTE-A based HetNet.

The mobility of users between macrocells and femtocells is quite difficult due to the large number of candidate femtocells in dense urban scenarios and the characteristics of the femtocell entity. These characteristics are mainly the different femtocell access modes and the radio resource allocation method. In the case of handover between macrocells and picocells, other issues and challenges should be considered. This HO is related to the procedure cell range expansion mechanism which is introduced in picocells deployment. The mobility trigger in this case is motivated by a load balancing and interference concern as the handover decision is made on the interference mitigation situation and picocell load unlike classical SINR-based user-to-cell associations [12][14].

2.5 Conclusion

This chapter has presented the generic LTE-A HetNets architecture. Then, fundamentals of LTE physical and MAC layers and more particularly the most important features related to our work were given. The next chapter will present an overview of the current literature on interference avoidance issue.

Chapter 3

Interference Mitigation: A state of the art

Recently, the interference issue in 4G wireless systems has been widely addressed in the literature. Two categories of solutions for this problem can be identified: Interference Cancellation (IC) and Interference Mitigation (IM) [28]. The basic principle of the interference cancellation is that the receiver subtracts the interference signal from the transmitted one to successfully decode the desired signal information. Generally, IC is defined as a combination of techniques that allows the communication to operate even under high levels of interference [29]. From the information theory point of view, the performance of the mobile received signals can be improved owing to the multiuser interference canceling principle [30].

The first IC algorithm, proposed in the 90's, aimed to acquire the Shannon capacity of multi-user additive white Gaussian noise, allowing the mobile terminals to use the multi-channels and a large spreading factor while assuming accurate channel estimation [31]. Other works on IC techniques have been analyzed in details in [32][33][34]. These schemes are difficult to implement in practical systems due to the complex procedure used to estimate the interfering signal and cancelling it from the received one, and to the possible unsuccessful signals subtraction that might be caused by error occurrence [35].

IM is another efficient to deal with the interference issue that has attracted the attention of both academic and industry researchers. The IM techniques usually attempt to avoid the interference through preventing it from the source or even from occurring. This can be achieved by selecting an efficient reuse factor such as restrictions on frequency resource, power allocation and antenna planning that meet network performance goals. We will detail in the following sections the main IM techniques and study their feasibility in HetNets scenarios.

3.1 Interference Mitigation: Problem description and motivations

In cellular networks regardless their types, i.e., homogenous or heterogeneous, the UEs at cell range borders experience high interference from neighboring transmitters as their distance-dependent attenuation is a critical issue. With the regard to the

conventional scheduling schemes that aim at increasing the network throughput, such as maximum-SINR scheduler, UEs with poor signal channel conditions will suffer from starvation compared to the cell center UEs which monopolize most of the assigned RBs. Moreover, the cell-edge UEs are not contributing to the increase of the total cell throughput even if a fair scheduler such as proportional fairness [36] or weighted fair queuing [37] is used.

There are several types of interference mitigation schemes in the literature that improve the SINR without sacrificing cell center UEs throughput. When considering low complexity approaches, fixed frequency reuse schemes do not imply signaling coordination among cells as they use fixed bandwidth and power allocation initialized during the network-planning phase. While adaptive frequency reuse schemes coordinate adjacent cells for resource and power allocation to achieve a better system performance by dynamically adapting to the time-varying network conditions [38]. Nevertheless, this increase in performance is obtained at the expense of an implementation complexity and large delay and signaling overhead between the operating cells.

We can classify the techniques of interference mitigations in two different categories depending on the type of networks, which can be either homogenous or heterogeneous depending on the different types of base stations deployed in the geographical area. Note that the term homogeneous refers to the conventional homogeneously deployed cellular systems which consider a network of high-power base stations also called macrocell BSs. All the BSs have similar characteristics, such as the transmit power levels, and antenna configurations, and they all provide unrestricted access to every mobile subscriber in the network. While the reference to a heterogeneous network indicates the use of multiple types of low power nodes overlaid to the traditional macrocells such as picocell, femtocell BSs, and relay nodes. Accordingly, in the following sections we detail the techniques of interference mitigation in both homogenous or heterogeneous cases and give a more in-depth insight on the interference issue in HetNets scenarios. We also provide at the end of the chapter a detailed classification of IM solutions in both homogenous and heterogeneous networks.

3.2 Interference Mitigation in Homogenous Networks

In 4G LTE specifications [14], the different schemes that can be adopted to mitigate the interference can be divided into two groups of solutions namely: fixed frequency partitioning and dynamic frequency partitioning. The former includes all the key methods like Fractional Frequency Reuse (FFR), Soft Frequency Reuse (SFR) and Partial Frequency Reuse (PFR). While the latter gathers both the centralized and decentralized dynamic frequency assignment schemes.

3.2.1 Interference mitigation using fixed resource partitioning

In order to mitigate inter-cell interference, OFDMA based networks can exploit their physical layer flexibility to enable several types of frequency reuse schemes [39].

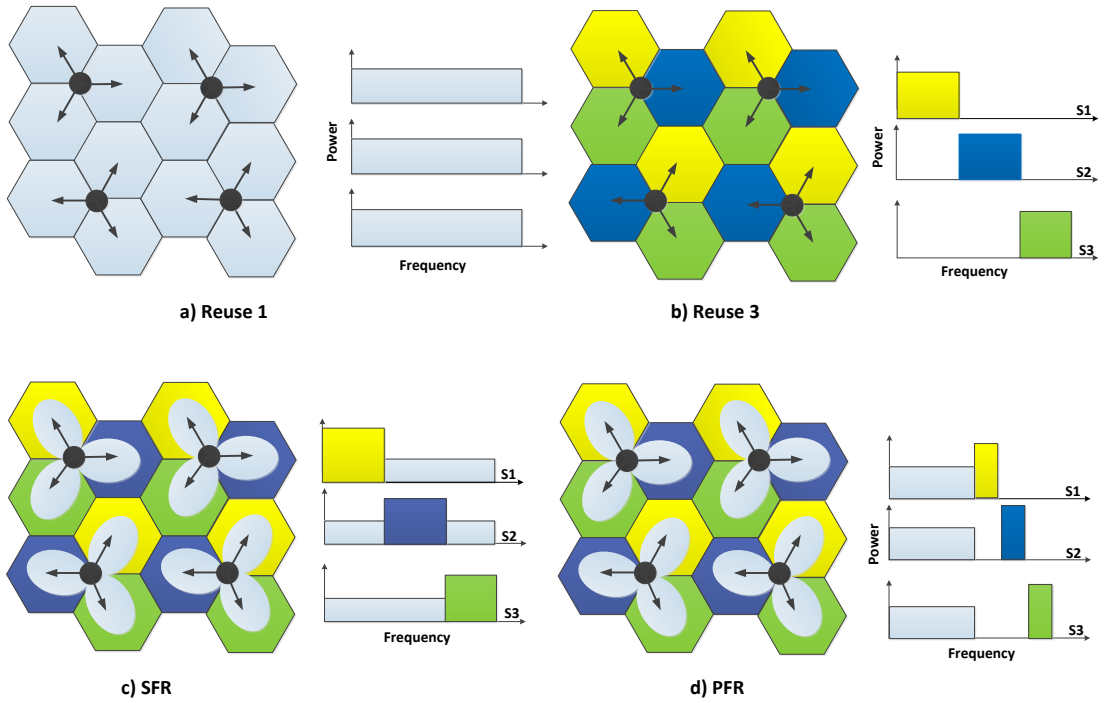

Figure 3.1: frequency reuse schemes

- **Universal reuse scheme** (also called reuse factor of 1) in which all the available sub-carriers are reused in each cell or sector without any restriction to the frequency resource usage or power allocation. Hence, in such scheme inter-cell interference is an issue that could degrade the network performance.

- **Frequency reuse scheme** in which the available sub-carriers are divided into S groups and each cell among neighboring cells will be assigned one group of sub carries, and then the Frequency Reuse (FR) factor of S can be achieved. This strategy eliminates the possibility of inter-cell interference among adjacent cells, however this is done at the expense of resource loss due to the partitioning. Figures 3.1 a and b show both methods for FR 1 and 3 schemes respectively, where the transmission power per resource group is constant [40][41].

In order to overcome the disadvantages of reuse 1 and S schemes, the FFR method was introduced for the GSM [42]. The basic idea is that FFR explores the trade-off between spectrum usage that may be obtained with reuse 1, and interference mitigation that can be achieved using FR S. In FFR allocation, the users are divided into two groups according to their locations (cell center and edge users) and geometries, so that the users with good geometries, e.g. close to the inner-zone (cell-center) belong to the inner-bands while users located in the outer-zone (cell-edge) are assigned to the outer-bands [43]. In FFR solutions, higher power is allocated to the resources used for the cell-edge UEs, while the boundary that separate the inner and outer zones is adjusted based on the distance, signal strength or signal quality, etc. Other solutions which can be considered as special cases of FFR are illustrated in figure 3.1 c and d namely PFR [44] and SFR [45].

The analysis presented in [42] studied the effect of power coordination in FFR schemes, and it demonstrated that several predefined power and frequency planning S outperform the pure FFR scheme where equal power is used across the entire sub-carriers. In general, SFR or PFR schemes are able to reduce the inter-cell interference due to cell-edge users are assigned by a specific band while cell-center users have exclusive access to all bands (cell-edge and cell-center bands). It is worth to notice here that all the previously mentioned schemes for inter-cell interference control in the frequency and power allocation domains are mostly based on static and fixed pre-planned frequency allocation, that does not cope with the time-frequency varying factors such as spatial distribution, users QoS, traffic dynamics, etc. [46].

3.2.2 Interference mitigation using dynamic resource partitioning

The static frequency reuse schemes are not capable of handling inter-cell interference efficiently especially when the macrocell layer is dealing with several time-varying network conditions such as users mobility. As the LTE system is mostly based on macrocells deployment only, it is referred to as homogeneous network, since all MBSs are of the same type and have similar maximum transmission power level. In this context, dynamic frequency reuse for interference mitigation was considered as an interference coordination (IC) technique [47].

Mostly the interference mitigation is based on the beamforming by which each MBS eliminates or reduces the effect of the interfering signal. In addition, the IC schemes (such as the coordinated spectrum scheduling and/or power allocation) can be implemented through the exchanged messages between two or more neighboring MBSs using the backhaul S1-interface via MME/S-GW. Moreover, different approaches optimizing jointly the frequency and power allocation have been also studied in LTE system, which differ in their complexity their and the required feedback information from the mobile terminals [48]. However, as the deployment of LPNs is expected to be widely used in LTE-A system, the inter-cell interference between macrocells and LPNs is expected to be more aggressive compared to the homogeneous case.

3.3 Interference Mitigation in Heterogeneous Networks

A HetNet consists of a classical macrocells layout with some LPNs placed throughout their coverage zones. Consequently, a HetNet shows completely different interference characteristics compared to a homogeneous deployment and attention must be paid to these differences when planning the frequency reuse. We are interested in this dissertation in the interference generated in two-tier systems, and more especially: Macrocell/Femtocell and Macrocell/Picocell systems. The interference in two-tier networks can be generally of two types [49]:

- **Co-tier** interference which occurs between cells belonging to the same tier, for example between two neighboring femtocells or macrocells,

- **Cross-tier** interference which occurs between cells belonging to different tiers, such as femtocell and macrocell or vice-versa.

This thesis focuses exclusively on the inter-cell interference mitigation in two-tier heterogeneous networks (macro-femtocell, and macro-picocell systems) where the same frequency spectrum is shared between macrocells and LPNs.

3.3.1 IM in two-tier Macro-Femtocells context

Generally, the impact of interference between different tiers, in our case (macro-femtocells) depends on the techniques used for spectrum assignment and/or the access method used by the network.

3.3.1.1 Frequency Spectral Assignment

Interference in cross-tier heterogeneous networks can be mitigated via appropriate frequency reuse schemes especially when the operator exploits several licensed bands [24]. Several options can be considered for frequency allocation:

1. **Fully dedicated band:** each tier of the overlaid network is assigned a different frequency band, consequently the cross-tier interference is totally avoided. Nevertheless, this approach shows low network spectral efficiency because each tier can only access a sub-set of the entire frequency resources. If we consider the case of LTE which is based on OFDMA technology, the terminology "Orthogonal allocation" is usually used and the available sub-channels are divided into two sub-sets, a sub-set is used only by the macrocell tier while the other is dedicated to the femtocell tier.

2. **Shared spectrum band:** (universal reuse scheme): both tiers share the same frequency band leading to the use of the total frequency band. Despite this positive aspect (in terms of spectral efficiency), this method produces severe interference that would degrade the overall network performance and has to be handled. In LTE OFDMA systems, this allocation is referred to as "Co-channel" assignment.

3. P**artially shared band:** is an intermediate solution which provides a trade-off between the spectral efficiency and the cross-tier interference by combining the fully dedicated and the shared spectrum approaches. In this assignment scheme, macrocell users can access the whole frequency spectrum, while femtocells operate in a sub-set of it. In case some MUEs experience a high interference in the shared spectrum due to their vicinity of the coverage of the other tiers, they are moved to the dedicated band (see Figure 3.2 c). This approach is referred to as "hybrid assignment" in LTE system [49] [50].

Note that in practical systems, operators usually exploit a single frequency band to be used among tiers and in this case the shared spectrum solution is the most effective approach to adopt in terms of spectral efficiency.

Therefore, in this thesis we focuses exclusively on the mitigation of the cross-tier interference in a shared spectrum deployment.

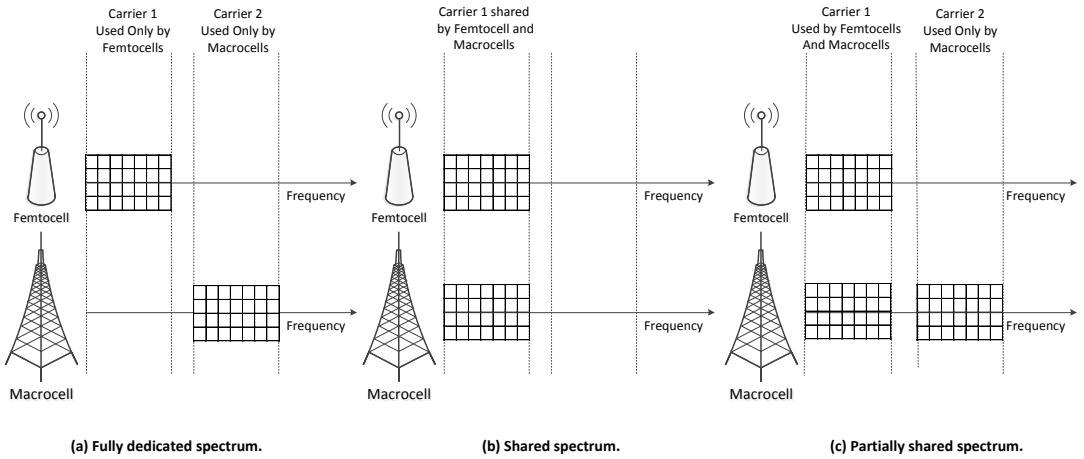

Figure 3.2: Assignment of carrier frequencies

3.3.1.2 Femtocell Access Modes and Interference

In this section, we discuss the different available access modes of femtocells and their competition with the interference issue. A femtocell can operate in one of the three access methods called open, closed and hybrid access modes. Each mode has its own cons and pros as described below.

- **Interference in closed access femtocells**: when a femtocell operates in a closed access mode [51] [52], the non-subscriber users cannot be served by the femtocell, even if they show a stronger received signal. Hence, in this mode a strong interference is generated between the transmitters at both tiers i.e. macrocell and femtocell users. For example, in the DL direction, when a non-subscriber user is passing close to a femtocell base station, the transmitted signal from femtocell could damage the communication especially if the received signal from the serving MBS is weak due to the path-loss between the source and destination. Alternatively, in the UL direction, the nonsubscriber user in the vicinity of the femtocell could also jam the communication between the subscriber user and it's serving FBS [49]. Figure 3.3 illustrates an example of a closed femtocell deployment and generated interference on both DL and UL directions.

The work presented in this thesis (chapters 4 and 5) focuses mainly on closed access mode femtocells, in which access permission is granted exclusively to CSG users.

- **Interference in open access femtocells**: when a femtocell operates in an open access mode [51], all mobile users (subscribers or non-subscribers) have an authorized access. In this scenario, each mobile user is served by the cell (macrocell or femtocell) that provides the strongest signal quality. As a result, the interference problem between cross-tier is reduced and the network throughput is enhanced [49]. However, the big challenge of open access femtocell deployment is the increasing number of handovers between

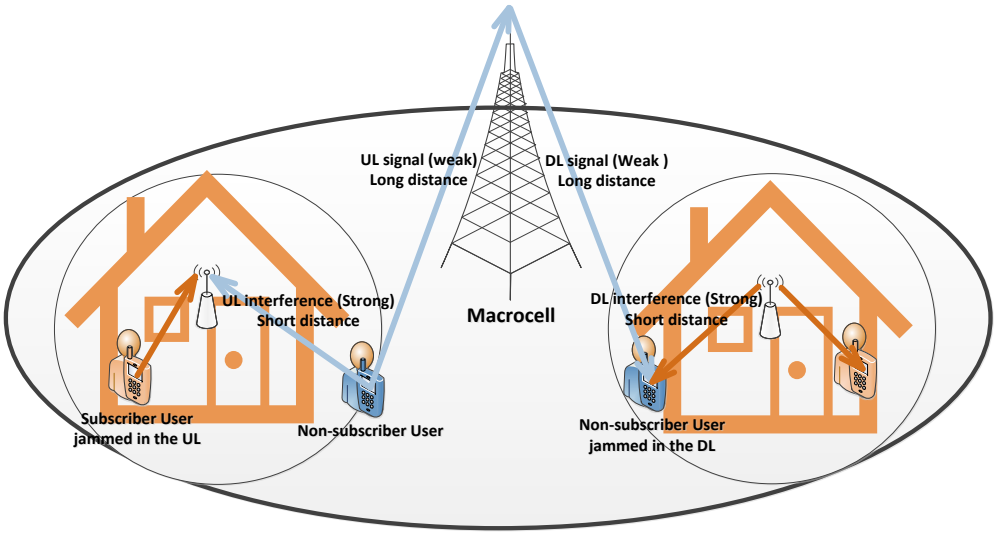

Figure 3.3: Interference in closed access femtocells

tiers [51]. The main characteristics and differences between open and close access modes are summarized in Table 3.1. We can conclude that the open access mode mitigates the cross-tier interference but increases the number of handovers, while open access femtocells are more appealing to users for a both throughput experience at the expense of an increased cross-tier interference (see Figure 3.4) [49].

- **Interference in hybrid access femtocells**: in order to cope with the disadvantages of both open and closed access modes, the hybrid access scheme is proposed as a combination of both of them. Here, a femtocell does not provide service to only its subscriber users but also to non-subscriber users. Moreover, hybrid access femtocells have the capability to deal with the cross-tier interference problem by giving access to an interfered non-subscriber user within a limited QoS and low priority [53][54]. Nevertheless, this scheme similarly to open access mode increases the probability of handover failures which affects the performance of non-subscriber users.

In order to analyze the open and closed access modes performances as regards to the interference issue, a comparative study was developed in [55]. In [56] the capacity of a macrocell in an environment where a number of femtocells are integrated in its umbrella was derived. The authors in [57] investigated the impact of cross-tier interference involved in a scenario where several macrocells and femtocells co-exist together. These studies proved that the closed access mode decreases significantly the performance of the macrocell tier especially when the transmission power of femtocells is not adequately adapted to mitigate the interference [54].

3.3.1.3 Taxonomy of Macrocell-Femtocells IM techniques

So far, many research works have addressed the cross-tier interference issue in macro/femtocell systems. We organized, in the following, the different works into

Table 3.1: Open and Closed access modes comparison

Open access femtocells	**Closed access femtocells**
More handovers and lower interference	Higher interference and low handover rate
Serving indoor and outdoor Users	Serving only subscriber users
Shopping malls, offices	Home, professional
Security issues	Easier billing
Higher network throughput	Lower network throughput

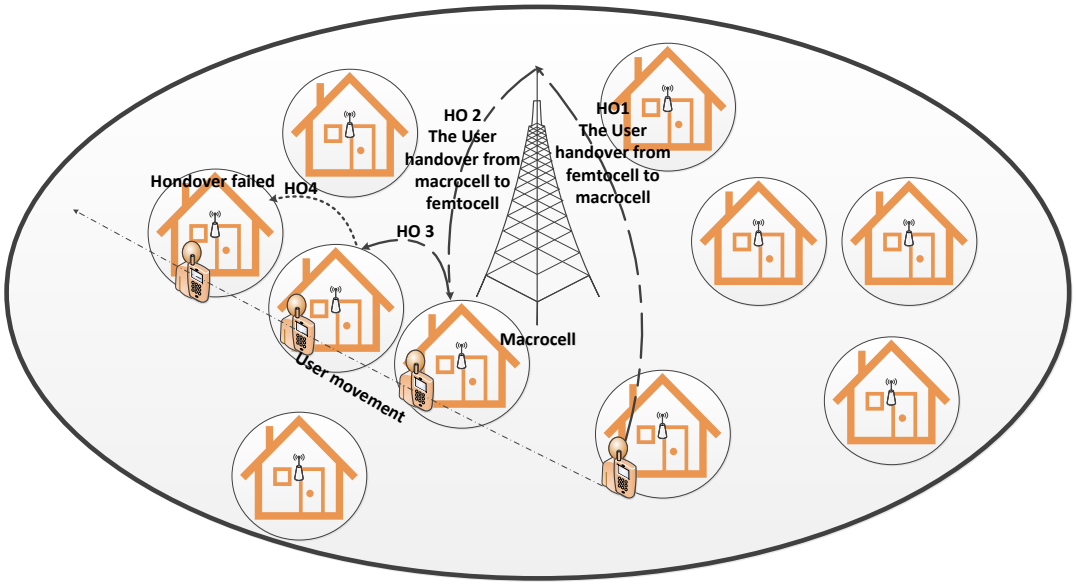

Figure 3.4: Open access femtocells scenario

categories according to their similarity in the adopted methodology for tackling the interference problem.

A) Distributed IM using power management in non OFDMA based system

Self-organization techniques play a great role in the deployment of femtocells especially when dealing with the power-based interference mitigation approaches. To alleviate the interference impact, the femtocell tunes its transmission power dynamically according to the changing conditions of the environment like the passing non-subscriber users in its vicinity, and the presence of interfering neighboring cells, etc. Generally, such power self-organized femtocells are deployed inside household shapes, by this way they reduce the interference on outdoor users who are passing close to their border area and minimize the number of handover attempts with macrocells. Many solutions proposed in the literature belong to this self-organization category [58-62].

In [58], an auto-configuration power control scheme for 3G UMTS is proposed. The scheme uses the pilot signals from femtocells in order to limit their cell range

and DL interference caused to the macrocell user. Each femtocell sets its transmitted power equal or less than the estimated power from the closest macrocell user. A theoretical throughput analysis is provided and the pilot power calculation is evaluated using system level simulations.

The authors in [59] presented a transmit power calibration technique in which femtocells use feedback reports from both macrocell and femtocell users, in order to calibrate femtocell DL and beacon transmit power such that a tradeoff between the good coverage and interference is achieved. To do so, femtocells use a Network Listening (NL) capability that allows monitoring the surrounding residential femtocell signals.

A self-organization coverage adaptation for femtocells was presented in [60]. The coverage adaptation scheme uses information on mobility behavior of the indoor and outdoor users. Upon getting such information, each femtocell sets its transmit power such it reduces the number of outdoor users attempts to connect to it.

In [61], the authors introduced two dynamic femtocell pilot adjustment algorithms that propose a tradeoff between femtocell coverage and interference by exploiting both spatial and temporal information. In this solution, the femtocells allow information exchange among neighboring femtocells, like the outage probability of their users and the local radio environment, in order to decrease or increase pilot powers. Note that the signaling exchange needs inter-tier cooperation across the core network.

The femtocell performance optimization problem under buildings coverage constraints and the interference with regards to outdoor users was considered in [62]. The authors aimed to maximize the capacity of the target indoor users and cells capacity by maximizing the total sum of femtocells transmit power.

Discussion These studies showed that the cross-tier interference can be mitigated using power management. However, those approaches often lead to insufficient indoor coverage, due to the fact that the femtocell base stations have only one omnidirectional antenna which is not located necessarily right in the best coverage location of the household. This causes in some situations coverage holes inside user premises. In order to resolve this issue, FBSs can be installed with multiple antennas. However, 3G multiple antennas equipments were not successfully commercialized due to the equipment size, price and complexity constraints.

B) Distributed IM using power and/or resource management in OFDMA based system

Recent contributions for interference mitigating proposed distributed power control and/or resource management technique for 4G OFDMA-based femtocells. Here, the key concept is to allocate dynamically different users with different transmit powers to the sub-channels by exploiting channel variation in both frequency and time domains [63]. Thus the interference mitigation can be handled not only by the overall power or antenna diversity but also by advanced OFDMA sub-channel allocation. Consequently, the disadvantage of coverage power control and multiple antennas installation can be overcome.

The DL power control issue in decentralized OFDMA networks was addressed in [64] where the main objective was to minimize the overall transmission power in the network. The authors proved that the optimal solution requires global link information through coordinator between the different tier-cells. In addition, it is also shown that the proposed distributed power allocation algorithm based on local information close to the global optimum derived by a centralized DL power controller.

Distributed Q-learning algorithms were analyzed for two-tier macrocell and femtocell systems in [65, 66, 67, 68]. Here, femtocells continuously interact with their local environment in a decentralized manner through trails and errors, and gradually adapt the channel selection strategy until reaching convergence, while mitigating their interference towards the MBSs. Nevertheless, for a better performance further improvements of the learning algorithms by means of global information exchange might be needed among and between tiers.

The Broadband evolved Femtocell (BeFEMTO) [69] [70] project addressed the cross-tier interference and developed advanced femtocell technologies for LTE-advanced system. It aimed at enabling a cost effective provisioning of ubiquitous broadband services based on self-organizing femtocell networks, and evaluating optimized solutions limiting the interference impact on MUEs. In interference mitigation technique in which femtocells self-configure their maximum DL transmit power was integrated to the REM. In order to do so, femtocells have to monitor the RSRP performed by the MUEs before adjusting their transmit power [71].

In [72], decentralized power allocation approaches are proposed under the assumption of limited MUE channel information. In the neighbour-friendly scheme, FBSs allocate the total adjusted power on sub-channels in order to maintain targeted FUEs' sum-rates while mitigating the interference on MUEs. However, some assumptions about channel stability over several frames may not be valid especially in mobility scenarios.

In [73], the authors proposed decentralized strategies for OFDMA femtocell systems based on the Game Theory (GT) approach. A non-cooperative scheme handles the interference generated by each FBS towards other FBSs as well as to macrocell users. In particular, different FBSs compete against each other to find out the optimal resource allocation under the constraint of inducing a limited interference to macrocell users. Nevertheless, the approach shows some limitations especially in the case of exact channel quality knowledge, which leads to a resource allocation that degrades macrocell users' performance.

Both distributed and centralized interference mitigation methods are proposed in [74]. The key idea of the proposed scheme is that the femtocells should avoid using the same frequency resources during the UL and DL scheduling time. This is accomplished using the sensing process performed independently by the femtocells and the centralized scheduling scheme carried out by the MBS. The performance showed that the centralized scheduling method performs better than the distributed one in term of system throughput.

In [75], two self-organization approaches for OFDMA-based femtocells are presented, in which the femtocell is able to sense the air interface and dynamically tune its sub-channels allocation in order to reduce inter-cell interference and enhance

the system capacity. In the considered sensing phase, the technique uses either the exchanged messages by femtocells or measurement reports sent periodically by the femtocell users. In the tuning phase, the scheme provides the best sub-channel assignment which minimizes system interference and maximizes network performance. However, the effect of message broadcasting and network listening mode should be further analyzed in order to find the throughput consumption needed from the network capacity systems.

In [76] and [77], a framework on a joint spectrum assignment and transmission power optimization for OFDMA-based femtocells is presented. Femtocells perform the spectrum assignment and power adaptation based on users' reported measurements, which sense the interference from macrocell and other neighboring femtocells. Despite the enhanced performance, the obtained gain of this framework was not compared with other centralized schemes.

Discussion As presented above, distributed IM techniques for OFDMA systems achieve the interference mitigation goal through frequency domain allocation and/or FS transmit power adjustments. Distributed have the advantage of the self-organization feature which suits perfectly the non-operated femtocells deployment. Nevertheless, these approaches show some limitations as they usually assume limited channel knowledge for macrocell users or channels stability in all subcarriers over several frames. Other works proposed some sub-optimal solutions at the expense of intense global information exchange between neighboring femtocells. Finally, the optimal solutions are usually obtained for simple scenarios (single carrier, fixed SNR, no mobility, etc.).

C) Centralized/MBS-assisted IM using power and/or resource management in OFDMA based systems

The centralized approaches rely on a central entity and a global knowledge of the parameters related to the different link gains whose transmission may induce extensive signaling and generate long delays. Another category of the interference mitigation solutions are MBS-assisted approach which propose to take benefit of the centralized architecture of cellular networks to propose more optimized approaches schemes through the possibility of signaling exchange between the different tiers. This technique assumes that the MBSs, usually referred to as cells coordinators, or their users assist femtocells to their power control or resource allocations. This is to say that the interfering femtocells have perfect channel knowledge of their own users, as well as the non-CSG users in their vicinity. Thus, the signaling exchange is mandatory to enable efficient resource adaptations to such dynamic context.

Recently, several techniques have been introduced as coordinated power and/or resource allocations [78-84]. In [78], MUEs assist femtocells power control scheme to keep the interference caused by femtocells as low as possible. They report the RSRP with the corresponding cell's physical cell identity and CQI message to the macrocell. Thereafter, the macrocell identifies the interfering (aggressive) femtocells and sends them an interference message through its interfered MUEs by the uplink (UL) direction. However, involving the MUEs in signaling messages relaying MUEs would decrease the capacity of the network especially in high dynamic scenarios

with high number of interfering femtocells and varying interference conditions. Not to mention the necessity to implement the functional compares in the terminals to enable the relaying capability.

The authors in [79] showed that the use of Radio Environment Maps (REM) information facilitates and increases the efficiency of practical power control mechanisms of femtocells. Moreover, the study proved that under unknown shadowing terms, the use of statistical information retrieved from the REM database leads to almost similar performance as the ideal case.

DL power allocation methods are proposed in [80] and [81], where no control information exchange is assumed between the MBS and FBSs. Instead, each FBS predicts the RB allocation to its close-by MUEs based on their overheard CSI (Channel State Indicator) feedback from MUEs to MBS. Based on this MUE allocation prediction, each FBS can perform resource allocation to FUEs while mitigating interference towards close-by MUEs. However, interference mitigation among FBSs is not considered.

In [82], the authors develop a stochastic geometry scheme for two-tier cellular systems. They showed that the throughput degradation of the macrocell can be mitigated owing to the opportunistic collaborative channel knowledge exchange for both UL and DL directions between the two tiers of the network. But to obtain such performance gain, the MBS need to be fully informed about the channel gains, and this requires a huge amount of feedback signaling through backhauling.

The hybrid spectrum sharing is investigated in the DL direction for the mixed macrocell and femtocells deployment in [83]. Here, femtocells deployed within the macrocell coverage are differentiated into inner and outer femtocells, where they operate in dedicated and shared spectrum frequency allocations, respectively. Femtocells can flexibly select one favorable mode to achieve higher capacity according to the relevant spatial condition, i.e., the relative location of FBS regarding to MBS. More specifically, the authors used the estimated RSRP (called P_r in LTE network) at femtocell or FUEs and compared it to P_{th} (corresponds to a pilot power threshold) in order to indicate whether the femtocell is located in the inner or outer zone. In addition, besides interference minimization the authors also focused on the signaling overhead reductions.

In [84], an Intra-cell Handover (IHO) approach is proposed. In this method, MUEs or FUEs have the capability to be transferred from one sub-channel to another in case of interference or fading, if a free or a better sub-channel is available in their serving cell. A second scheme is proposed as a centralized downlink power control procedure executed by the MBS, which uses the RSS to measure the interference. This scheme helps in alleviating the interference, but its major limitation is the generated signaling overhead since each sub-frame allocation should integrate a new command to every interfering femtocell. Besides, the interfering femtocell should have a good knowledge about the DL sub-channels used by the MUEs.

Discussion The analysis of these techniques showed that pure centralized approaches are unfeasible in such dynamic scenario while coordinated MBS-assisted IM approaches have the potential to significantly optimize network performance. They may outperform the distributed approaches as they take benefit from the

MBSs assistance. However in this context, the number of exchanged messages and their size should be reduced as much as possible to limit the overhead. In addition, almost all these solutions to enhance macrocell users performance priority to the detriment of femtocell users. However maintaining an acceptable QoS for femtocell users should be taken into account too to avoid them severe service degradation. In order to clarify all the above studied approaches (homogenous and heterogeneous networks solutions), figure 3.5 illustrate a classification diagram of interference categories in LTE/LTE-A networks.

This thesis proposes a MBS-assistance IM approach using for dynamic power control. A MBS instructs femtocells to minimize their transmit power on certain RBs, in order to decrease inter-cell interference to victim cell-edge users (non-CSG users), while meeting a high QoS for femtocell users.

3.3.2 IM in two-tier Macro-Picocells context

The interference mitigation problem generated in a scenario where the macro and picocells co-exist is different from the one presented in macro and femtocells context. This is mainly due to the open access nature of picocells' deployment as they are managed by the network operator. As a consequence unlike the closed access mode femtocells, picocells can always handle the macrocell users. Hence, the mobile terminals are always associated with the cell offering higher quality of RSRP. Nevertheless, the user association with the highest RSRP might not always be desirable due to the following reasons:

Load-balancing: As the range of picocell area is much smaller than the one of macrocell and due to the mobility behavior of most mobile users, the number of mobile terminals served by the PBSs is much smaller than the MBS users' number. Consequently, the amount of traffic in the picocell may be changing very often, leading to an unbalanced load among different tiers.

Mobility-consideration: As in any other open access small cell, the mobile users served by the picocell experience the interference from either macrocells and/or neighboring picocells. Moreover, the users' mobility behavior may make them change very often their served cell, or the undesired strength signal is detected where the Radio Link Failure (RLF) procedure is declared and the mobile user desires to re-initiate to the strongest RSRP cell. Consequently, the number of handover procedures is expected to increase compared to the homogenous networks scenario.

In order to improve significantly the system performance by taking advantage of the picocells spectrum, a user may be better served by the PBS even if it is receiving a weaker signal power than the one received from the MBS. Additionally, in order to reduce the number of failed handovers, LTE-A system has proposed a technique called Cell Range Expansion (CRE) in which a bias value is added to the picocell RSRP during the handover operation [85] [86]. Consequently, the CRE technique could make more mobile users benefiting from the picocell capacity, mitigate significantly the cross-tier interference in the UL direction, and enhance the offloading capacity of macrocell users. However, these advantages come at the expense of a

reduced DL signal quality to those users in the CRE region. Moreover, due to the high difference in transmit power, the DL signal from a PBS in the CRE region is much smaller compared to the received from the MBS. Hence, those PUEs passing through the expanded region will experience a strong interference situation. Therefore, whenever CRE is used, an enhanced Inter-Cell Interference Coordination (e-ICIC) technique between macro and picocells may be required to mitigate the DL interference. There are some issues to be considered by the e-ICIC techniques as follows:

- Decreasing the DL interference received from the macrocells without extremely degrading the QoS offered to their served users,
- The deployment of an e-ICIC process should not be complex and iterative, and its parameters should be dynamically adapted according to the network dynamics (for example, number of offloaded users to picocells, number of users located in the CRE region, types of application used by the users at macro or picocell, and users mobility in both tiers, etc.),
- Finally, the e-ICIC technique should confine the backhaul signaling messages needed for the coordination proposes.

The work presented in this thesis (chapter 6) focuses on open access picocells which gives access permission to all users. In addition, we deal with the mitigation of the cross-tier interference generated by a shared spectrum band (co-channel assignment).

3.3.2.1 Taxonomy of Macrocell-Picocells IM techniques

In a HetNet where picocells are deployed as an under laid-layer, the DL interference caused by macrocells might be mitigated through the use of interference cancellation techniques at individual mobile terminals or alternatively collaborative IM solutions. Adaptive or fixed resource partitioning is an effective solution for interference mitigation. Adaptive e-ICIC schemes provide smart assignment of resource spectrum in time, frequency and space domains among interfering cells. Recently, many dynamic e-ICIC techniques for IM have been developed. They can be grouped into two categories:

- **Time domain and joint time-power control techniques:** the main principle of time-domain solutions is that the macrocell gives up a portion of its resource spectrum during a certain time of each sub-frame reducing the amount of interference to the underlying picocells. In LTE-A, this process is called Almost Blank Sub-frames (ABSs) mechanism. In addition, the jointly coordinated time domain with the power transmit control is also an attractive way for interference mitigation. Thus the interference is mitigated not only by the ABSs scheme but also within the DL transmitted power.
- **Frequency domain and joint frequency-power control techniques:** the principle of frequency domain techniques is that the macrocell mutes some of its OFDMA RBs, and grant them to the picocells to serve their users without being interfered. Like time domain, the frequency muting schemes may be

also considered also within the overall power control. Note that, a simple beamforming power control techniques from the interfered MBSs can improve the SINR of picocell users but cannot fully mitigate such severe interference. Thus, the sole power allocation schemes have not been considered in the macro-picocells context.

In e-ICIC approaches, the time and frequency domain techniques are implemented by the MBS which then announce the allocation instructions to the neighboring (or underlying) picocells. Whereas, the power control is applied by either MBS or PBS through transmitted power adjustments or adaptive biased values.

Time and joint time-power solutions

A Cell Selection Offset (CSO) scheme based on the expected user data rate was proposed in [87]. The authors showed that the impact of ABS ratio is more important than the bias value in terms of average user data rate. Thus, a mobile user prefers to be served by the macrocell regardless the picocell' value bias as it was proved that the users had more chance to be scheduled by the macrocell rather than the picocell base station. However, considering the ABS ratio for the cell selection process would increase the number of handovers for a mobile terminal. The ABS and non-ABS frames is issued every TTI which means that the handover demand is fluctuating every sub-frame, which will highly impact the user's data delivery.

The impact of a dynamic picocell range expansion value was considered in [88]. In the proposed scheme, the picocell adapts the size of its region boundary depending on the average logarithmic throughput rate of the MUEs. Moreover, the average throughput rate of each mobile user was chosen to be the metric for changing the cell selection bias value. It was shown that the unitization of time based e-ICIC scheme through the ABS mode offers significant gain for picocell users. Obviously, the ABS mode technique reduces the macrocell capacity. In addition, the implementation of such model in the picocells requires to know the throughput information of the overlaying macrocell users. Particularly, this would impose sharp synchronizations between the MBS and its underlying PBSs.

Frequency and joint frequency-power solutions

The adaptive resource partitioning based on load balancing among macro and picocells is seen as an effective approach for IM in co-channel deployments. Resource partitioning configuration allows the avoidance of interference by switching off some resources, enabling the UEs in the CRE region to receive data more efficiently, as they are scheduled in those protected resources. To do so, a macrocell informs the picocell which resources in a sub-frame will be scheduled to the MUEs and which resources would be protected for picocell users. Such information exchange is enabled through the coordination management introduced in LTE Rel-10 via the X2 interface backhaul.

Several models have been proposed to define the *Muting Ratio*, the amount of resources which might be protected by the macrocell. In [89], the authors proposed a model in which the muting ratio depends on the number of picocell users suffering

from strong interference when the picocell biasing is applied. The *Muting Ratio* β of MBS M is expressed as follows

$$\beta = \frac{|\mathcal{N}_l|}{|N_I|} \tag{3.1}$$

where $\mathcal{N}_l$ is the set of PUEs in the CRE region of picocell P_l, and N_I is the set of MUEs served by macrocell M.

Another approach was proposed in [90], in which a part of the licensed shared resources are reserved for PUEs operation. The basic concept of the proposed method is very close to the work in [89], except for the partition strategy which is expressed as

$$\beta = \frac{|\mathcal{N}_l|}{|\mathfrak{N}_l|} \tag{3.2}$$

where $\mathfrak{N}_l$ is the set of all PUEs in P_l including $\mathcal{N}_l$. The authors showed that the scheme provides better cell edge throughput gain compared to [89].

Another frequency approach was proposed in [91]. The main difference of the proposed model compared to [89] and [91] is that the e-ICIC scheme between macro and picocells includes both frequency partitioning and power-resource coordination. The proposed frequency-power arrangement divided the available frequency in each cell into two distinct sub-bands in every cell, one is named Normal Band (NB), and the other is termed as Platinum Band (PB). In each picocell, both normal and platinum bands are exploited with the maximum transmission power level. While in the macrocell only the normal band is used with the maximum power level. The frequency partition scheme defines β as a function of the number of cell-edge PUEs and the total number of users (including PUEs and MUEs)

$$\beta = \frac{|\mathcal{N}_l|}{|N_{total}|} \tag{3.3}$$

where N_{total} is equal to $N_I \cup \mathfrak{N}_l$ sets.

A decentralized procedure for joint interference management and cell association inspired from Reinforcement Learning (RL) was proposed in [92]. The authors developed a joint time-power e-ICIC technique in which picocells learn their cell range bias and DL transmit power allocation. This method outperforms the classical resource partition schemes such as [89] in terms of throughput. However, the proposed dynamic Q-learning algorithm should be evaluated in terms of time processing and complexity.

The work in [93] proposed a scheme to determine UEs bias values using a Q-learning algorithm, in which each UE learns independently from its past experience its bias value that minimizes the number of outage UEs. It was shown that the Q-learning approach can perform better than no learning schemes. It improved the average throughput at almost all ratios of RBs and enhances the cell-edge UE spectral efficiency compared to the schemes using a common bias value. In addition, the authors showed that UEs can keep having the Q-table data when they move to another PBS coverage area, this helps the learning algorithm to converge faster. However, as for the previous work [92], the required learning time should be deeply investigated since long convergence time would make the approach infeasible for real-time systems.

In [94], the authors proposed an analytical model to study the relation between UEs aggregate spectral efficiency and some parameters, such as the CSO value,

relative densities, and the duty cycle[1]. In the developed study, investigations about optimal values of CSO were limited to the selected simulation scenarios due to the difficulty of modeling such systems analytically. The authors showed that the throughput is higher when a PUE is scheduled using the protected resources blocks rather than non-protected resources. However, scheduling all PUEs in the CRE region using the protected RB is not necessarily optimal as the received signal varies from one PUE to another because of the channel diversity.

Discussion The above detailed works proposed various e-ICIC schemes adapted to picocells range expansion paradigm. Although, these time, frequency, and joint power control approaches can mitigate the interference, this is done at the expense of a decreased capacity. There are still several challenges that come into play and which have not been considered yet, for example the mobility of users, the user's application type, number of resources blocks required by the application, QoS requirements like packet size, minimum data rate, etc.

Additionally, scheduling restriction involves a negative performance if the channel quality between resources (protected and non-protected) are not exploited individually for each user. For every individual user in the picocell area, the SINR is higher when it is scheduled in the protected resource. However, scheduling all CRE users in protected resources may not necessarily preferred since the throughput difference between resources varies from a user to another. If a macrocell interference signal for specific resources sufficiently weakened before it reaches to a picocell user, the difference between the protected or non-protected resources for a CRE user is the same or very small, thus those resources can be allocated to CRE users. On the other hand, if macrocell interference is strong, scheduling a CRE user in the non-protected resource introduces large throughput loss. Hence, simply swapping the CRE user' non-protected to protected RB would be necessary and significantly improve the network performance especially for the CRE users. Finally, we can conclude that the scheduling restriction has negative impacts on network capacity which can be summarized as:

- Firstly, it leads to the reduction of user diversity gain since the scheduling in each resource is restricted to a subset of users instead of the set of entire users.
- Secondly, the gain from each time and frequency diversity is reduced due to the loss of freedom in allocating the time (frequency) resources other than those allowed by the restriction. Such performance loss should be minimized.

This thesis proposes a new dynamic and mobility-aware frequency partitioning approach in macro-picocells deployments. The proposed e-ICIC scheme decreases the interference on cell-edge users (PUEs in CRE region) while providing high throughput to macrocell users. Furthermore, the scheduling restriction of PUEs on protected resources is relaxed to better benefit from the frequency diversity.

[1]The duty cycle is a repeating on/off pattern which defines how often the pattern repeats (usually in milliseconds) while the duty cycle value is the fraction of the period that the transmission is turned on. Currently, 3GGP proposes blank sub-frame duty cycles of 1/8, 2/8, 3/8, and 3/20 [95].

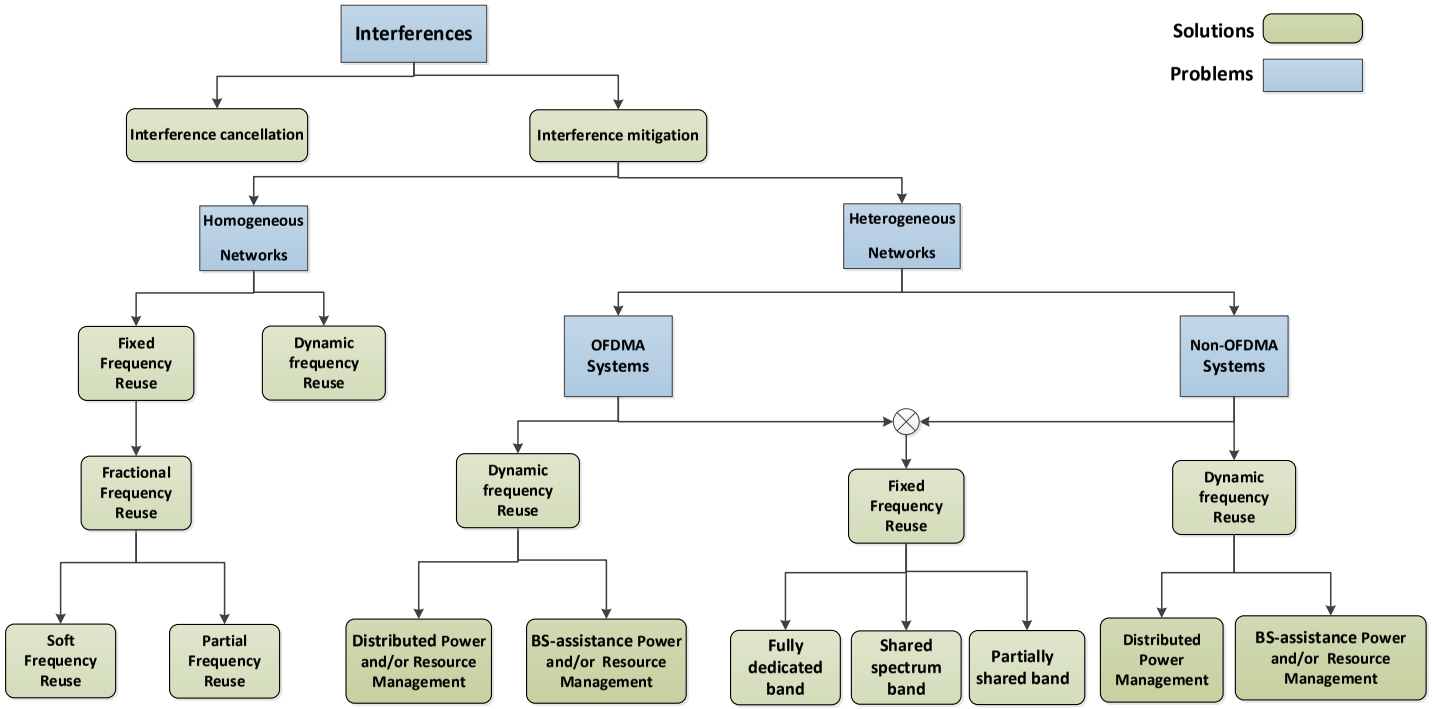

Figure 3.5: Main developments of selective interference avoidance for LTE/LTE-A networks

3.4 Conclusion

In this chapter, we presented a review of some reference solutions proposed for interference avoidance issue, and more particularly those focusing on interference mitigation. Our analysis showed that the interference issue is addressed differently depending on the considered two-tier deployment scenario (macro-picocell or macro-femtocell). Therefore, we will study this interference issue by considering both scenarios. In the macrocell-femtocell case, our study showed that full centralized IM approaches which rely on a central entity and a global knowledge of the different link gains whose transmission may induce extensive signaling and generate long delays. Whereas, the distributed approaches have the advantage of the auto-organization but need high coordination to attain optimal performance under realistic assumptions (mobility, etc.). Therefore, we are interested in the MBS-assisted approach in which the MBS supports the FBSs in making their resource usage decisions using some global and local information and/or the reported measurements from MUEs/-FUEs.

In the macrocell-picocell case, we will make use of context-information on users' locations and mobility to mitigate the interference on victim users under cell range expansion assumption In the following chapters, we will details our proposed schemes for interference mitigation for both scenarios.

Part I

Macrocell and Femtocells

Chapter 4

Interference Mitigation in Mobile Environment through Power Adjustment

4.1 Introduction

LTE introduced the use of femtocells beside the classical macrocells due to their low cost, low power-consuming access points that use the licensed spectrum and their ability to enhance the indoor coverage through simple deployment inside residences. Femtocells are usually connected to the network operator's MBSs through a backhaul connection. In one hand, these small indoor devices can offer within their small coverage area a high spectral efficiency in terms of throughput to their UEs, as these users enjoy better signal quality due to the proximity between transmitter and receiver. On the other hand, this technology offers a capacity offload to MUEs as it helps them to achieve higher throughput. In case of co-channel deployment of MBSs and FBSs which has been proved more performant than the orthogonal one [17], the cross-tier interference from the transmitting FBS can cause significant damage to MUEs performance, especially when the MUEs are passing very close to the coverage area of the interfering FBS. This type of interference is the key issue for an effective FBS deployment and an integrated MBS/FBS coexistence.

In this chapter, we mainly focus on BS-assisted methods for power allocation which exploit the RRC signaling messages like the RSS. Moreover, cross-tier interference is described as the undesired signal received at a femtocell because of the simultaneous transmissions of surrounding macrocells and vice versa. The term cross-tier indicates that macrocells and femtocells belong to a different tier. Moreover, the DL cross-tier interference occurs when a given macrocell user is located in an area where the signal coming from its own MBS is not large enough with respect to the sum of the interference coming from its neighboring FBSs. Cross-tier interference may be specially significant in CSG-femtocell deployments, because macrocell users may not be allowed to connect to nearby femtocells at shorter path losses than their macrocells due to connectivity rights. Thus, a severe DL interference from femtocells should be controlled by the MBS to increase the performance requirement of macrocell users.

In particular, we propose a power control mechanism in a mobile environment which key benefits are to achieve higher performance for non-CSG users, as well as avoiding potential service degradation to femtocell users by taking into account mobile users locations and SINR at both macro and femtocell sides. Furthermore, by adjusting adequately the FBSs transmit power we aim to give the priority to MUEs while maintaining the communication quality of FUEs. For that purpose, our mechanism takes into consideration the number of affected FUEs, i.e. those who experience a channel quality under a minimum target SINR due to the power adjustment strategy. Note that the channel quality of FUEs does not depend only on the interfering MUEs and the new FBS transmission power, but also on their respective positions and mobility within their coverage area. In our proposal, we propose allowing the FBS to return back an "*Objection*" report to the MBS in case the requested power adjustment is significantly impairing the performance of a large number of its users.

Moreover, to alleviate the signaling exchange between the macro and femtocells, we propose an algorithm at the network side to decrease the signaling overload caused by the proposed BS-assisted power control scheme. The proposed signaling mechanism generates RSS Measurement Reports (MRs) only if a significant change in the received signal values is observed. To do so, the MBS needs to track the last values of the received RSSs while on the FBSs side the same power allocation is maintained until a new explicit RSS MR is received.

The remainder of this chapter is organized as follows. Section 4.2 describes the system model and the main assumptions. Details of the proposed scheme are presented in Section 4.3. In section 4.4 the cooperative macrocell/femtocell signaling strategy is explained and in Section 4.5 the simulation environment and results are presented. Finally, Section 4.6 concludes the chapter.

4.2 System Model and Assumption

We consider a macrocell/femtocell overlay system in which L femtocells are geographically positioned in streets located at the edge of the coverage area of one MBS referred as M (see Figure 4.1). We assume that I MUEs are uniformly distributed within the MBS coverage area and are not allowed to access a neighboring femtocell F_l, $(l = 1, ..., L)$ when they approach its coverage area. In other words, all the outdoor users are considered non-CSG users for F_l's operator. Each F_l serves J FUEs uniformly distributed in its coverage area. The transmissions are OFDMA-based and all MUEs and FUEs share the same frequency band divided in K RBs. We also assume that MBS M is fully loaded and cannot execute any intra-channel allocation to mitigate the potential interference caused to MUEs. To perform the resource allocation of their RBs, both MBS and FBSs require their UEs to periodically report their signal quality expressed by the CQI in terms of SINR. The received DL SINR of a MUE_i associated with MBS M on RB k $(k = 1, ..., K)$ can be expressed as

$$SINR^k_{M,MUE_i} = \frac{\frac{p^k_M}{PL_{M,MUE_i}} |G^k_{M,MUE_i}|^2}{\sum_{F_l \in \mathcal{Z}_{i,k}} \frac{p^k_{F_l}}{PL_{F_l,MUE_i}} |G^k_{F_l,MUE_i}|^2 + N_0}, \tag{4.1}$$

where p_M^k is the current transmit power allocated on RB k by the serving cell MBS M, and $|G_{M,MUE_i}^k|$ is the channel fast fading gain between MBS M and MUE$_i$ on RB k. Similarly, $p_{F_l}^k$ is the transmit power of neighboring femtocell F_l on RB k, while $\mathcal{Z}_{i,k}$ represents the set of all interfering FBSs on user MUE$_i$ on RB k. Similarly, $|G_{F_l,MUE_i}^k|$ is the channel fast fading gain between MUE$_i$ and the neighboring F_l on RB k. PL_{M,MUE_i} and PL_{F_l,MUE_i} represent the pathloss from MUE$_i$'s serving cell MBS M and neighboring F_l respectively, and N_0 is the power of the additive white Gaussian noise.

Similarly, the DL $SINR_{F_l,FUE_j}^k$ of a given FUE$_j$ associated with a femtocell F_l on RB k can be expressed as

$$SINR_{F_l,FUE_j}^k = \frac{\frac{p_{F_l}^k}{PL_{F_l,FUE_j}}|G_{F_l,FUE_j}^k|^2}{N_0 + A_j^k + \sum_{\substack{F_m \in \mathcal{V}_{j,k} \\ m \neq l}} \frac{p_{F_m}^k}{PL_{F_m,FUE_j}}|G_{F_m,FUE_j}^k|^2}, \tag{4.2}$$

where $p_{F_l}^k$ is the current transmit power allocated on RB k by the serving femtocell F_l, and $|G_{F_l,FUE_j}^k|$ is the channel fast fading gain between FUE$_j$ and its serving femtocell F_l. $p_{F_m}^k$ is the transmit power of a neighboring FBS F_m, while $\mathcal{V}_{j,k}$ represents the set of all interfering FBSs on user FUE$_j$ on RB k. $|G_{F_m,FUE_j}^k|$ is the channel fast fading gain between FUE$_j$ and its neighboring FBS F_m. PL_{F_l,FUE_j} stands for the pathloss between FUE$_j$ and FBS F_l while A_j^k is the interference generated by MBS M on resource block k [51], namely

$$A_j^k = \frac{p_M^k}{PL_{M,FUE_j}}|G_{M,FUE_j}^k|^2. \tag{4.3}$$

In this scheme we take benefit from the REM concept as a support to our interference mitigation techniques. The term REM is generally used to refer to a database (local and/or global) which gathers location-dependent information about the environment where the radio system operates [96]. The REM concept is useful to develop optimized resource allocation and eICIC (enhanced Inter-Cell Interference Coordination) solutions that require to capture the evolution of random processes such as the channel quality, user mobility and traffic dynamics. Therefore, we propose in this paper to make use of local REM databases at both MBS and femtocell sides to store local information. More specifically, the MBS REM registers all the RSSs recently fed back by the MUEs to inform about the interference condition caused by the neighboring FBSs on their respective allocated RBs.

For our system model needs, we define the following parameters in the MBS REM table:

- $SINR_{MUE}^{target}$: the predefined SINR requirement threshold of each MUE$_i$ and each allocated RB k. This threshold corresponds to the minimum acceptable channel quality which will trigger the interference mitigation process.

- $SINR_{FUE}^{target}$: the predefined SINR requirement threshold for each FUE$_j$ and each allocated RB k. This value corresponds to the outage situation.

- RSS_{M,MUE_i}^k and RSS_{F_l,MUE_i}^k: the received signal strength by MUE$_i$ from MBS M and FBS F_l on RB k, respectively [97]. They are expressed as

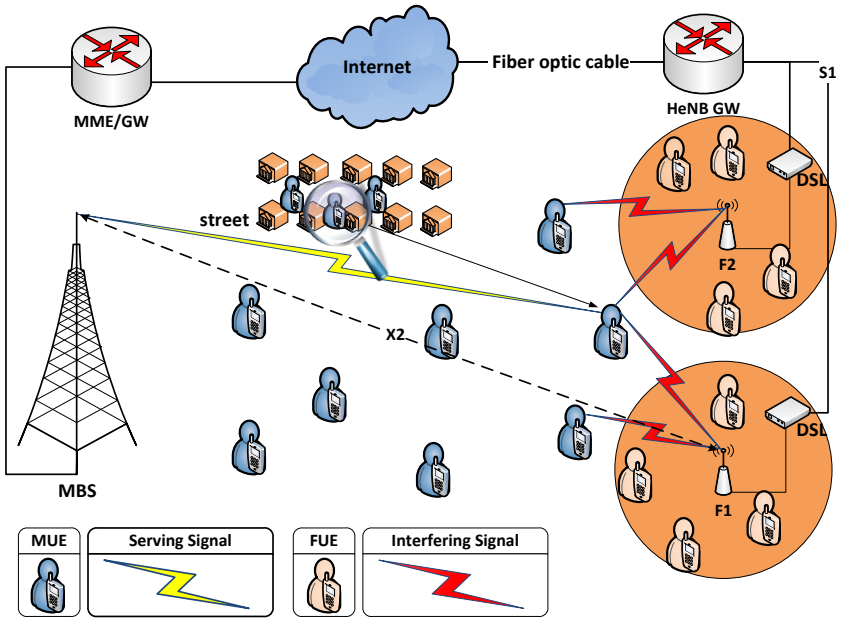

Figure 4.1: Two-tier Macrocell and Femtocell architecture

$$RSS^{k}_{M,MUE_i}=\frac{p^{k}_{M}}{PL_{M,MUE_i}}, \tag{4.4}$$

$$RSS^{k}_{F_l,MUE_i}=\frac{p^{k}_{F_l}}{PL_{F_l,MUE_i}}. \tag{4.5}$$

- $\Delta SINR$: a positive protection margin, expressed in dBs, used together with $SINR^{target}_{MUE}$ to determine if MUE_i experiences a bad serving channel. This is confirmed if the following condition is verified,

  $$SINR^{k}_{M,MUE_i} < SINR^{target}_{MUE}+\Delta SINR. \tag{4.6}$$

- ΔP: a positive power protection margin, measured in dBs and used with the reported $RSS^{k}_{F_l,MUE_i}$ to check whether RSS^{k}_{M,MUE_i} from the serving MBS M is indicating a pending connection loss. This is verified if the following condition is true,

  $$RSS^{k}_{M,MUE_i} < RSS^{k}_{F_l,MUE_i}+\Delta P. \tag{4.7}$$

Note that ΔP and $\Delta SINR$ values should be adequately tuned to avoid a potential oscillatory behavior. For example, if ΔP is too low, MUE_i may suffer too long from the interfering F_l before MBS M initiates the interference mitigation strategy. Inversely, if ΔP is too high, MBS M activates the interference mitigation procedure even if the interference from neighboring F_l is insubstantial, which leads to an increase in the signaling overhead.

- *New-RSS-Table*: is a table continued in the macrocell REM. It records all the *RSSs* newly returned by the MUEs to inform about the interference condition caused by the neighboring FBSs on their respective allocated RBs when conditions (4.6) and (4.7) are fulfilled.

- *Old-RSS-Table*: contains the old values of New-RSS-Table get from previous frames and saved as a data mining in the REM of macrocell M.

4.3 Proposed power adjustment scheme in macro /femtocell mechanism (PAMF)

In this section, we detail our BS-assisted power control scheme for DL interference caused by FBSs to a given mobile MUE_i. The advantage of our scheme is twofold: (i) increasing the spectral efficiency of MUE_i, and (ii) be aware of the negative impact on an interfering F_l while decreasing its radiated power.

Initially, MUEs are randomly positioned within M coverage and each active MUE_i periodically sends to M a MR report including the $SINR^k_{M,MUE_i}$ experienced on each allocated RB. Before performing the resource allocation procedure based on the adopted scheduling strategy, M first checks the quality of the users communication channels based on the returned measurement reports.

If condition (4.6) is fulfilled, M asks the concerned users to send another measurement report in terms of RSS which contains the received pilot signal of the current serving cell and all neighboring cells regardless their types (M or FBSs). The RSS reports help M in identifying the source of interference and checking whether it is caused by neighboring cells or the consequence of another effect such as fast fading or some noise signals. For this purpose, condition (4.7) is checked to determine if the $RSS^k_{F_l,MUE_i}$ of a user MUE_i from neighboring cell F_l is greater than the RSS^k_{M,MUE_i} of the serving cell. If so, M identifies the interfering F_l for victim MUE_i. To keep track of the $RSS^k_{F_l,MUE_i}$ evolution perceived from each interfering FBS, M makes use of the temporary "*New-RSS-Table*" to record the current reported $RSS^k_{F_l,MUE_i}$ values.

To mitigate the generated interference, we propose that M takes power adjustment decisions according to these two steps:

- ***Step1***: Interference detection and power adjustment

Using the *New-RSS-Table*, if M detects more than S victim MUEs, then it instructs all the interfering FBSs to decrease their radiated transmission power. Note that this strategy gives full priority to MUE users. The amount of the new transmission power to apply by each FBS is given here after.

M first computes the Maximum Interference $MI^k_{MUE_i}$ which can be tolerated by an MUE_i victim as follows:

$$MI^k_{MUE_i} = \frac{RSS^k_{M,MUE_i}}{SINR^{target}_{MUE}} - N_0. \tag{4.8}$$

Then, M asks each interfering FBS on the *New-RSS-Table* to decrease its power on RB k from $p^k_{F_l}$ to $p'^k_{F_l}$ according to

$$p'^k_{F_l} = \underbrace{MI^k_{MUE_i} \cdot \frac{RSS^k_{F_l,MUE_i}}{\sum_{l=1}^{L} RSS^k_{F_l,MUE_i}}}_{I^k_{F_l,MUE_i}} \cdot \underbrace{\frac{p^k_{F_l}}{RSS^k_{F_l,MUE_i}}}_{PL^k_{F_l,MUE_i}}, \tag{4.9}$$

where $p^k_{F_l}$ represents the transmitted power of the interfering F_l in RB k and $RSS^k_{F_l,MUE_i}$ the measured received signal strength from F_l by an MUE$_i$ for which RB k has been allocated. Note that the first term of the equation noted $I^k_{F_l,MUE_i}$ represents the maximum interference that F_l is permitted to cause an MUE$_i$, and the second term, referred to as $PL^k_{F_l,MUE_i}$, is the pathloss between them (this information can be derived from "*New-RSS-Table*").

- ***Step2***: FBSs objection

Decreasing blindly the transmission power of an *FBS* may harshly impact the quality of service of its FUE users or even worse cause connections interruptions. To avoid such a situation and offer FUEs some minimum quality, we propose to take into account the number of affected FUEs, noted N_{F_l}, i.e. those which signal quality falls below a minimum tolerance value ($SINR^{target}_{FUE}$). Thus, after applying the adjustment requests sent by M, each interfering F_l checks if the number of its affected FUEs (i.e. those which DL $SINR^k_{F_l,FUE_j}$ is smaller than $SINR^{target}_{FUE}$) is over a certain value N^{TARGET} as follows:

$$N_{F_l} > N^{TARGET}, \tag{4.10}$$

where

$$N_{F_l} = \sum_{j=1}^{J} f(j)$$

$$f(j) = \begin{cases} 1 & if\ (SINR^k_{F_l,FUE_j} < SINR^{target}_{FUE}) \\ 0 & otherwise \end{cases}$$

where N^{TARGET} is a tunable system parameter and represent the maximum tolerable number of affected FUEs.

If condition (4.10) is verified, F_l will create and send back an *Objection* message to the macrocell expressing its declination to the latest power decrease instruction due to a high number of affected FUEs. It is worth to notice at this point, that our power adjustment strategy depends jointly on the number of affected outdoor and indoor users (MUEs and FUEs) which may vary over time depending on users mobility and traffic dynamics.

To describe the operational functions of our power adjustment strategy, we summarize the distinct cases the different stakeholders (MUEs, M and FBSs) can face in the flowchart illustrated in Figure 4.2. In a typical interference scenario, an active mobile MUE$_i$ getting closer to an F_l coverage may endure an important interference which degrades its DL signal quality. This situation is reported to the serving cell M through the RSS reports. Depending on the number of victim MUEs (S), the affected FUEs (N_{F_l}) as well as the presence of a prior *Objection* message, three different cases can be distinguished:

- *Case* 1: Initially, to mitigate the interference of its MUEs and since no *Objection* report has yet been received, M prepares for each victim user a MR type B corresponding to the power decrease instruction (steps from (1) to (12)). On the interfering F_l side, the received power mitigation report is analyzed and executed. At this point, F_l checks the number of type B reports. No *Objection*

is generated by F_l as long as the number of victim MUEs is greater than S even if its FUEs may indicate a service degradation.

- *Case* 2: This case is similar to case 1 except that here the number of MUEs victims is less than S. In this situation, F_l is allowed to emit an *Objection* report to M if there is at least N^{TARGET} of its FUE users that have been affected by the recent power decrease, i.e. those who show an $SINR^k_{F_l,FUE_j}$ smaller than $SINR^{target}_{FUE}$ (condition 4.10). It is worth to notice that an *Objection* report received from an interfering F_l in the current frame is analyzed and the resulting actions will take effect in next frames.

- *Case* 3: When M receives an *Objection* from a given F_l, it avoids restating the power decrease instruction. The major difference of this case is that M monitors the ongoing interference and keeps track of the number of its victim MUEs (verifying equation 4.5). It creates then, for each user, another type of report (type A) and sends it to F_l. At F_l side, type A reports are counted and an *Objection Cancellation* is issued if the number of type A reports is found greater than S.

4.4 Macrocell /femtocell signaling reduction strategy

In our interference mitigation scheme, different signaling messages can be exchanged between M and the underlying FBSs. These messages include RSSs reports, the power adjustment instruction reports (type B), the interference measurement reports (type A) and the *Objection* messages. Type A and B measurement reports are sent each frame (or each in frames, $w \geq 1$) for every victim MUE and for each corresponding allocated resource block as long as the interference situation keeps going. This results in a significant signaling overhead which may consume bandwidth, processing time and energy at both M and FBSs sides. However, in practical scenarios, some victim MUEs may show, for some time period, a fixed mobility behavior and thus experience almost unchanged $SINR^k_{M,MUE_i}$ and RSS^k_{M,MUE_i}/ $RSS^k_{F_l,MUE_i}$ values. To take into account such situations and overcome this signaling overhead issue, we propose a Signaling Overhead Reduction Algorithm (SORA) to be implemented at the macrocell side. In SORA, M keeps track of the evolution of the $RSS^k_{F_l,MUE_i}$ values for each victim user and each corresponding RB k by using two REM tables: *Old-RSS-Table* and *New-RSS-Table*. Every w frames (in our simulations, we set w=1), M compares the $RSS^k_{F_l,MUE_i}$ values, i.e. the latest reported $RSS^k_{F_l,MUE_i}$ and the previous $RSS^k_{F_l,MUE_i}$ stored in *Old-RSS-Table* and decides in case of a negligible change that there is no need to send new power adjustment instructions and MRs type B (see figure 4.2) to the interfering F_l. This, in reality, stands for an implicit report transmission to F_l until a new report with an updated $RSS^k_{F_l,MUE_i}$ value is received. Each w frames, the content of *Old-RSS-Table* is updated using *New-RSS-Table*, whereas *New-RSS-Table* is refreshed with the new reported $RSS^k_{F_l,MUE_i}$ values. Finally, it is worth to notice that the amount of the decreased signaling overhead depends on users radio environment and mobility (see algorithm 4.1).

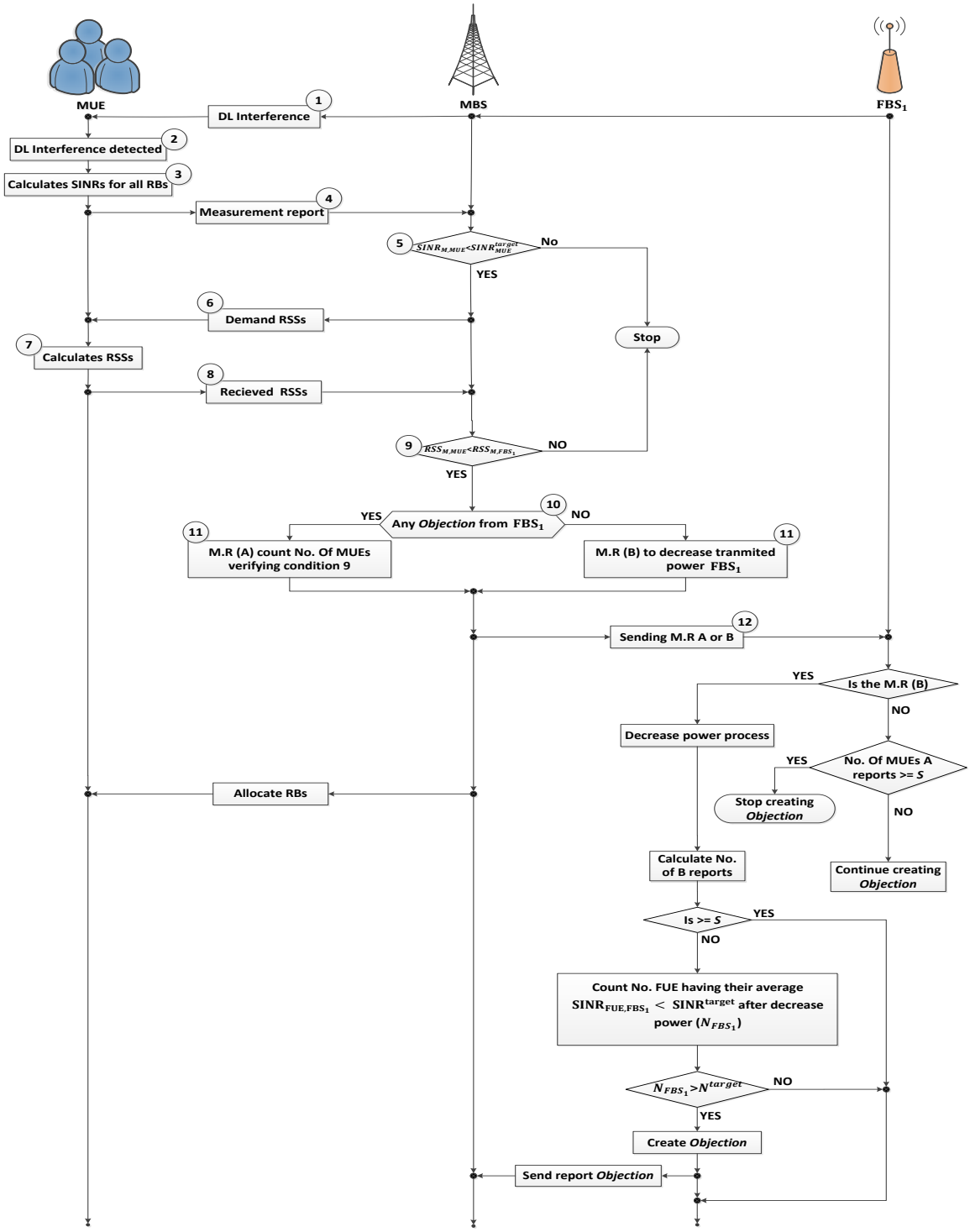

Figure 4.2: Power allocation flow chart

Algorithm 4.1 SORA signaling overhead reduction mechanism

Let U be the set of MUEs of macrocell M,
Let $Z_{i,k}$ be the set of interfering FBSs on user MUE$_i$ on RB k,
Let R_i be the set of RBs allocated to MUE$_i$
Set Old-RSS-Table $=\emptyset$ // set empty, the set of interfering FBSs
Initiate $SINR^{TARGET}$
1: **for all** MUE$_i \in U$ **do**
2: **for all** $k \in R_i$ **do**
3: **if** $SINR^{k}_{M,MUE_i} < SINR^{target}_{MUE}$+$\Delta$SINR **then**
4: **for all** $F_l \in \mathcal{Z}_{i,k}$ **do**
5: **find** $RSS^{k}_{F_l,MUE_i}$
6: **if** $RSS^{k}_{M,MUE_i} < RSS^{k}_{F_l,MUE_i}$+$\Delta P$ **then**
7: **add** $RSS^{k}_{F_l,MUE_i}$ **to** *New-RSS-Table*
8: **end for**
9: **end if**
10: **end for** // *each RB*
11: **for all** $RSS^{k}_{F_l,MUE_i}$ **in** each Table *(new* **and** *old)*
12: **Dif** $\leftarrow(RSS^{k,new}_{F_l,MUE_i} - RSS^{k,old}_{F_l,MUE_i})$
13: **if Dif** $> \epsilon$ **then** *send a new B reports* // where ϵ is a small margin value
14: **end for** // *all* $RSS^{k}_{F_l,MUE_i}$
15: **Update** *Old-RSS-Table*
16: **end for** // *all users in macro.*

4.5 Simulation Analysis

4.5.1 Simulation Model

To investigate the performance of our proposed power allocation and signaling reduction mechanisms, we implemented series of simulations using LTE-Sim simulator [98]. LTE-Sim is an open source framework to simulate LTE-A networks. It encompasses several aspects of LTE-A networks, including both the E-UTRAN and the EPS. It supports several scenarios and environments such as single and multi-cell environments, QoS management, multi users network, user mobility, handover procedures, and frequency reuse techniques. It includes several features allowing both researchers and practitioners to test enhanced techniques for improving 4G cellular networks, such as new physical functionalities, innovative network protocols and architectures, high performance scheduling strategies and so on. In order to implement our scenario, the network topology consists of macrocell M and several neighboring FBSs positioned in a street with a reasonable distance from M (>300m). Each FBS is placed in a building and serves a maximum of eight users registered as CSG users and who move at a low speed compared to the outdoor users (3km/h vs. 30km/h). MUE users are randomly positioned within the macrocell and move according to a random walk mobility model. The simulation parameters are detailed in Table 4.1.

We used a path loss propagation model as specified in 3GPP TSG WG4 [97] as follows:

$$PL^{k}_{M,MUE_i}[\text{dB}]=128.1+37.6\times log_{10}(D \times 0.001), \tag{4.11}$$

Table 4.1: Simulation Parameters

Parameters	Values	Parameters	Values
Macrocells	1	Thermal noise density	-174dBm/Hz
Femtocells	20	Carrier frequency	3.5 GHz
MUEs	5-40	UE noise figure	2.5 dB
Bandwidth	5MHz	ΔSINR	1 dB
Total RBs	25	ΔRSS	1 dB
Macro Tx power	43 dBm	Macrocell radius	1km
Femto Tx power	23 dBm	FUEs average speed	3km/hour
$SINR_{MUE}^{target}$	5.7 dB	MUEs average speed	30km/hour

$$PL_{F_l,FUE_j}^{k}[\text{dB}]=128.1+37.6\times log_{10}(D\times 0.001)+B, \tag{4.12}$$

where B is the external Wall Attenuation (20 dBm), if the user is in the outdoors, and D is the distance between the UEs and their serving cell.

4.5.2 Performance evaluation

4.5.2.1 PAMF scheme performance

We evaluated the performance of our power allocation scheme using the well-known scheduling algorithms: Modified Largest Weighted Delay First (MLWDF) and Exponential Proportional Fairness (EXPPF) to capture the effect of the scheduling strategy on our results. All MUE/FUEs in the cell have three different types of application flows (Video, VoIP, CBR). The Video service is a 242 kbps data source with H.264 coding [99], whereas the VoIP flows generate 20 bytes packets using an ON/OFF model [100]. Best Effort service is generated as an HTTP traffic. Quality of Service in terms of throughput is measured for both scheduling algorithms, i.e. MLWDF and EXPPF, for our proposed power allocation scheme, and for the basic scenario where no power adjustment strategy is considered. The basic reference scenario is noted "Basic" in the figures.

Figure 4.3 shows the average throughput of Video flows for different numbers of MUE users. The performance gain in throughput for our proposed power adjustment strategy is observed whatever is the scheduling algorithm, especially when the number of users is above 20 users with an improvement of more than 16.4% of the total throughput. This observation can be easily explained as follows. When the number of mobile MUEs increases, there is a high probability that some of them get close to femtocells coverage and thus experience potential severe interference situations. In these cases, our PAMF strategy can operate and the gain in throughput is observed. Inversely, when the scenario includes few MUE users, interference situations occur rarely resulting in very low throughput enhancement compared the Basic scenario.

Figures 4.4 and 4.5 depict the average throughput of MUEs VoIP and CBR flows respectively for a varying number of MUEs. As it can be seen, our proposal using both scheduling algorithms performs better than the basic strategy and realizes a

maximum gain of 13.3%. These results show that the power reduction strategy has almost the same impact on the types of service. Yet, a lower reduction in the gain can be observed for VoIP and CBR flows due to their reduced number of allocated RBs compared to Video flows.

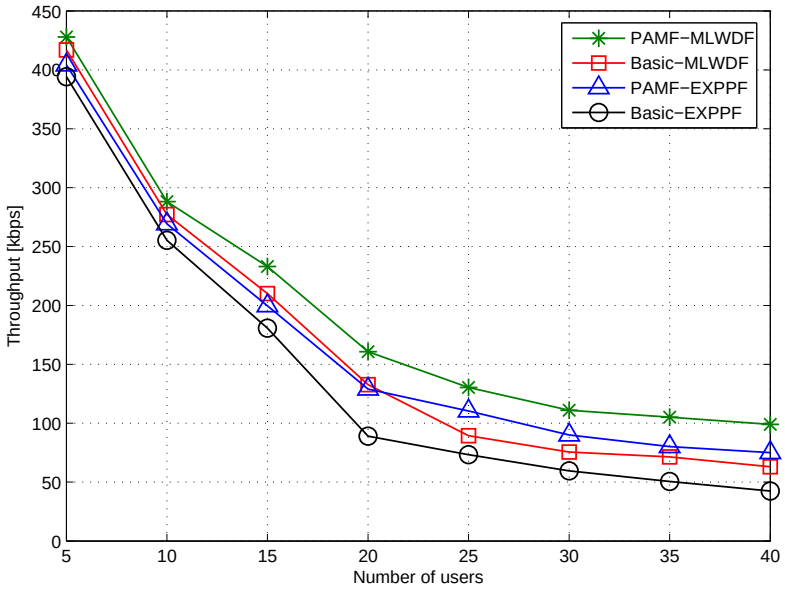

Figure 4.3: Average per-user throughput of MUEs for Video flows

To show the awareness of our power adjustment algorithm to FUE users QoS, we illustrate in each of the Figure 4.6, 4.7 and 4.8 the average per-user throughput of VoIP, Video and CBR flows respectively of FUE users for a varying number of MUEs. We compare the performance of PAMF with the Basic algorithm and with a version of PAMF which adopts the same power adjustment method but without the objection procedure from femtocells. The latter scheme is referred to "POW-ALO-MLWDF" in the figure.

We can observe in Figure 4.6 that PAMF is better than POW-ALO-MLWDF and shows a gain of 11%. This highlights the benefits of the objection method in conserving some quality to FUE users. We can also observe that PAMF results show a small reduction (about 4%) in the throughput of FUEs compared to the Basic scenario which corresponds to the cost of the power adjustment strategy which is done in favor of MUEs' quality and at the expense of FUEs' performance.

Figures 4.7 and 4.8 depict the average throughput of Video and CBR flows respectively. We can observe in Figure 4.7 that the PAMF scheme outperforms the POW-ALO-MLWDF mechanism and show a gain approximately 12%. However, compared to VoIP traffic the PAMF scheme achieves a slight better performance (less degradation compared to the Basic scenario), due to the higher number of allocated RBs for Video flows. While, Figure 4.8 illustrate the obtained results for CBR traffic. We can observe almost the same behavior of the three schemes which confirm the stability of the performance again traffic differentiation.

We can conclude that our proposed PAMF strategy shows a better performance

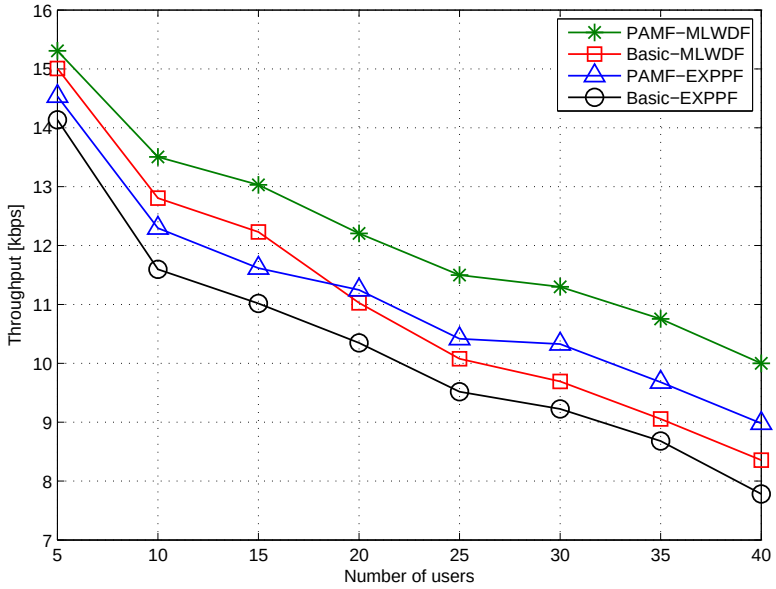

Figure 4.4: Average per-user throughput of MUEs for VoIP flows

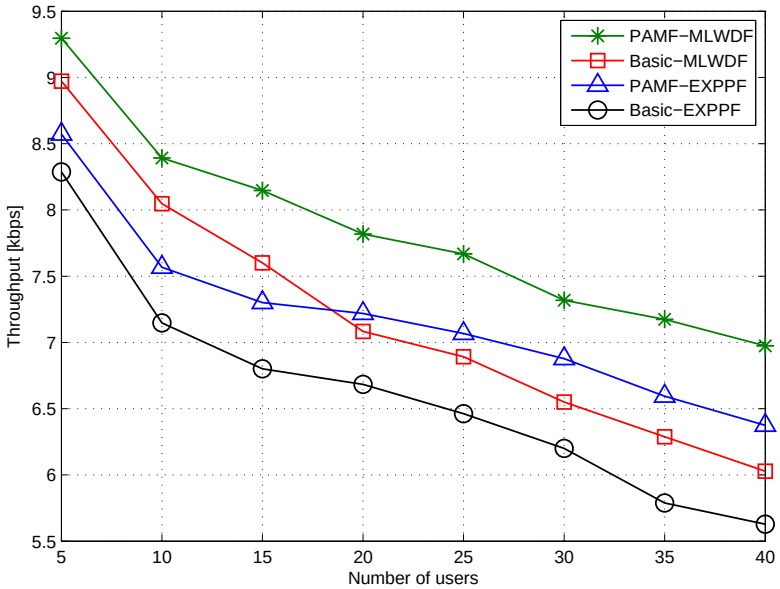

Figure 4.5: Average per-user throughput of MUEs for CBR flows

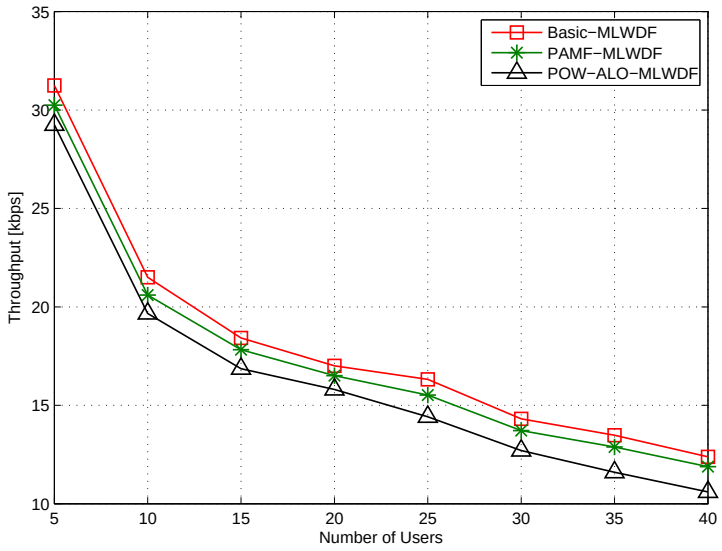

Figure 4.6: Average per-user throughput of FUEs for VoIP flows as a function of the number of MUEs

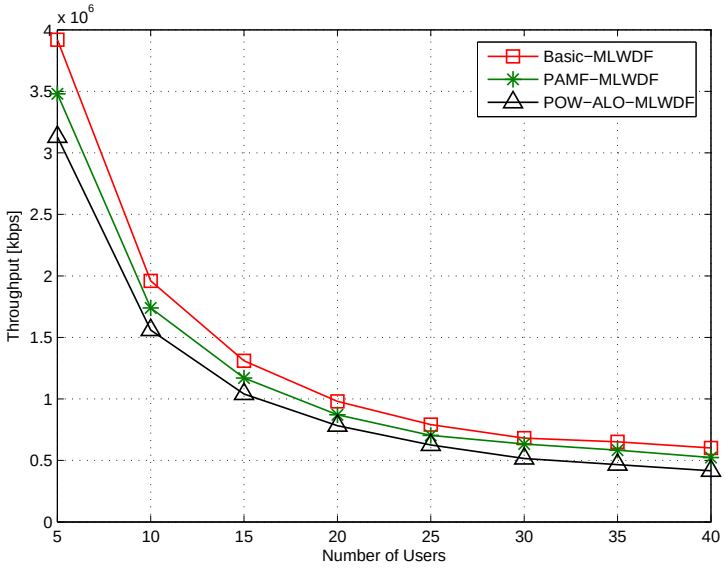

Figure 4.7: Average per-user throughput of FUEs for Video flows as a function of the number of MUEs

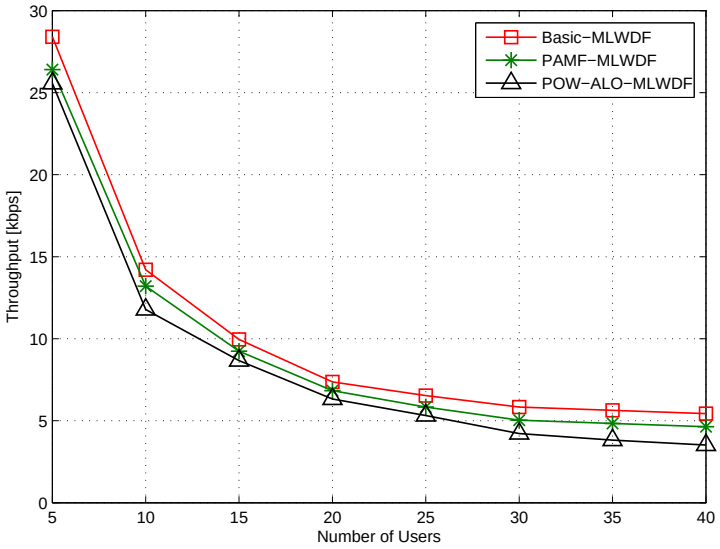

Figure 4.8: Average per-user throughput of FUEs for CBR flows as a function of the number of MUEs

for scenarios that involve a high number of mobile MUEs. In low users density, the proximity of MUEs and FBSs generating a high interference happens too rarely to observe a significant gain in the average user throughput. Hence, as our PAMF scheme is intends for dense urban environments, it is able to achieve the highest performance in realistic urban scenarios.

4.5.2.2 SORA mechanism performance

To analyze the performance of SORA scheme in terms of signaling overhead, we realized a set of experiments in which we obtained SORA mechanism to our PAMF scheme and compare it to the basic version of PAMF (noted Basic in Figure 4.9). Moreover, to highlight the effect of mobility on the generated signaling we considered two cases of mobility: 3km/h and 30km/h.

Figure 4.9 illustrates the average number of MRs B to decrease the transmit power sent by the macrocell M. We can observe that 15% of RSS reports do not change when the victim's speed is around 30km/h, while it increases up to 24% for a pedestrian profile (speed around 3km/h). Moreover, the total number of the generated MRs in high mobility scenarios is higher, since the probability that MUEs pass close to the FBSs coverage is greater.

4.6 Conclusion

This chapter addressed the interference issue in a two-tier macro-femtocells system involving a user mobility environment. We proposed PAMF a power allocation scheme which aim is to increase the throughput of non-CSG UEs at the expense of a decreased power from femtocells. The advantage of our power allocation strategy

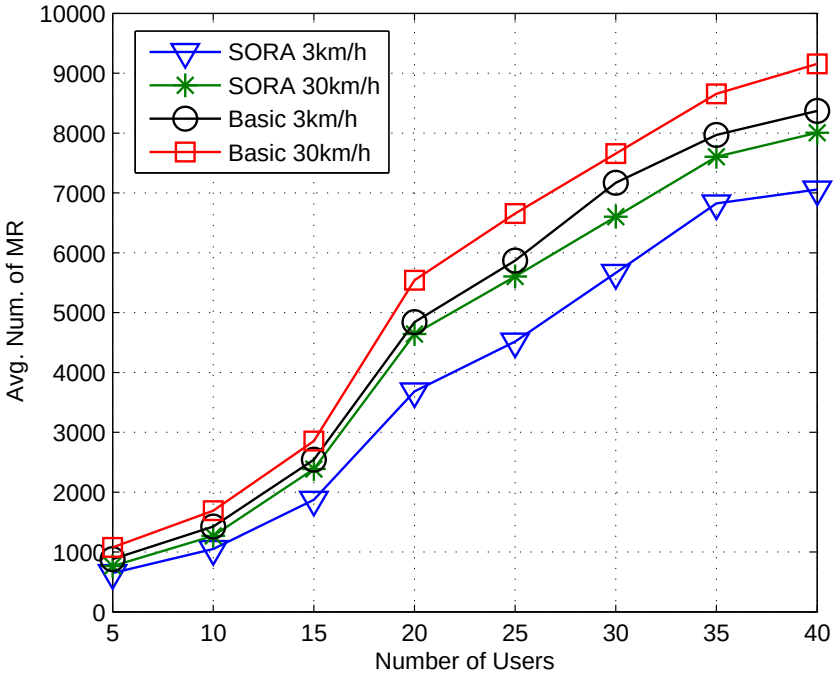

Figure 4.9: Average Number of MRs sent by the macrocell

is threefold: (i) mitigate the interference affecting the MUEs, (ii) be aware of the service degradation caused to FUEs due to the power adjustment of their FBSs, and (iii) reduce the signaling overhead caused by the power adjustment strategy. The simulation results showed the effectiveness of our mechanisms in terms of throughput and signaling overhead when using two well-known scheduling algorithms for resource block allocation, namely MLWDF and EXP-PF.

Nevertheless, when employing our power adjustment strategy on CSG-femtocells, the DL signal from the interfering femtocells has been treated equally without being aware of the possible correlation and additive effect interference on some MUEs which can be affected by more than one interfering FBS. Therefore, in order to take into account more advanced context information on users' locations and the shared interference effect measure, in the next chapter, our investigation by proposing a coordinated power adjustment technique based on context information.

Chapter 5

Power adjustment mechanism using context information for interference mitigation in two-tier heterogeneous networks

5.1 Introduction

In our previous contribution (chapter four), we proposed an MBS-assisted power adjustment strategy for interference mitigation in a mobility environment where macrocells and femtocells are co-located. The key benefits of this scheme were to achieve higher performance for non-CSG macrocell users while avoiding potential service degradation of femtocell users by taking into account FUEs outage situations and users SINR at both macro and femtocell sides. In this chapter, we involved the above mentioned contribution by proposing two different context-aware and cooperative power adjustment strategies for IM with different degrees of awareness of femtocell users' performance. Our key objective is to improve the spectral efficiency of MUEs while preserving a high throughput to FUEs.

In particular, the proposed power control schemes make use of femto and macro users' context information in terms of positioning, for setting the appropriate prioritization weights among the current victim macro users and the femto users in outage.

Our two context-based and adaptive power control schemes, called respectively Global Power Adjustment (GPA) and Selective Power Adjustment (SPA), differ in their selection strategy of the set of FBSs executing the power adjustment as well as the amount of power to reduce. The main advantage of our proposed approach over traditional ones is that it is based on power adjustment parameters whose values are dynamically adapted to the interference impact of each femtocell on the global interference situation. To estimate such femtocell's liability on the global interference, we use a *Score Function* which quantifies this value based not only on the RSS feedback returned by MUEs, but also on some context information (such as the number and location of MUEs/FUEs) retrieved from the MBS and FBS load REM databases. Exploiting this context information about users' number and

localization enriches the decision policy and brings added value knowledge to the power allocation decision process. Finally, we discuss and analyze the effect of the *Score Function* weighting parameters on the global system performance in terms of MUEs and FUEs throughput.

The rest of this chapter is organized as follows: Section 5.2 describes the system model and the main assumptions. Section 5.3 presents the proposed power adjustment schemes based on both users context factors and the dynamic power adjustment parameters. In Section 5.4, the simulation environment and results are presented, while in section 5.5 concludes the chapter.

5.2 System Model and assumptions

In our system, a single macrocell base station is deployed in which femtocells access points are geographically positioned in streets located at the cell-edge of the macrocell coverage (see Figure 5.1). We consider all the assumptions and the system model parameters have mentioned in section 4.2 (chapter four) are supposed the same as uses in this chapter.

We consider in this work the system model described in section 4.2 of chapter 4. All SINR equations (equations 4.1 and 4.2) remain valid. Moreover, here again we make use of the local MBS and FBS REM databases to registers all the RSSs recently fed back by the MUEs to inform about the interference condition caused by the neighboring FBSs on their respective allocated RBs when conditions (4.6) and (4.7) are fulfilled. Moreover, the context parameters (to be defined in the next section) will also be recorded in each local REM to help the power adjustment decisions. The REM databases are also used to store other less dynamic parameters such as $SINR^{target}_{MUE}$, $SINR^{target}_{FUE}$, $\Delta SINR$ and ΔP values.

5.3 The Proposed Power Control Strategies

5.3.1 Optimization Problem Formulation

Since the femtocells are deployed in the macrocell coverage area with full frequency reuse, the transmission signal from FBSs will generate a strong interference to neighboring MUEs, causing a large degradation of their received $SINR^{k}_{M,MUE_i}$. Therefore, the goal of the considered femtocell power adjustment is to minimize the sum of the transmit powers of all femtocells, over all RBs, while satisfying both MUEs' and FUEs' SINR requirements simultaneously.

Since it is assumed that all RBs are fully loaded, i.e., they are all allocated to MUEs beforehand, the considered femtocell power allocation optimization problem can be formulated as

$$\min_{p^k_{F_l}} \sum_{l=1}^{L} \sum_{k=1}^{K} p^k_{F_l}, \tag{5.1}$$

$$\text{s.t.} \quad SINR^{k}_{M,MUE_i} \geq SINR^{target}_{MUE} + \Delta SINR \quad \forall i \in \{1, ..., I\}, \forall k \in \mathcal{K}_i,$$

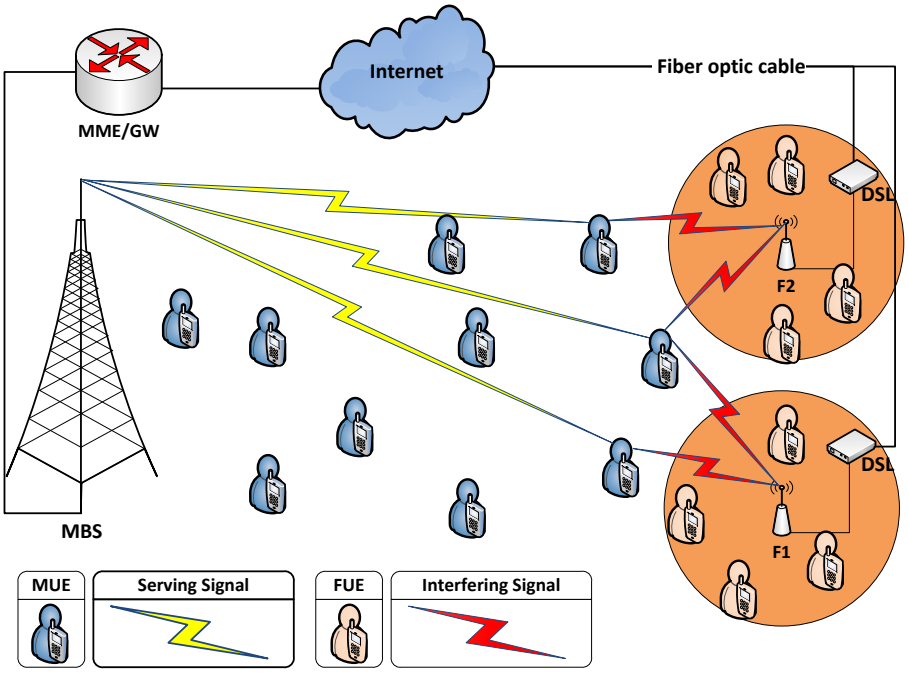

Figure 5.1: Two-tier Heterogeneous Network

$$SINR^{k}_{F_l,FUE_j} \geq SINR^{target}_{FUE} \quad \forall j \in \{1,...,J\}, \forall l \in \{1,...,L\}, \forall k \in \mathcal{K}_j,$$

$$p^{k}_{F_l} \geq 0 \quad \forall F_l \in \{1,...,L\}, \forall k \in \{1,...,K\},$$

$$\sum_{k=1}^{K} p^{k}_{F_l} \leq P^{Max}_{Fl} \quad \forall k \in \{1,...,K\},$$

where $\mathcal{K}_i$ denotes the set of RBs allocated to MUE$_i$, $\mathcal{K}_j$ the set of RBs allocated to FUE$_j$ and $P^{Max}_{F_l}$ denotes the maximum transmit power of femtocell F_l. Note that similar optimization problems were considered in [101] and [102], but for a much simpler system such as single-carrier transmission and fixed SINR levels, i.e., without any multipath fading. Even under such simplified assumptions, it was shown that the global optimization problem required a huge computational complexity as well as extensive control signaling for information exchange, which in return make it hardly suited for implementation. Thus, the global optimization of our problem by a centralized approach may be even more difficult and intractable. Therefore, we propose a MBS-assistance approach for femtocell power control, which may be categorized as an MBS-assisted power adjustment scheme.

5.3.2 Proposed Power Control Strategies

In our model, various MUEs are randomly positioned within MBS M's coverage and each active MUE$_i$ periodically sends to MBS M a CQI in terms of $SINR^{k}_{M,MUE_i}$ as expressed in (1) and experienced on each allocated RB k. Before performing the resource allocation procedure based on the adopted scheduling strategy, MBS M

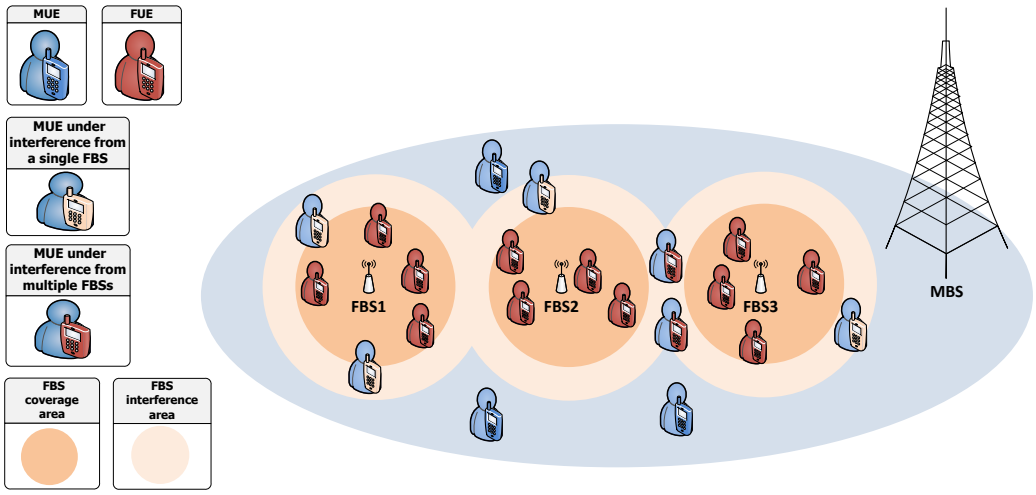

Figure 5.2: Macrocell/Femtocells interference scenario

first checks the quality of MUEs' communication channels based on the returned CQI [17][51][103].

For all MUEs and for all their allocated RBs for which condition (4.6) is fulfilled, MBS M asks the concerned users to send a Measurement Report (MR) in terms of RSSs of the received pilot signals from their current serving cell and all neighboring femtocells. The RSS reports help MBS M to identify the source of interference and to check whether it is caused by neighboring cells or if it is a consequence of any other effect such as fast fading or noise. For this purpose, condition (4.7) is checked to determine if for a given MUE_i, the signal received from the neighboring femtocell F_l covers the signal of its serving macrocell. If so, MBS M identifies F_l as an interfering cell for victim MUE_i and F_l is added to the set of interfering FBSs on MUE_i, $\mathcal{Z}_{i,k}$: $\mathcal{Z}_{i,k} \leftarrow \mathcal{Z}_{i,k} \cup \{F_l\}$. To keep track of the $RSS^k_{F_l,MUE_i}$ evolution perceived from each interfering FBS, MBS makes use of a local REM table to record the latest reported $RSS^k_{F_l,MUE_i}$ values.

In order to mitigate the interference generated by each interfering FBS in its local REM table, MBS M initiates the power adjustment decision process as follows. First, for each victim MUE_i, MBS identifies all the RBs k on which MUE_i suffers from interference (i.e., those which fulfill condition (4.7)). Then, it retrieves from the REM table the set of femtocells causing this interference on MUE_i on RB k (i.e, the set $\mathcal{Z}_{i,k}$).

The main objective of our approach is to express, for each interfering femtocell, its impact level on the interference situation. To do so, we define the *Score Function* $f(F_l)$ for each interfering femtocell F_l in the REM table as follows:

$$f(F_l) = \theta_1 R_{F_l} + \theta_2 N_{F_l} - \theta_3 Q_{F_l}, \tag{5.2}$$

where R_{F_l}, N_{F_l} and Q_{F_l} are the context parameters defined as follows:

- $\mathcal{R}_{F_l}$: the set of MUEs impacted by femtocell F_l only (i.e., which verify condition (4.7)) and R_{F_l} denotes its cardinality,

  $\mathcal{R}_{F_l}=\{MUE_i,\ i=1,\ldots,I;\ \exists k \in \mathcal{K}_i,\ \mathcal{Z}_{i,k}=\{F_l\}\}$,
  $R_{F_l}=|\mathcal{R}_{F_l}|$.

- $\mathcal{N}_{F_l}$: the set of MUEs located in the overlapping areas between F_l and any neighboring F_m, and N_{F_l} denotes its cardinality,

  $\mathcal{N}_{F_l}$=$\{MUE_i,\ i$=$1,...,I;\ \exists F_m \in \mathcal{L},\ \exists k \in \mathcal{K}_i,$
  $\mathcal{Z}_{i,k} \supseteq \{F_l\} \underset{m \neq l}{\cup} \{F_m\},\ |\mathcal{Z}_{i,k}| \geqslant 2\},$
  N_{F_l}=$|\ \mathcal{N}_{F_l}\ |$.

- $\mathcal{Q}_{F_l}$: the set of FUEs observing an outage after decreasing the power of their serving cell F_l and Q_{F_l} denotes its cardinality,

  $\mathcal{Q}_{F_l}$=$\{FUE_j,\ j$=$1,...,J;\ SINR^k_{F_l,FUE_j} < SINR^{target}_{FUE}\}$,
  Q_{F_l}=$|\mathcal{Q}_{F_l}|$.

Finally, θ_i, $(i = 1, ..., 3)$ are the weighting factors reflecting the priorities of the context parameters.

The context parameters refer to the number of victim MUEs and FUEs as well as their respective locations within the interference area. By assigning different weights to the MUEs affected by only one FBS and those affected by multiple FBSs in equation (5.2), we differentiate the impact of those two types of interference situations in the Score Functions. Thus, these context parameters will help in identifying the set of femtocells which have the greater and shared impact on a given interference situation and hence allow for an adapted and coordinated power adjustment proportional to this impact. Figure 2 illustrates a simple scenario in which both interference situations are observed. In this example, R_{FBS_1}=2, and R_{FBS_2} or R_{FBS_3}=1. While, N_{FBS_2} or N_{FBS_3}=2.

The *Score Function* $f(F_l)$ defined in equation (5.2) can be either positive or negative. A positive $f(F_l)$ score means that the associated femtocell F_l impacts more importantly the MUE than the FUEs under its coverage, and thus has the ability to tolerate more reduction of its transmission power. Conversely, a negative score value reflects a serious outage situation of F_l's FUEs. Note that $f(F_l)$ is evaluated at each frame as long as the interference lasts. Its value will vary according to the power adjustment strategy to be applied in the current frame as well as the mobility of MUEs.

The main objective now is to estimate the exact amount of power to be used by each interfering femtocell for the adjustment purpose. To resolve this problem, we propose two power adjustment strategies baptized Global Power Adjustment (GPA) and Selective Power Adjustment (SPA). GPA and SPA offer a different degree of awareness of FUE performance and consequently impacts the MUE performance as well due to the tradeoff between their conflicting requirements in terms of spectral efficiency. More specifically, GPA and SPA implement a different selection mechanism of the interfering femtocells which are to apply the power adjustment and the amount of the power adjustment (increase or decrease). Besides, the associated power adjustment parameters to be introduced hereafter offer an additional leverage in managing the compromise between FUE and MUE performances.

For each victim MUE_i on RB k, MBS M retrieves from the REM table the set of femtocells responsible for this interference and determines their respective Score

Functions values. Then, MBS M finds the maximum interference $MI^k_{MUE_i}$ which can be allowed by a victim MUE$_i$ on RB k as

$$MI^k_{MUE_i} = \frac{RSS^k_{M,MUE_i}}{SINR^{target}_{MUE}} - N_0. \tag{5.3}$$

Afterwards, MBS M computes for each interfering F_l in the REM table the new value of its transmission power $p'^k_{F_l}$ in RB k as

$$p'^k_{F_l} = \alpha^k_{F_l} \ . \ \beta^k_{F_l} \ . \ p^k_{F_l}, \tag{5.4}$$

where we have

$$\beta^k_{F_l} = \frac{MI^k_{MUE_i}}{\sum_{l=1}^{L} RSS^k_{F_l,MUE_i}}. \tag{5.5}$$

$p^k_{F_l}$ represents the latest transmitted power of the interfering F_l in RB k, and $RSS^k_{F_l,MUE_i}$ is the measured received signal strength from F_l by MUE$_i$ for the allocated RB k. First, the previous power level $p^k_{F_l}$ is adjusted by the parameter $\beta^k_{F_l}$ which represents the allowed per-femtocell interference level, where $MI^k_{MUE_i}$ has been normalized by the sum of all RSSs of interfering femtocells. Hence, $\beta^k_{F_l}$ is the same for all F_l and the received RSS by MUE_i after this adjustment becomes $\frac{RSS^k_{F_l,MUE_i}}{\sum_{l=1}^{L} RSS^k_{F_l,MUE_i}}$.

Next, the resulting power is further adjusted by the boosting factor $\alpha^k_{F_l}$ whose value is proportional to $f(F_l)$ score. Using the boosting factor $\alpha^k_{F_l}$ enables to adapt the power allocation proportionally to the femtocells' role in the interference situation rather than uniformly as usually performed in traditional power adjustment approaches. However, the amount of power boosting will be limited by a tunable system parameter x, $(0 < x \leq 1)$ which represents the maximum allowed power reduction/increase ratio of the nominal power $\beta^k_{F_l} p^k_{F_l}$, i.e., $p'^k_{F_l} \in [\beta^k_{F_l} p^k_{F_l}(1-x), \beta^k_{F_l} p^k_{F_l}(1+x)]$. Therefore, we have

$$\begin{cases} 1 - x < \alpha^k_{F_l} \leq 1 & if\ f(F_l) \geqslant 0 \\ 1 < \alpha^k_{F_l} \leq \min(1 + x, \frac{P^{Max}_{F_l}}{\beta^k_{F_l} p^k_{F_l}}) & otherwise, \end{cases}$$

Moreover, the $\alpha^k_{F_l}$ value for each F_l should be inversely proportional to its corresponding score $f(F_l)$. Indeed, the higher the $f(F_l)$ score, the greater the impact of F_l on the MUE interference so the more it should reduce its interference by setting a lower $\alpha^k_{F_l}$, with $1 - x \leq \alpha^k_{F_l} \leq 1$. On the contrary, a lower $f(F_l)$ value implies a larger $\alpha^k_{F_l}$. In particular, the case $f(F_l) < 0$ means that the proportion of unsatisfied FUEs is greater than that of victim MUEs, and hence $\alpha^k_{F_l}$ should be increased within the range $[1, \min(1 + x, \frac{P^{Max}_{F_l}}{\beta^k_{F_l} p^k_{F_l}})]$. Thus, we propose the following setting of $\alpha^k_{F_l}$ in each case,

$$\begin{cases} 1 - \min(x, \frac{f(F_l)}{\max\limits_{\mathcal{Z}_{i,k}} f(F_l)}) & if\ f(Fl) \geqslant 0 \\ \min(1 + \min(x, \frac{f(F_l)}{\min\limits_{\mathcal{Z}_{i,k}} f(F_l)}), \frac{P^{Max}_{F_l}}{\beta^k_{F_l} p^k_{F_l}}) & otherwise, \end{cases} \tag{5.6}$$

where $\frac{f(F_l)}{\max\limits_{\mathcal{Z}_{i,k}} f(F_l)}$ and $\frac{f(F_l)}{\min\limits_{\mathcal{Z}_{i,k}} f(F_l)}$ act as the weights for FBS F_l when $f(F_l)$ is positive or negative respectively.

At this step, the selection of the set of the interfering femtocells that are to apply the boosting factor $\alpha_{F_l}^k$ defines the power adjustment strategy. As mentioned above, we propose two adjustment strategies: GPA and SPA.

5.3.3 Global Power Adjustment (GPA)

In the GPA strategy, we propose to apply the power adjustment using the boosting factors to all the interfering femtocells. It is worth noticing here, that GPA strategy acts on all femtocells participating in the interference whatever their *Score Function* values. Therefore, GPA will create a balance between the offered throughput to victim MUEs and the performance of FUEs which may suffer from the power adjustment (see Algorithm 5.1).

5.3.4 Selective Power Adjustment (SPA)

The aim of this second strategy is to apply $\alpha_{F_l}^k$ adjustment parameters only for those femtocells which show a positive *Score Function* ($f(F_l) \geq 0$). The rest of interfering femtocells ($f(F_l) < 0$) are allocated a fixed and neutral parameter value $\alpha_{F_l}^k = 1$. Such a strategy will give more priority to MUEs in terms of throughput since femtocells suffering from a severe FUE outage situation will not benefit from an adapted power reduction proportional to their "suffering" level. As a consequence, in SPA strategy $\alpha_{F_l}^k$ are derived as follows

$$\begin{cases} 1 - \min(x, \frac{f(F_l)}{\max\limits_{\mathcal{Z}_{i,k}} f(F_l)}) & if\ f(F_l) \geqslant 0 \\ \alpha_{F_l}^k = 1 & otherwise \end{cases}$$

Similarly to GPA, the adjustment process in SPA is repeated recursively at each frame until the interference caused to MUE_i on RB k fades (see Algorithm 5.2).

5.3.5 Required signaling information exchange between cells

The required signaling information between the macrocell and femtocells may be exchanged through two main possibilities: i) the backhaul connection using the core network infrastructure (Optic Fiber), through the S1 interface and femtocell gateway [104] [105], ii) the direct X2 interface between macrocells and femtocells [63]. These two communication means will impact differently the performance mainly in terms of delay and signaling overhead.

The X2 interface enables the support of resource management functionalities operating in short time scales such as interference, mobility and handover [104]. Therefore, the X2 interface is more suitable to support the signaling exchange in our power adjustment strategy as the S1 interface will reduce longer delays. In fact, power adjustments and several context information (i.e. RSS, SINR, ..., etc) have to be periodically exchanged between the MBS and femtocell local REMs, and the delay imposed by the interface should be at a shorter time-scale compared to this periodicity in order to allow a real-time response of the operations.

Algorithm 5.1 *GPA* algorithm

Let $\mathcal{I}$ be the set of MUEs of MBS M,
Let $\mathcal{L}$ be the set of FBSs,
Let $\mathcal{Z}_{i,k}$ be the set of interfering FBSs on MUE_i in a RB k,
Let $\mathcal{K}_i$ be the set of RBs allocated to MUE_i, $\mathcal{K}_i \neq \emptyset$,
initiate $SINR_{MUE}^{target}$
add $\mathcal{Z}_{i,k}$ **in** *REM-Table*
for all $MUE_i \in \mathcal{I}$ **and for all RB k** $\in \mathcal{K}_i$ **do**
 initiate $\mathcal{Z}_{i,k} \leftarrow \phi$
 if $SINR_{M,MUE_i}^{k} < SINR_{MUE}^{target} + \Delta SINR$ **then**
  calculate RSS_{M,MUE_i}^{k}
   for all $F_l \in \mathcal{L}$ **do**
    calculate RSS_{F_l,MUE_i}^{k}
    if $RSS_{M,MUE_i}^{k} < RSS_{F_l,MUE_i}^{k} + \Delta P$ **then**
     $\mathcal{Z}_{i,k} \leftarrow \mathcal{Z}_{i,k} \cup \{F_l\}$
    end if
   end for
  add $\mathcal{Z}_{i,k}$ **in** *REM-Table*
 end if
end for
for all $MUE_i \in \mathcal{I}$ **and for all RB k** $\in \mathcal{K}_i$ **do**
 get $\mathcal{Z}_{i,k}$ **from** *REM-Table*
 if $\mathcal{Z}_{i,k} \neq \phi$ **then**
  for all $F_l \in \mathcal{Z}_{i,k}$ **do**
   calculate R_{F_l}, N_{F_l} **and** Q_{F_l} **from** *REM-Table*
   calculate $f(F_l) \leftarrow (\theta_1 R_{F_l} + \theta_2 N_{F_l} - \theta_3 Q_{F_l})$, //where $0 \leq \theta_i \leq 1$, $i = 1, 2, 3$
   case $f(Fl) \geq 0$
    calculate $p_{F_l}^{'k} \leftarrow \alpha_{F_l}^{k} \,.\, \beta_{F_l}^{k}.p_{F_l}^{k}$, //power adjustment at F_l
    where $\beta_{F_l}^{k} \leftarrow \frac{MI_{MUE_i}^{k}}{\sum_{l=1}^{L} RSS_{F_l,MUE_i}^{k}}$, $\alpha_{F_l}^{k} \leftarrow 1 - \min(x, \frac{f(F_l)}{\max\limits_{\mathcal{Z}_{i,k}} f(F_l)})$
   case $f(Fl) < 0$
    calculate $p_{F_l}^{'k} \leftarrow \alpha_{F_l}^{k} \,.\, \beta_{F_l}^{k}.p_{F_l}^{k}$, //power adjustment at F_l
    where $\beta_{F_l}^{k} \leftarrow \frac{MI_{MUE_i}^{k}}{\sum_{l=1}^{L} RSS_{F_l,MUE_i}^{k}}$, $\alpha_{F_l}^{k} \leftarrow \min(1 + \min(x, \frac{f(F_l)}{\min\limits_{\mathcal{Z}_{i,k}} f(F_l)}), \frac{P_{F_l}^{Max}}{\beta_{F_l}^{k} p_{F_l}^{k}})$
  end for
 end if
end for
update *REM-Table*

Algorithm 5.2 *SPA* algorithm

Let $\mathcal{I}$ be the set of MUEs of MBS M,
Let $\mathcal{L}$ be the set of FBSs,
Let $\mathcal{Z}_{i,k}$ be the set of interfering FBSs on MUE_i in a RB k,
Let $\mathcal{K}_i$ be the set of RBs allocated to MUE_i, $\mathcal{K}_i \neq \emptyset$,
initiate $SINR_{MUE}^{target}$
add $\mathcal{Z}_{i,k}$ **in** *REM-Table*
for all $MUE_i \in \mathcal{I}$ **and for all RB k** $\in \mathcal{K}_i$ **do**
 initiate $\mathcal{Z}_{i,k} \leftarrow \phi$
 if $SINR_{M,MUE_i}^{k} < SINR_{MUE}^{target} + \Delta SINR$ **then**
  calculate RSS_{M,MUE_i}^{k}
   for all $F_l \in \mathcal{L}$ **do**
    calculate RSS_{F_l,MUE_i}^{k}
    if $RSS_{M,MUE_i}^{k} < RSS_{F_l,MUE_i}^{k} + \Delta P$ **then**
     $\mathcal{Z}_{i,k} \leftarrow \mathcal{Z}_{i,k} \cup \{F_l\}$
    end if
   end for
  add $\mathcal{Z}_{i,k}$ **in** *REM-Table*
 end if
end for
for all $MUE_i \in \mathcal{I}$ **and for all RB k** $\in \mathcal{K}_i$ **do**
 get $\mathcal{Z}_{i,k}$ **from** *REM-Table*
 if $\mathcal{Z}_{i,k} \neq \phi$ **then**
  for all $F_l \in \mathcal{Z}_{i,k}$ **do**
   calculate R_{F_l}, N_{F_l} **and** Q_{F_l} **from** *REM-Table*
   calculate $f(F_l) \leftarrow (\theta_1 R_{F_l} + \theta_2 N_{F_l} - \theta_3 Q_{F_l})$, //where $0 \leq \theta_i \leq 1$, $i = 1, 2, 3$
   case $f(Fl) \geq 0$
    calculate $p'^{k}_{F_l} \leftarrow \alpha^{k}_{F_l} \ . \ \beta^{k}_{F_l} . p^{k}_{F_l}$, //power adjustment at F_l
    where $\beta^{k}_{F_l} \leftarrow \frac{MI^{k}_{MUE_i}}{\sum_{l=1}^{L} RSS^{k}_{F_l,MUE_i}}$, $\alpha^{k}_{F_l} \leftarrow 1 - \min(x, \frac{f(F_l)}{\max\limits_{\mathcal{Z}_{i,k}} f(F_l)})$
   case $f(Fl) < 0$
    calculate $p'^{k}_{F_l} \leftarrow \alpha^{k}_{F_l} \ . \ \beta^{k}_{F_l} . p^{k}_{F_l}$, //power adjustment at F_l
    where $\beta^{k}_{F_l} \leftarrow \frac{MI^{k}_{MUE_i}}{\sum_{l=1}^{L} RSS^{k}_{F_l,MUE_i}}$, $\alpha^{k}_{F_l} \leftarrow \alpha^{k}_{F_l} = 1$
  end for
 end if
end for
update *REM-Table*

As regards to the signaling load, the amount of exchanged information becomes more stringent as the number of femtocells increases. In this respect, the backhaul connection may provide enough bandwidth for the signaling overhead but introduces harsh delay constraints, making it difficult to satisfy the real-time requirements [106]. It is worth noticing that the coordination between cells in our proposed scheme requires a limited signaling load for each updating cycle, namely:

- the measurement report $\mathcal{Q}_{F_l}$ which represents the number of F_l 's FUEs in outage situation. This message is triggered by F_l and sent to the corresponding MBS.
- the values of $p'^{k}_{F_l}$ for each RB k and each F_l, to be sent by the MBS to the corresponding FBS F_l.

5.4 Simulation Analysis

5.4.1 Simulation environment

To investigate the performance of our proposed power allocation mechanisms, we implemented various simulation scenarios using LTE-Sim simulator [98]. The network topology consists of one MBS M and several neighboring FBSs positioned in a street with a reasonable distance from M. Each FBS is placed in a building and serves a maximum of four users registered as CSG users and moving at a low speed compared to the outdoor users (3km/h vs. 30km/h). MUEs are randomly positioned within the macrocell and move according to a random walk mobility model constrained by the street layout of 30m. The main simulation parameters are detailed in Table 5.1.

We used path loss models as specified in 3GPP TSG WG4 [97] with an external Wall Attenuation of 20 dBm. In a first set of experiments the *Score Function*'s weighting parameters θ_1, θ_2, and θ_3 have a fixed value of 0.3, 0.3 and 0.4, respectively. Note that the effect of these weighting parameters will be analyzed in subsection 5.4.3.

5.4.2 Power adjustment strategies performance

In this first set of experiments, we evaluate the performance of our power allocation schemes using extensive simulations and gain further insight on the influence of the involved parameters on the macrocell/femtocell throughput performance. Regarding the scheduling module, we used the reference Modified Largest Weighted Delay First (MLWDF) algorithm. All MUEs/FUEs in the cell support three different types of application flows: Video, VoIP, and CBR. The Video service is a 242 kbps data source with H.264 coding [99], whereas the VoIP flows generate 20-byte packets using an ON/OFF model [100]. CBR traffic is generated at a rate of 5-byte packets per second. Quality of Service in terms of throughput is measured for our proposed power allocation strategies GPA and SPA, and compared with the Basic scheme where no power adjustment strategy is considered, as well as the Reference scheme proposed in [51], and which can be viewed as classical femtocell power adjustment

Table 5.1: Simulation Parameters

Parameters	**Values**
Number of Macrocells	1
Number of Femtocells	30
Number of MUEs	10-60
Number of FUEs	4
Bandwidth	10MHz
Total number of RBs	50
Macro Tx power	43 dBm
Femto Tx power	23 dBm
Thermal noise density	-174dBm/Hz
Carrier frequency	3.5 GHz
UE noise figure	2.5 dB
Macrocell radius	1 km
Femtoocell radius	20m
FUEs, average speed	3km/hour
MUEs, average speed	30km/hour
$\text{SINR}_{MUE}^{target}$	5.7 dB
$\text{SINR}_{FUE}^{target}$	12.6 dB
ΔP	0.1 dB

scheme that is unaware of the FUEs' performance. The Basic and Reference schemes are noted "Basic" and "Ref." in the figures, respectively.

Figure 5.3 shows the average per-user throughput of MUEs for the supported Video flows. We can easily observe that for all the schemes, the throughput degrades with the number of active MUEs as this number is correlated to the generated traffic. Moreover, we can also see that the gain in throughput for our proposed strategies is higher than for the Basic and Ref. strategies especially when the number of users is increased from 30 to 60. We have an improvement of 13% to 18% and 11% to 15% compared to the Basic and Ref. schemes, respectively. This increase in throughput for higher user density is mainly due to an increased probability of interference situations when MUEs approach the femtocells' coverage. Figure 3 also shows that SPA strategy performs better than GPA since it gives a higher priority to MUEs, providing them a higher average throughput.

Figure 5.4 illustrates FUEs' average per-user throughput for Video flows, when varying the number of active MUEs. As the power adjustment in general degrades the transmission power of femtocells to mitigate the interference effect on victim MUEs, the GPA scheme offers as expected a better average throughput for FUEs. However, we observe a similar FUE throughput performance for both SPA and Reference schemes, while the proposed SPA scheme provides a higher MUE throughput.

Figure 5.5 depicts the average per-user throughput of VoIP flows for MUEs. Here again, our GPA and SPA strategies perform better than the Basic or Reference schemes and offer a gain of almost 12% and 16%, compared to the Basic scheme, and 9% and 14% compared to the Reference scheme. Moreover, we observe that the voice traffic is slightly less impacted by the gain in throughput, which is due

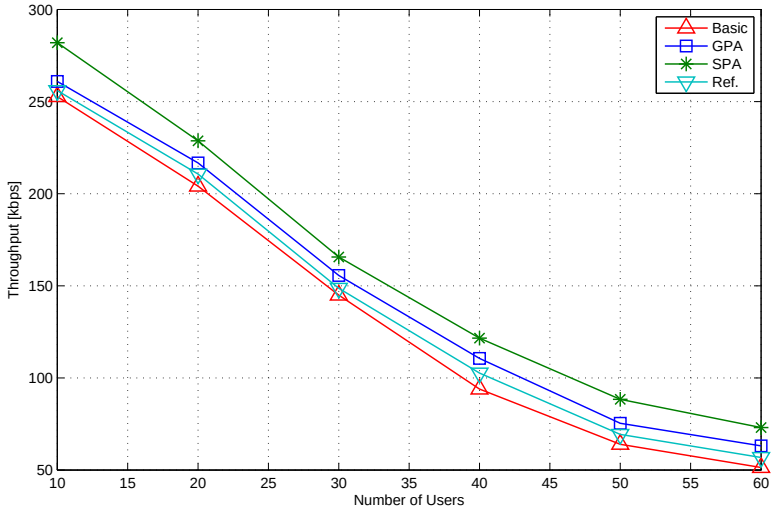

Figure 5.3: Average per-user throughput of MUEs for Video flows

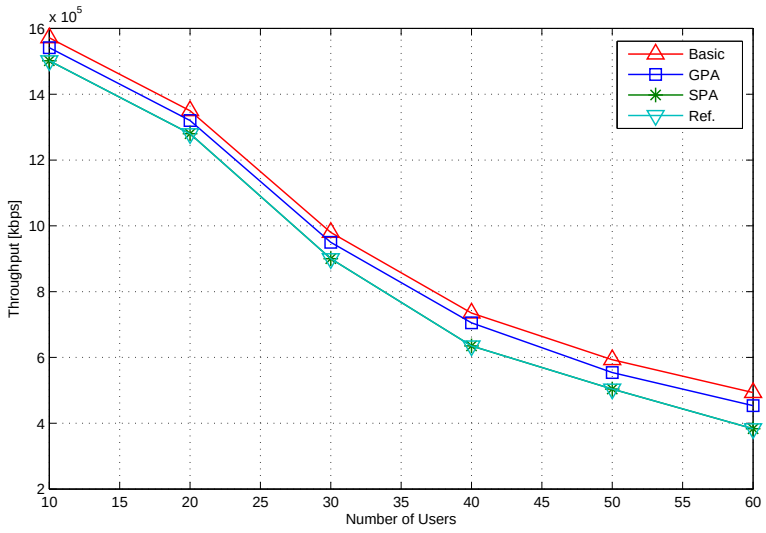

Figure 5.4: Average per-user throughput of FUEs for Video flows as a function of the number of MUEs

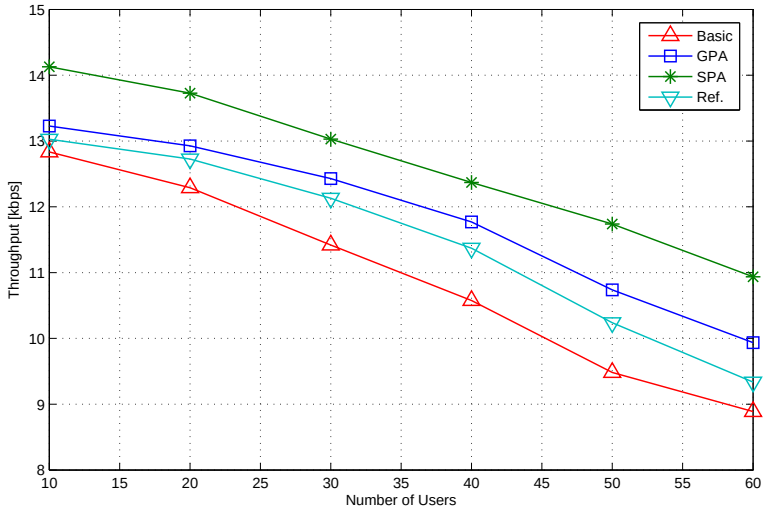

Figure 5.5: Average per-user throughput of MUEs for VoIP flows

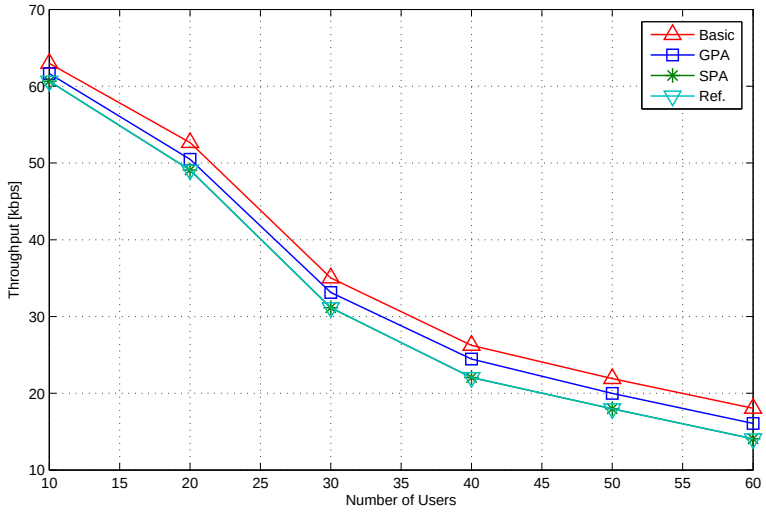

Figure 5.6: Average per-user throughput of FUEs for VoIP flows as a function of the number of MUEs

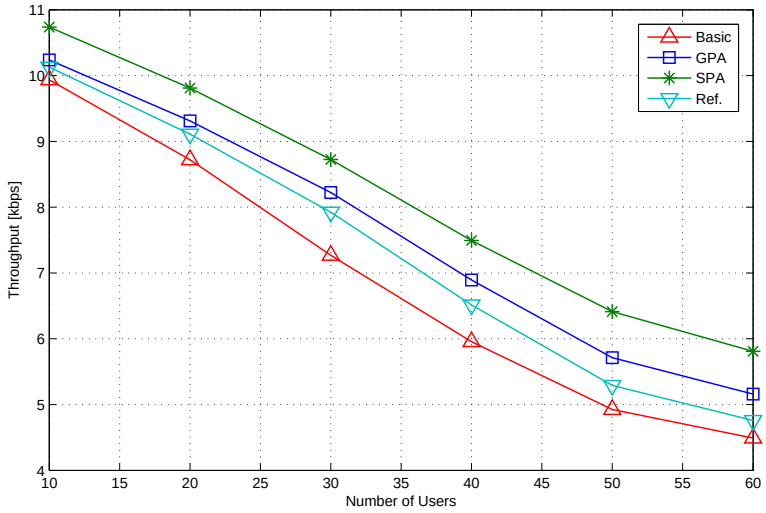

Figure 5.7: Average per-user throughput of MUEs for CBR flows

to the fact that voice flows usually require less RBs compared to Video flows given the lower data rate and packet size. The same behavior is observed for CBR flows (Figure 5.7) which shows almost a similar performance gain.

Figures 5.6 and 5.8 show the average per-user throughput with VoIP and CBR flows for FUEs, respectively. We can observe that the throughput degradation compared to the Basic scheme is only 5% and 7% as regards to GPA and SPA (who achieves a similar throughput as Reference scheme), respectively. Note that the throughput degradation against the increasing number of MUEs here is slightly less important than for Video case (figure 4), since Video flows monopolize most of the available RBs. Finally, since the GPA strategy in its design is more aware of the throughput degradation of FUEs, it outperforms SPA and Reference strategies regardless of the traffic class.

In order to better analyze the effect of the different strategies on the overall system throughput, figures 5.9 and 5.10 show the overall throughput for VoIP and CBR traffics, respectively. We can observe that SPA outperforms GPA and the Reference scheme, while the Basic scheme offers the lowest performance. SPA strategy achieves the highest performance since it improves the spectral efficiency of MUEs while being agnostic to FUEs throughput degradation. On the contrary, GPA tries to offer a tradeoff between MUEs and FUEs performances at the expense of a reduced performance in terms of system capacity.

Finally, note that the throughput gain achieved by our proposed techniques is more significant when the density of active UEs increases. Hence, these power adjustment strategies fit perfectly the dense and mobile scenarios of urban areas.

5.4.3 Analysis of the impact of the weighting parameters

In this section, we investigate and analyze the effect of the *Score Function* weighting parameters θ_i, $(i = 1, 2, 3)$ on the performance of our GPA and SPA schemes. As defined in equation (5.2), the score of a given interfering FBS F_l depends on the

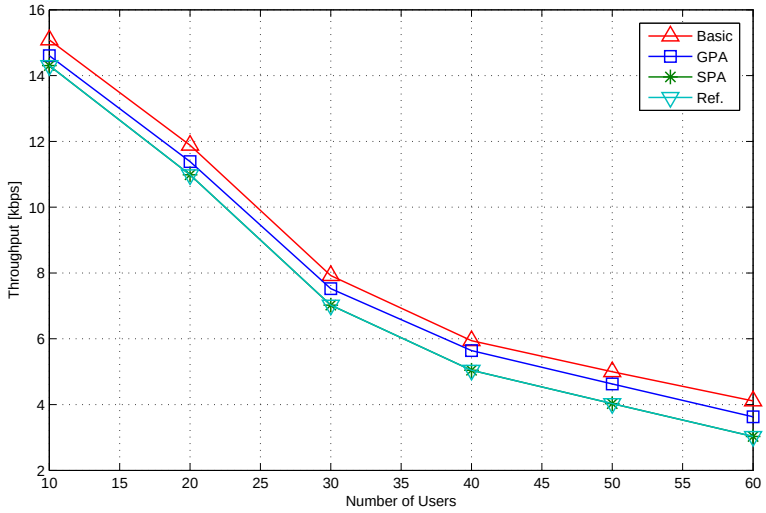

Figure 5.8: Average per-user throughput of FUEs for CBR flows as a function of the number of MUEs

values of θ_i parameters which rule the balance between the three context parameters. For a better understanding of the weighting parameters effect, we recall in the following their respective role in the score function:

- θ_1 : rules the weight of the "single interference source" situation as it is associated to the context parameter R_{F_l}. The single interference situation refers here to the case where the victim MUEs suffer from the interference occurring only from the current FBS F_l.

- θ_2 : acts on the weight of the "multiple interference sources" situation which indicates that the victim MUEs of sub-set $\mathcal{N}_{F_l}$ are suffering from the interference of other FBSs besides F_l's interference.

- θ_3 : is used to determine the weight of the outage FUEs on the global F_l score. In other words, θ_3 manages the degree of awareness of the FUEs' performance within the power adjustment strategy.

It is worth mentioning here that distinguishing the single and multiple interference situations provides a good means to take advanced and adapted power adjustment decisions. For example, the power adjustment strategy may demand more power decrease from FBSs involved in multiple interferences than those creating single interference to rapidly heal the global interference situation. Moreover, note that the association of the θ_i weighting factors and the adopted power adjustment strategy (GPA or SPA) provides two complementary means to realize the best tradeoff between MUEs' and FUEs' performance.

To simplify the analysis and discussion, we organize the experiments in three different and significant cases (see Table 5.2):

1. **Case A:** corresponds to the scenarios which give a higher priority to FUEs over MUEs while maintaining the same weight between multiple and single

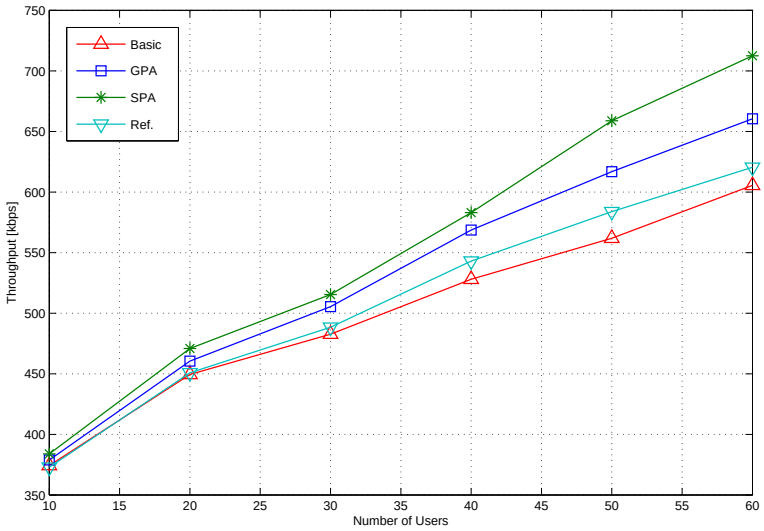

Figure 5.9: The overall system throughput for Voip flows as a function of the number of MUEs

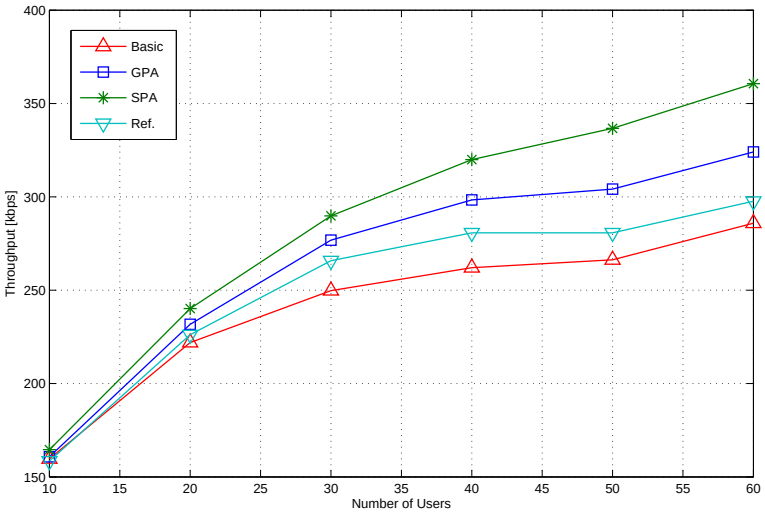

Figure 5.10: The overall system throughput for CBR flows as a function of the number of MUEs

Table 5.2: Conducted Test Ids and corresponding θ_i values

	Test Ids	θ_i Values
Case A Priority to FUEs	1	(0.1, 0.1, 0.8)
	2	(0.2, 0.2, 0.6)
Case B MUEs/FUEs Balanced	3	(0.25, 0.25, 0.5)
	4	(0.4, 0.1, 0.5)
	5	(0.1, 0.4, 0.5)
Case C Priority to MUEs	6	(0.3, 0.3, 0.4)
	7	(0.4, 0.4, 0.2)

interference situations. This case meets the following conditions, θ_1=θ_2 and θ_3 >θ_1+θ_2.

2. **Case B:** corresponds to the balanced mode where FUEs and MUEs share the same priority. In this case, we have θ_1+θ_2 = θ_3.

3. **Case C:** represents the opposite situation of Case A since we give more priority to MUEs by setting θ_3<θ_1+θ_2.

We evaluate in the following the performance of our power allocation schemes in each of the cases mentioned above. To do so, we assume here CBR traffic flows with 20 and 40 active MUEs using the same simulation parameters provided in Table 1. The three different cases described above are conducted using the θ_i values provided in Table 2. The average throughput for MUEs and FUEs achieved for each test are presented in figures 11 and 12, respectively. Note that the Basic and Reference schemes are also depicted in figures 11 and 12, in order to provide a baseline performance and to have a better insight on how the parameters affect the results compared to the reference schemes. Except for the MUE throughput with test Id 1, the proposed schemes always outperform the Reference one. Therefore, the following discussion will mainly focus on the weighting parameters' effect on our GPA and SPA strategies.

First of all, comparing the cases where $\theta_1 + \theta_2 < \theta_3$, i.e., tests 1 and 2, to the cases where $\theta_1 + \theta_2 > \theta_3$, i.e., tests 6 and 7, we observe that FUEs are prioritized against MUEs in the first cases and vice versa in the latter ones. Thus, the achieved throughputs are in concordance with the corresponding set of θ_i values, as higher values of θ_1+θ_2 enable higher MUE throughput but lower FUE throughput given the constraint $\theta_1 + \theta_2 + \theta_3 = 1$. We observe that the value of $\theta_1 + \theta_2$ has more significant effects on the MUE throughput than the value of θ_3 on the FUE throughput, given the higher vulnerability of MUEs under FBS interference in our target scenario. Although smaller θ_3 implies a lower FUE throughput, figure 12 shows that there is only a slight decrease, even with the SPA strategy where FBSs are not allowed to increase their power. We can also confirm that a very good trade-off between MUE and FUE throughput is achieved in the balanced case (Case B, test Ids 3,4,5) where $\theta_1 + \theta_2 = \theta_3$.

Moreover, we study the effect of the discrimination of θ_1 and θ_2 values, corresponding to different prioritization weights given to MUEs affected by only one femtocell and those affected by several femtocells. These scenarios are represented

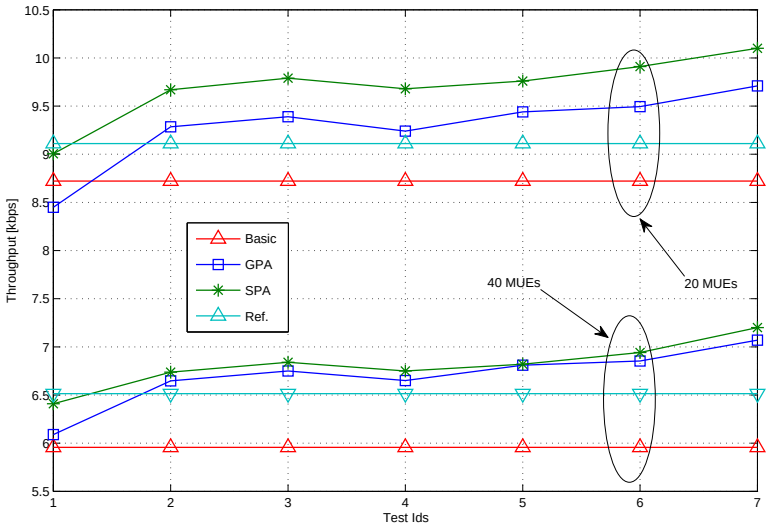

Figure 5.11: Average per-user throughput of MUEs (20 or 40 MUEs) for CBR flows in different scenarios

by Test Ids 4 and 5 in Table 2, assuming $\theta_1 + \theta_2 = \theta_3$. Clearly, choosing $\theta_2 > \theta_1$ (Test Id 5) provides a higher throughput to MUEs. Thus, giving a larger weight on the interference caused by multiple femtocells allows to decrease their power simultaneously, and hence to improve the average MUE throughput. However, the power decrease on those femtocells does not decrease much the FUE average throughput, as shown in figure 12, validating the efficiency of the proposed power adjustment strategies. In addition, note that compared to the completely balanced scenario (Test Id 3), the achieved MUE throughput is further enhanced by selecting $\theta_2 > \theta_1$ (Test Id 5), especially for the GPA strategy for both numbers of MUEs, while keeping the FUE throughput at the same level. This shows the utility of defining distinct θ_1 and θ_2 values depending on the number of interference sources.

Finally, the results obtained for different sets of θ_i values show that the selected power adjustment strategy, namely GPA or SPA, along with the appropriate tuning of the θ_i values enable to achieve the required MUE/FUE prioritization level in terms of throughput in an efficient manner.

5.5 Conclusion

This chapter has addressed the interference issue in a collocated macro/femtocell HetNets within an urban mobility environment. We proposed femtocell power adjustment methods whose key objective was to increase the average throughput of non-CSG MUEs by limiting the amount of interference caused by femtocells. The main contribution of our approach was to introduce power adjustment parameters whose values are dynamically adapted to the weight of each interfering femtocell through their Score Functions on the global interference situation. Given these weights, the two proposed power adjustment strategies have the common objective

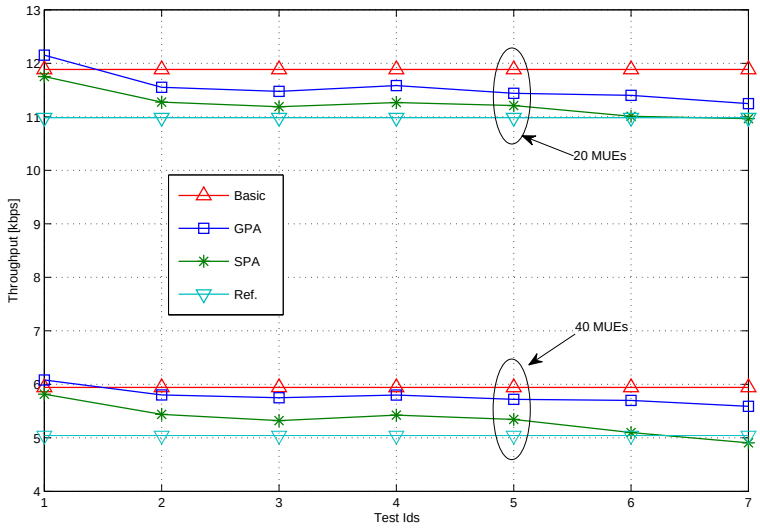

Figure 5.12: Average per-user throughput of FUEs (20 or 40 MUEs) for CBR flows in different scenarios

of mitigating the interference on victim MUEs while implementing two different degrees of awareness of FUE's throughput degradation. The simulation results have shown the effectiveness of both proposed strategies in terms of macrocell and femtocell average throughput for different types of traffic. Moreover, it was shown that the proposed priority weights used in the femtocells' Score Functions provide an efficient means for achieving the desired level of macrocell/femtocell throughput trade-off. System-level simulations show that our schemes enhance the throughput of macrocell users while maintaining a high performance for femtocell users compared to conventional power allocation.

In the next chapter, we will investigate the interference mitigation issue in tow-tier macrocell-picocell HetNet. The picocell deployment poses the interference issue differently compared to the femtocell user. Our aim in the next chapter is to investigate this problem make the Cell Range Expansion perspective under uses mobility assumptions.

Part II

Macrocell and Picocells

Chapter 6

Mobility-Aware Dynamic Inter-Cell Interference Coordination in HetNets with Cell Range Expansion

6.1 Introduction

Picocells are one of the key solutions in HetNets which can efficiently relieve saturated areas and improve the overall system capacity of a region covered by a scarce macrocell penetration regardless the coverage type (indoor or outdoor). Despite its benefits, the classical cell selection procedure which is achieved by comparing and selecting the cell with the maximum RSS as the user serving cell, introduces uneven traffic load distribution in the network, since most of the UEs would connect to the MBS rather than the PBS. Consequently, the macrocell would overload whereas the picocells would offload.

In order to overcome the inadequate data offloading problem, the concept of Cell Range Expasion (CRE) has been introduced recently in 3GPP LTE-A by defining a positive bias value to be added to the PBS RSS during the cell-selection. In this way, more MUEs are offloaded to picocells even if the RSSs of the selected picocells are below those of macrocells (see Figure 6.1) which is return enhances the throughput performance of the entire system.

But a straightforward co-channel deployment in the picocells range expansion area would make PUEs suffer from severe interference caused by nearby macrocells, thereby degrading their SINR at picocells. To protect the PUEs from such SINR degradation, an e-ICIC technique should be applied. LTE-A introduced several time and frequency domain e-ICIC techniques such as the Almost Blank Subfames (ABS) strategy in which the aggressor cell periodically stops its transmission during predefined subframes, or the dynamic frequency partitioning that turns-off dynamically some resource blocks to enable PUEs transmission under reduced interference conditions. In the latter strategy, PUEs in the CRE region experience better performance if they are scheduled in the restricted protected resources [89, 90, 91]. However, such scheduling restriction diminishes the user diversity gain, due to the loss of freedom in allocating the time-frequency resources.

In this chapter, we propose a mobility-aware e-ICIC scheme which turns-off some

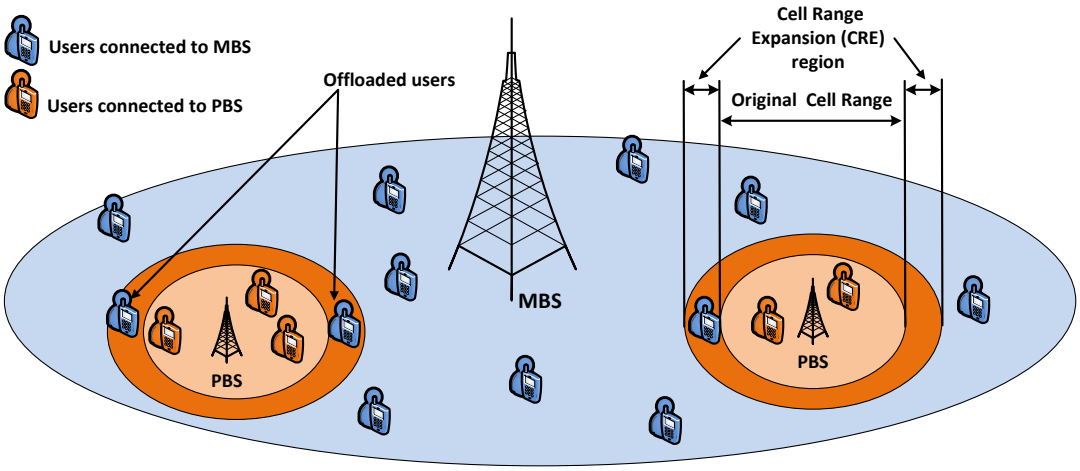

Figure 6.1: Cell range expansion (CRE)

of the RBs in the macrocell in function of the mobility behaviour of the range-expanded picocell users, thereby providing an efficient trade-off between macrocell and picocell achievable throughputs. Note that in this study, we consider dynamic frequency partition for the DL communication in a co-channel macro-picocell deployment. Our proposed strategy makes use of PUEs mobility information to adapt dynamically the muting ratio value that acts on the frequency partitioning degree. The PBS periodically estimates the traveling time of the offloaded CRE users which, combined to the bandwidth required of both MUEs and PUEs, helps the MBS to better estimate the optimal value of the muting ratio. Furthermore, our strategy lifts the above mentioned scheduling restriction and makes the entire RBs available to all PUEs in the allocation process.

The rest of this chapter is organized as follows. In Section 6.2, we describe the system model and cell selection schemes for HetNets. Section 6.3 presents the classical e-ICIC frequency partitioning technique while section 6.4 details our mobility-based e-ICIC method. The performance evaluation and analysis discussed in section 6.5. Finally, section 6.6 draws the conclusion.

6.2 System Model

We consider a macrocell/picocell overlay system in which L picocells are geographically positioned in a macrocell coverage area with an MBS referred to as M. We assume that I MUEs are uniformly distributed within the MBS area and are allowed to access to a neighboring picocell P_l, $(l = 1, ..., L)$ when they pass randomly through its coverage area. Each P_l serves J PUEs distributed randomly within its coverage. The transmissions are OFDMA-based and all MUEs and PUEs share the same frequency band divided in k RBs. To perform the resource allocation of their RBs, both MBS and PBSs require their UEs to periodically report their signal quality expressed by the channel quality indicator in terms of SINR. The received DL SINR of a given MUE_i associated with MBS M on resource block k can be expressed

as

$$SINR^k_{M,MUE_i}=\frac{\frac{p^k_M}{PL^k_{M,MUE_i}}|G^k_{M,MUE_i}|^2}{\sum_{P_l\in\mathcal{U}_{i,k}}\frac{p^k_{Pl}}{PL^k_{P_l,MUE_i}}|G^k_{P_l,MUE_i}|^2+N_0}, \tag{6.1}$$

where p^k_M is the current transmit power allocated on RB k by the serving cell MBS M, and $|G^k_{M,MUE_i}|$ is the multipath channel fading gain between MUE_i and its MBS M on RB k. Similarly, $p^k_{P_l}$ is the transmit power of neighboring picocell P_l on RB k, while $\mathcal{U}_{i,k}$ represents the set of all interfering PBSs on user MUE_i on RB k. $|G^k_{P_l,MUE_i}|$ is the multipath channel fading gain between MUE_i and the neighboring P_l on RB k. PL^k_{M,MUE_i} and $PL^k_{P_l,MUE_i}$ stand for the pathloss between MUE_i and its serving cell MBS M and PBS P_l on RB k, respectively. N_0 is the power of the additive white Gaussian noise.

Similarly, the DL $SINR^k_{P_l,PUE_j}$ of a given PUE_j associated with a given picocell P_l on resource block k can be expressed as

$$SINR^k_{P_l,PUE_j}=\frac{\frac{p^k_{P_l}}{PL^k_{P_l,PUE_j}}|G^k_{P_l,PUE_j}|^2}{N_0+A+\sum_{\substack{P_m\in\mathcal{V}_{j,k}\\ m\neq l}}\frac{p^k_{P_m}}{PL^k_{P_m,PUE_j}}|G^k_{P_m,PUE_j}|^2}, \tag{6.2}$$

where $p^k_{P_l}$ is the current transmit power allocated on RB k by the serving picocell P_l, and $|G^k_{P_l,PUE_j}|$ is the multipath channel fading gain between PUE_j and its serving picocell P_l. $p^k_{P_m}$ is the transmit power of a neighboring PBS P_m, while $\mathcal{V}_{j,k}$ represents the set of all interfering PBSs on user PUE_j on RB k. $|G^k_{P_m,PUE_j}|$ is the multipath channel fading gain between PUE_j and its neighboring P_m. $PL^k_{P_l,PUE_j}$ stands for the pathloss between PUE_j and PBS P_l. A is the interference generated by MBS M on resource block k, namely
$A=\frac{p^k_M}{PL^k_{M,PUE_j}}|G^k_{M,PUE_j}|^2$.

Typically, the cell selection (macro/picocell) is based on the criterion of maximal DL-RSS. In other words, a UE is associated to the cell $S_{\max}$ with the strongest DL-RSS. The Max-RSS cell association rule is given by

$$S_{\max}=\arg\max_S\{RSS_S\}, \tag{6.3}$$

where S corresponds to the candidate cells, $S\in\{M\}\cup\{P_l,\text{l=1,...,L}\}$.

However, in practical scenarios this Max-RSS rule limits the number of UEs associated to picocells due to the high MBS transmit power level compared to that of PBSs. This limits the amount of traffic offload from macrocell to picocells, thereby reducing the potential capacity gains of HetNets [107]. Therefore, a positive bias value is introduced as follows

$$S_{\max}=\arg\max_S\{RSS_S+\alpha\}, \tag{6.4}$$

where α denotes a bias value which is chosen to be a positive non-zero value whenever the candidate cell S is a picocell and zero if S is the macrocell.

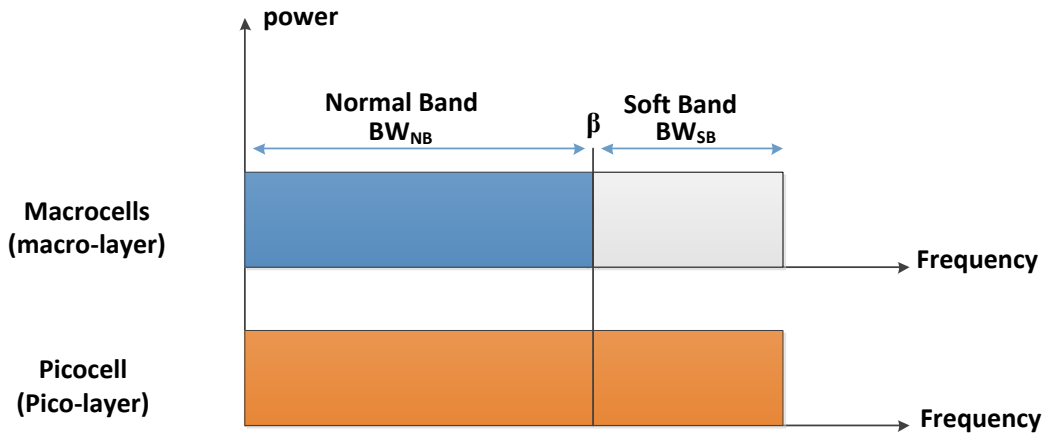

Figure 6.2: e-ICIC scheme with frequency partitioning

6.3 Reference e-ICIC Scheme with Frequency Partitioning

In the CRE concept, the offloaded macrocell users release their resource spectrum in the macrocell to be served by the picocell. However, they may experience a strong MBS interference depending on their locations in the CRE region. In the rest of this chapter, these offloaded macrocell users within the CRE region will be referred to as Range expanded PUEs (RPUEs).

In order to offer RPUEs a better performance, e-ICIC such as frequency resource partitioning among macrocell and picocells is usually performed. Figure (6.2) shows one of the classical e-ICIC schemes [90], where the resource spectrum (frequency band) is divided into two distinct sub-bands: the normal band (NB) which is shared by the macrocell and picocells and the soft band (SB), reserved for the picocell. These sub-bands are delimited by a dynamic parameter called *Muting Ratio* β, as expressed in equation (3.2), $\beta = \frac{|\mathcal{N}_l|}{|\mathfrak{N}_l|}$ [90].

However, this technique has several limitations, as listed below:

- As the *Muting Ratio* β is determined as the ratio of RPUEs over the total number of PUEs, the resource needs of MUEs are not considered which may result in poor macrocell performance.

- Most existing e-ICIC schemes in CRE context have either neglected the mobility factor of UEs on the design of β or simply mentioned its importance without further investigation [91]. Moreover, if the reference e-ICIC scheme based on equation (3.2) was directly applied in the case of mobile users, the PBS should inform periodically the MBS about the fluctuating numbers of PUEs and RPUEs (e.g. using backhaul or X2 interface, as recommended in LTE-A release 10 [108]). However, UEs locations may vary very frequently, especially in urban scenarios, causing high fluctuation and instability of the *Muting Ratio* β.

- From the viewpoint of picocells, the scheduling of RPUEs is restricted to the resources in the SB partition, so that the interference can be completely avoided. Such scheduling restriction may lead to the reduction of multi-user diversity gain as each sub-band is restricted to a sub-set of users against the entire set of users [109].

6.4 Proposed Mobility-Aware e-ICIC Scheme

To overcome the abovementioned limitations, we propose a mobility-aware frequency partitioning method in HetNets scenarios which aims are threefold; i) optimize the frequency partitioning by taking into account RPUEs mobility characteristics such as their traveling time duration in the CRE region, ii) provide a good trade-off between RPUEs and MUEs performance through the proposed resource partitioning, iii) take advantage of full multi-user diversity by allowing whenever possible the scheduling of RPUEs in the entire bandwidth.

The main characteristics of the proposed mobility-aware e-ICIC method are described as follows,

1. Like the traditional method, the available frequency resource partition between NB and SB changes dynamically, however, the RPUE's mobility profiles have been taken into consideration for determining the *Muting Ratio* β. In particular, we predict the traveling time T_j of each RPUE$_j$ within the CRE area and use it as a key parameter for evaluating the muting ratio. Arithmetic details and the problem formulation are explained in the next paragraphs of this section.

2. In order to avoid the frequent changes and thus instability of β, it is only updated for significant values of traveling times T_j, i.e., only if RPUEs are estimated to be staying long enough within the CRE area. Moreover, the contribution of each RPUE$_j$ in the calculation of β will be weighted by their traveling time T_j.

3. Finally, the RPUEs have the possibility to be scheduled within all available RBs whether in NB or SB.

6.4.1 Mobility Model and Traveling Time Estimation

In order to estimate the traveling time for each RPUE, we first define the following mobility model. We consider a random waypoint mobility model in which each UE's velocity and direction remain constant during a period of time T. We assume that each RPUE estimates and informs PBS about its position ϕ (x-axis and y-axis) periodically, so that the PBS can trace the entrance position of RPUEs within its coverage area. Let ϕ_1=(x_1, y_1) and ϕ_2=(x_2, y_2) be the successive positions of RPUE$_j$ at two different times t_1 and t_2, where ϕ_1 corresponds to its entrance point into the CRE area of PBS P_l and ϕ_2 the current location. We assume that PBS P_l 's position is known and referred to as ϕ_{P_l}=(x_{P_l}, y_{P_l}), while the MBS's position is given by ϕ_M=(x_M, y_M).

For any RPUE$_j$ positioned at the outer boundary of the CRE region, its RSS to MBS M and to PBS P_l satisfies the following equation,

$$p^k_M - PL^k{}_{M,PUE_j} = p^k_{P_l} + \alpha - PL^k{}_{P_l,PUE_j}[\text{dB}]. \tag{6.5}$$

While in the case of RPUE$_j$ being positioned at the inner boundary of the CRE region, its RSS to MBS M and to PBS P_l would verify

$$p^k_M - PL^k{}_{M,PUE_j} = p^k_{P_l} - PL^k{}_{P_l,PUE_j}[\text{dB}]. \tag{6.6}$$

The shape of the CRE boundaries defined by (6.5) and (6.6) will depend on the different involved parameters as illustrated in figure 6.3. Based on the knowledge of RPUE$_j$'s entrance position ϕ_1, the current position ϕ_2, its velocity v_j and equations (6.5)-(6.6), the traveling time T_j can be estimated as in the following.

First, the traveling time T_j for RPUE$_j$ is defined as the predicted time for RPUE$_j$ to go from point ϕ_2 to the exit point $\hat{\phi}=(\hat{x},\hat{y})$ of the CRE area, located either on the CRE outer boundary defined by (6.5) or its inner boundary (6.6), and which can be determined by the RPUE$_j$'s direction estimated from ϕ_1 and ϕ_2[110]. We describe the case where the estimated exit point is located on the outer boundary, the other case can be obtained similarly. Thus, T_j is given by

$$T_j = \frac{D_j}{v_j}, \tag{6.7}$$

where v_j represents the velocity of RPUE$_j$, which can be estimated from ϕ_1, ϕ_2, t_1 and t_2. Note that v_j can also be measured by an accelerometer embedded in the mobile terminal [110]. D_j is the travelled distance between points ϕ_1 and ϕ_2.

The exit point $\hat{\phi}=(\hat{x},\hat{y})$, belongs geometrically to the line defined by positions ϕ_1 and ϕ_2, satisfying

$$\hat{y} = \epsilon\hat{x} + \delta, \tag{6.8}$$

where $\epsilon = \frac{y_1 - y_2}{x_1 - x_2}$ and $\delta = \frac{x_1.y_2 - x_2.y_1}{x_1 - x_2}$.

Moreover, the exit point $\hat{\phi}$ satisfies equation (6.6) where we have $PL_{M,PUE_j} = A + B log_{10}(d_4)$, and $PL_{P_l,PUE_j} = C + B\, log_{10}(d_3)$ (see Table 6.1), with $d_4 = \sqrt{(x_M - \hat{x})^2 + (y_M - \hat{y})^2}$ and $d_3 = \sqrt{(x_{P_l} - \hat{x})^2 + (y_{P_l} - \hat{y})^2}$, i.e., the respective distances of point $\hat{\phi}$ to MBS (x_M, y_M) and PBS (x_{P_l}, x_{P_l}). Substituting the path loss expressions in (6.5) we obtain the relation

$$d_4 = \mathfrak{K} d_3, \tag{6.9}$$

where $\mathfrak{K} = 10^{\frac{p^k_M - p^k_{P_l} + C - A - \alpha}{B}}$.

Then, squaring both sides of (6.9) and replacing $\hat{y}$ by its expression in (6.8), we obtain

$$\mathfrak{K}^2((\epsilon\hat{x} + \delta - y_{P_l})^2 + (\hat{x} - x_{p_l})^2) = (\epsilon\hat{x} + \delta - y_M)^2 + (\hat{x} - x_M)^2 \tag{6.10}$$

Rearranging equation (6.10), we obtain the quadratic equation as follows

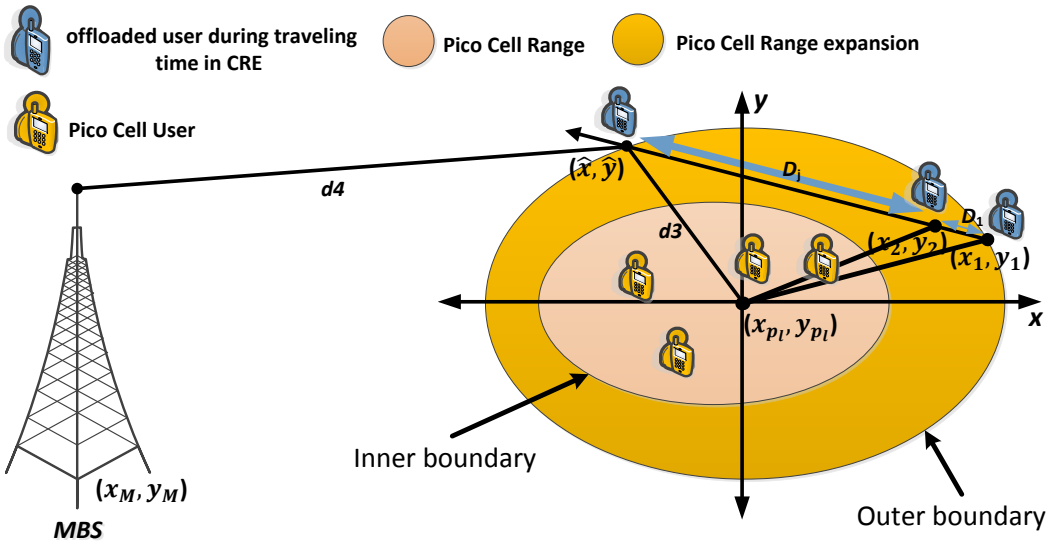

Figure 6.3: A scenario for traveling time prediction in CRE

$$\begin{cases} a\hat{x^2} + b\hat{x} + c = 0 \\ a = 1 + \epsilon^2 - \Re^2(1+\epsilon^2) \\ b = 2\epsilon(\delta - y_M) - 2x_M - (2\Re^2\epsilon(\delta - y_{P_l}) - 2\Re^2 x_{P_l}) \\ c = x_M^2 + (\delta - y_M)^2 - \Re^2(x_{P_l}^2 + (\delta - y_{P_l})^2) \end{cases} \tag{6.11}$$

Hence, we can deduce $\hat{\phi}=(\hat{x},\hat{y})$ position by $\hat{x}=\frac{-b+\sqrt{b^2-4ac}}{2a}$ and $\hat{y}$ from (6.8). Finally, we calculate the distance D_j as

$$D_j=\sqrt{(x_2-\hat{x})^2+(y_2-\hat{y})^2}. \tag{6.12}$$

6.4.2 Proposed Muting Ratio β

Once the traveling time T_j is estimated for each RPUE$_j$, it is used to determine the weight β_j of RPUE$_j$ on the overall muting ratio β. Clearly, to avoid unstable behaviors, only significant values of T_j that are larger than a threshold τ are taken into account in the updates of β. Therefore, we define the utility time U_j of RPUE$_j$ as

$$U_j=\begin{cases} T_j & \text{if } T_j \geqslant \tau \\ 0 & \text{otherwise.} \end{cases} \tag{6.13}$$

Then, the weight β_j of RPUE$_j$ is given by

$$\beta_j=\frac{U_j}{\sum_{j\in\mathcal{N}_l} U_j}, \tag{6.14}$$

Then, the proposed mobility-aware muting ratio is defined as

$$\beta=\frac{\sum_{j\in\mathcal{N}_l} \beta_j M_j}{\sum_{k\in\mathfrak{N}_M} M_k}, \tag{6.15}$$

Table 6.1: Simulation Parameters

Parameters	Values	Parameters	Values
Macrocells	1	Thermal noise density	-174dBm/Hz
Picocells	2	Carrier frequency	3.5 GHz
UEs	20-120	Macrocell radius	1km
Bandwidth	10MHz	Picocell radius	114 m
Total RBs	50	50% UEs average speed	30km/hour
Macro Tx power	46 dBm	50% UEs average speed	3km/hour
Picocell Tx power	30 dBm	Bias CRE value α	10 dB
Macrocell path loss 128.1+37.6log10(d), dB, d in km			
Picocell pathloss 140.1+37.6log10(d), dB, d in km			

where M_j and M_k are the amounts of RB units required by $RPUE_j$ and MUE_k users, respectively, while $\mathfrak{N}_M$ is the set of all MUEs. Note that M_j and M_k parameters are determined based on the user's application type (packet size, minimum data rate, etc.) as well as the CQI of each allocated RB which is mapped to the corresponding modulation and coding scheme level.

To implement the proposed scheme, note that the numerator of (6.15) may be determined by the PBS and then fed back to the MBS, which then calculates β by (6.15).

6.5 Numerical Results

To investigate the performance of our proposed mobility-aware e-ICIC scheme, we implemented the algorithms using *LTE-Sim* simulator [98], as it did not include the picocells nodes within macrocells coverage. In order to evaluate the performance our mobility aware model in the picocell range expansion scenario, the framework was extended to enable picocell deployments. More specifically, two major components has been largely modified in the simulator *FrameManager* and *NetworkManager* components. New classes and sub-classes were developed from scratch to extend the existing macrocell implementation based on LTE-advanced specifications, as proposed in [25] [85].

6.5.1 Simulation Conditions

In the simulated scenario, the network topology consists of one macrocell and two picocells whose PBSs are positioned at a distance of 519 m from the MBS and separated by an angle of 90 degrees, i.e., one PBS is placed on the x axis and the other on the y axis. All UEs are randomly positioned within the macrocell and picocell and move according to a random walk mobility model at two different speeds: 50% of UEs move at 30km/h and 50% at 3km/h. The simulation parameters are detailed in table 6.1.

6.5.2 Performance evaluation

We evaluate the Proposed and Reference e-ICIC (presented in section 6.3) schemes referred in the figures as *Prop. ICIC* and *Conv. ICIC* in terms of total achievable throughput in bits/second, assuming Proportional Fair Scheduling (PFS) for RB allocation. Three different types of application flows are considered: Video, VoIP and Best Effort generating with Constant Bit Rate (CBR) traffic. The Video service is a 242 kbps data source with H.264 coding [99], while the Best Effort service is generated as an HTTP traffic. The proposed e-ICIC scheme is evaluated for three different values of the threshold τ in equation (6.13), namely τ=0,1,2.5 sec.

6.5.2.1 Average throughput performance

Figures 6.4 and 6.5 show the total average throughput of picocells and macrocell in the case of Video flows, respectively, when varying the number of users from 20 to 120. We observe, for τ=0s, i.e., when all estimated values of traveling times T_j are taken into account in the muting ratio estimation, that picocells achieve the highest throughput performance, where the amount of improvement is approximately 8 to 10 % compared to *Conv. ICIC*. This is because our mobility-aware muting ratio β takes into account all RPUE$_j$s' required amount of RBs for resource partitioning, while RPUEs may be scheduled within all the bands (SB and NB) if the interference level allows it. In other words, if the RPUB have a strong interference from the NB then it can be scheduled by only on a SB. Meanwhile, our proposed resource partitioning does not infer any macrocell throughput decrease compared to *Conv. ICIC*, providing a good trade-off between macrocell and picocell performance. As the traveling time threshold increases (τ=1 and 2.5s), the picocell throughput decreases as small values of predicted traveling times are neglected leading to a smaller SB size, while the macrocell throughput is improved from 2.8% to 4.8%. Note that in any case, the proposed e-ICIC scheme always provides higher throughput compared to *Conv. ICIC* for both macrocell and picocells, proving the validity of our approach.

Figures 6.6 and 6.7 show the total average throughput of picocells and macrocell in the case of VoIP flows, respectively. As it can be seen, the selection of τ=0 combined with the scheduling algorithm offer better capacity compared to Reference e-ICIC scheme, achieving a picocell throughput increase of approximately 6% to 10.6%. For τ=2.5, a macrocell throughput gain of 6 to 7% over *Conv. ICIC* is observed. It is worthy to notice that, compared to Video traffic, voice flows are more impacted as they show high gain. This is due to the fact that the higher quality RBs allocated to voice flows comparing to the Video flows.

Figures 6.8 and 6.9 depict the total average throughput of picocells and macrocell in case of CBR flows, respectively. Likewise, the results show that the selection of τ=0s is the best strategy for picocells, achieving a picocell throughput increase of around 7 to 11% over the Reference e-ICIC scheme, without any macrocell throughput decrease. With higher values of τ, the macrocell throughput is increased while closely approaching the picocell throughput of τ=0s. For τ=2.5s, a macrocell throughput gain of 4 to 7% over *Conv. ICIC* is observed.

To better capture the effect of our strategy on the whole system, Figure 6.10 illustrate the overall system throughput (picocells and macrocell users) in the case

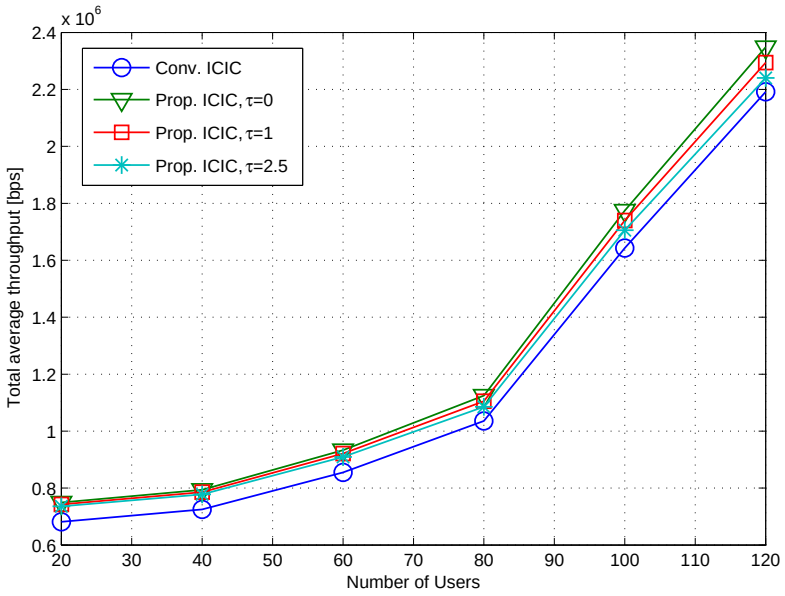

Figure 6.4: Total average throughput in Picocells (Video flows)

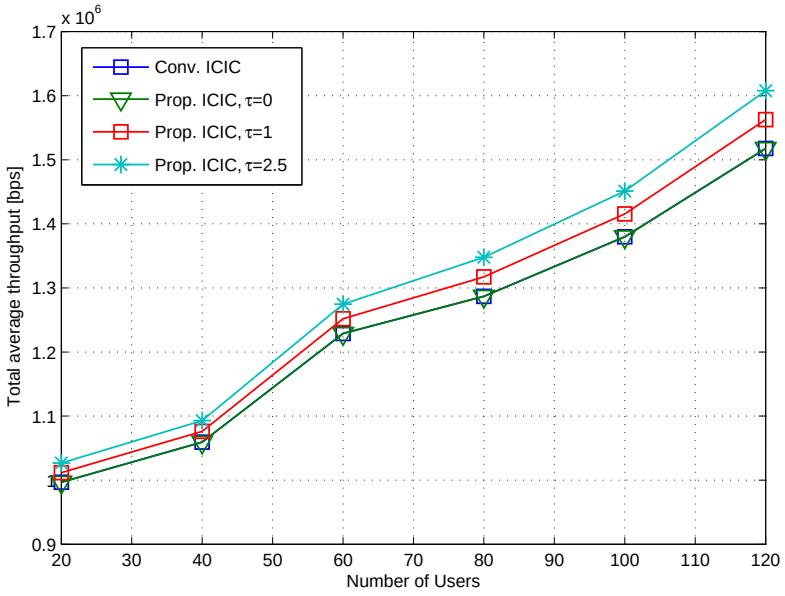

Figure 6.5: Total average throughput in Macrocell (Video flows)

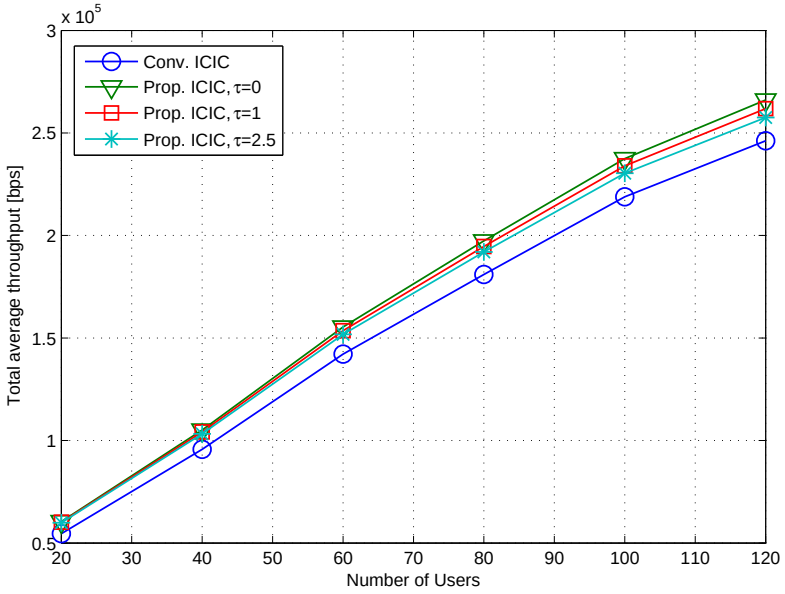

Figure 6.6: Total average throughput in Picocells (VoIP flows)

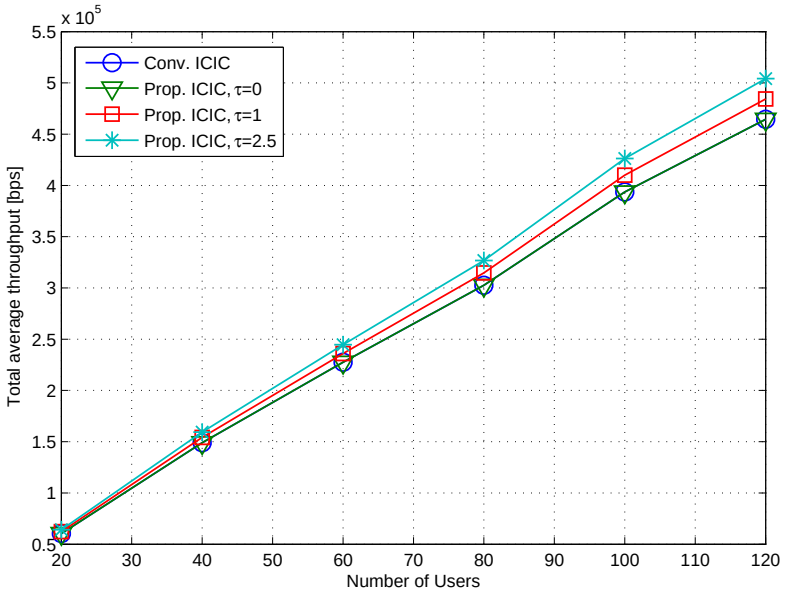

Figure 6.7: Total average throughput in Macrocell (VoIP flows)

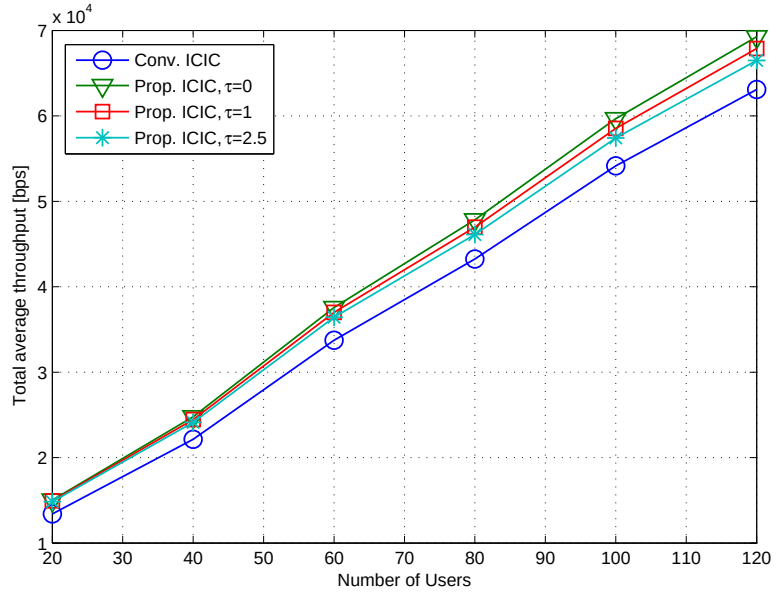

Figure 6.8: Total average throughput in Picocells (CBR flows)

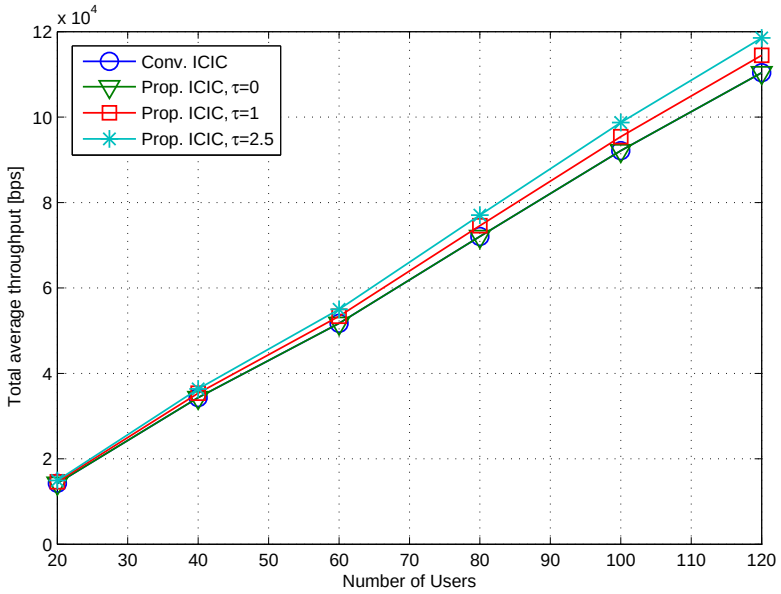

Figure 6.9: Total average throughput in Macrocell (CBR flows)

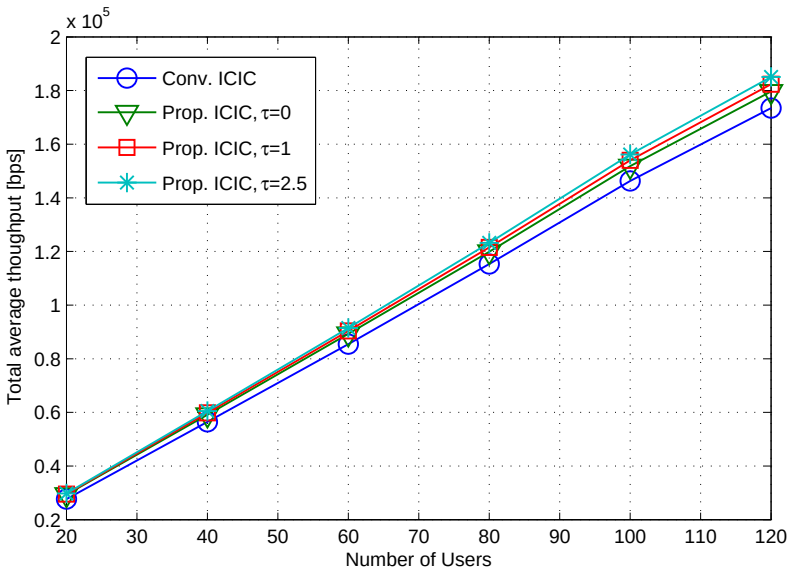

Figure 6.10: The overall system throughput (CBR flows)

of CBR flows. As it can be seen, the system capacity is improved with our Proposed scheme. The maximum gain of 5.5% is obtained with τ=2.5 owing to the combined of non-restricted RB assignment and the dynamic tuning of the muting ratio.

All these results show the effectiveness of our approach as well as the gain achieved to the macrocell and picocell users. Clearly, higher values of the muting ratio τ are in favor of the macrocell users' performance while the lower values advantage the picocell users. We can see for example that the τ=1 give the good balance between the gains of macro and picocells. Hence, τ can be seen as a system parameter which tuning can provide leverage to achieve the targeted balance between macrocell and picocells performances. Future work we aim to conduct further investigation on the optimal values of parameters τ.

6.5.2.2 Spectral sufficiency performance

In order to understand the ergodic capacity that can be perceived by a macrocell or picocell user, we evaluate in figures 6.11 and 6.12 the DL spectral efficiency in bit/subcarrier/cell as a function of the total number of users (20 to 120 UEs). As expected, the results show that the sitting the muting ratio to τ=0 always provides the best performance as their users relieved from interference and benefit from a longer SB bandwidth. While for higher values of τ, the macrocell spectral efficiency is enhanced (see Figure 6.11) with a gain of about 5 to 6% over *Conv. ICIC*.

Consequently, the trade-off between employing low or high τ value has some drawbacks to both MUEs and/or PUEs. Therefore, the adaptive τ with average mobility-aware and user prediction speed must be more investigated to provide the maximum spectral efficiency everywhere in cell.

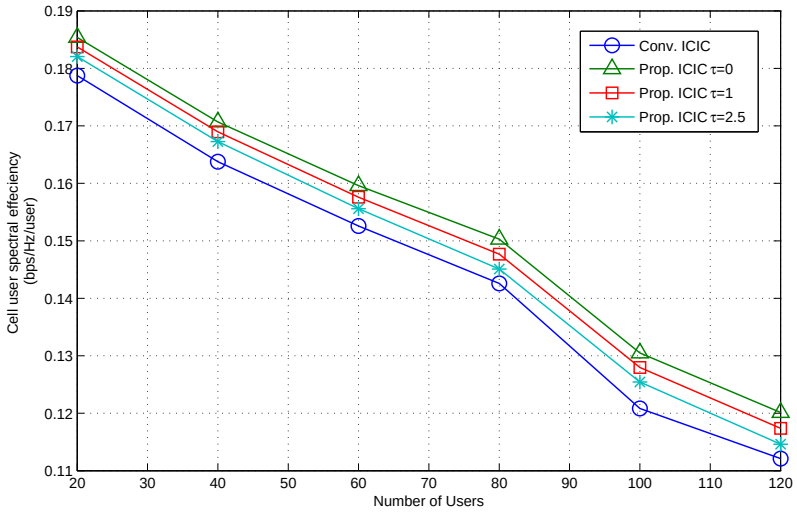

Figure 6.11: Total average spectral efficiency in Picocells

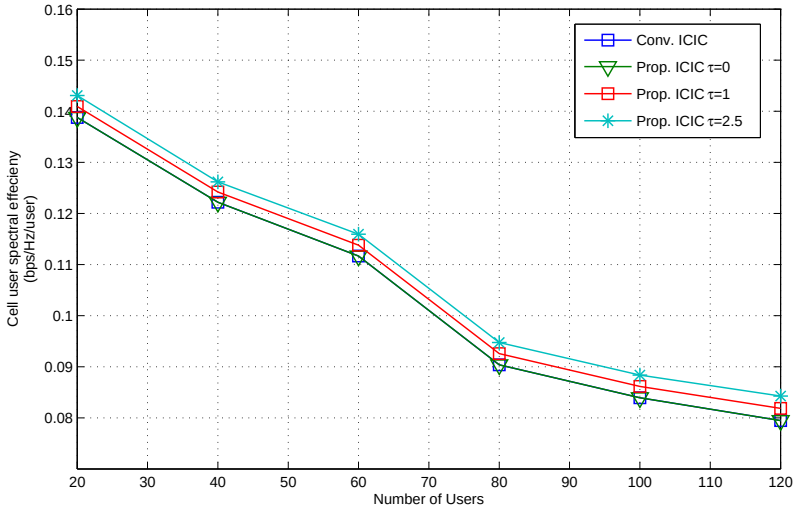

Figure 6.12: Total average spectral efficiency in Macrocell

6.6 Conclusion

In this chapter, we have proposed a novel mobility-aware e-ICIC technique in co-located macro/picocells with range expansion. In the proposed scheme, each PBS predicts the traveling time of each RPUE within its range-expanded area, which is then used as a key parameter for determining the muting ratio. The simulation results have shown that the proposed e-ICIC scheme provided an excellent trade-off between macrocell and picocell throughput, while outperforming reference e-ICIC. In our future work, we will investigate more advanced muting ratio definitions and use adapted optimization tools to derive optimal values. Moreover, it would be also interesting to study the other e-ICIC techniques such as time-dimension techniques in conjunction with user mobility.

Chapter 7

Conclusions

This final chapter summarizes the major contributions of this thesis and highlights numerous topics for future research.

7.1 Conclusions and Main Contributions

This thesis proposed novel methods of interference mitigation for HetNets, where the target deployment scenarios represented by two collocated networks; namely macro-femtocells and macro-picocells were examined. Both scenarios are considered as part of the LTE-A radio technology development where the PHY-OFDMA resources blocks are supposed to be the shared frequency band at both tiers with co-channel assignment.

Following the structure of our contributions in this thesis, we have introduced description of the HetNet architecture based on LTE-A.Then, we described all fundamental concepts and features related to MAC and PHY layers which are closely related to the interference management issue in *chapter 2*.

Then in *chapter 3*, we elaborated the literature review of the different existing approaches on the dynamic inter-cell interference mitigation problem for each of femtocells and picocells deployments as an underlying macrocell layer.

Chapter 4 focused mainly on the MBS assistance-based power allocation technique in which the decision of femtocell's power adjustment is made by the macrocell through information exchanged with the femtocell access points as well as received measurement reports from mobile terminals (MUEs/FUEs). The cross-tier interference was described in this scenario as the unwanted signal received from the CSG-femtocells that occurs when a macro user is located in the area where a signal received from its serving macrocell is not high enough with respect to the same one received from the neighboring femtocells. Our proposed approach concentrated on adjusting dynamically the transmission power of the femtocells according to the evolution of the interference situation especially for the varying mobile environments. The key advantage was to achieve high performance for non-CSG users, along with avoiding potential service degradation of femtocell users. This is done by allowing femtocells to make objections to the adjustments instruction when a given number of its users experience an outage situation. The results obtained for this scheme showed that the interference at a given macrocell can be better controlled while maintaining

a high QoS for femtocell users. Furthermore, in order to enforce our assistance-based technique, we proposed a method to alleviate the signaling messages exchanged in the integrated architecture. Accordingly, we proposed an algorithm at the network side to decrease the signaling overhead as much as possible, by authorizing the signaling exchange only when significant changes in the received interfering signal value from the interfering femtocells occur.

Although our optimization scheme on CSG-femtocell decreased a significant amount of interference in our first contribution in *chapter 4*, it did not completely benefit from the MBS-assistance strategy to better analyze and coordinate the different femtocell's local information for a better handling of the cross-interference situations. For that reason, based on the same system model presented in *chapter 4,* we enriched the proposal by defining two different adaptive power control schemes; namely global power adjustment and selective power adjustment which differ in their selection strategy of the set of interfering femtocells to execute the power adjustment and the amount of power to reduce. The main advantage of our proposed approaches in *chapter 5* over the traditional one or the contribution in *chapter 4* is that, the power mitigation solution is based on power adjustment parameters which its values are dynamically adapted to the interference weight of each femtocell on the global interference situation. To estimate such femtocells' liability on the global interference, we used a Score Function which quantified this value based not only on the received signal strength feedback returned by MUEs, but also on some context information (such as the number and the location of users) retrieved from radio environment map databases. Furthermore, we exploited this context information about user numbers and localization to enrich the decision policy and bring added value knowledge to the power allocation decision process. The degree of awareness of FUEs' throughput degradation outperforms significantly the reference schemes in our simulation results.

In order to overcome an inadequate data offloading problem between macrocells and picocells, as well as mitigating the inter-cell interference under the concept of cell range expansion, another aspect which has been considered in *chapter 6* is the use of the MBS-assistance-based solution for the dynamic frequency resource partitioning between tiers. Our proposed strategy made use of offloaded macrocell user's mobility information to adapt dynamically the muting ratio value that acts on the frequency partition degree. Moreover, the picocell base station periodically estimated the traveling time of the offloaded macrocell users using an analytical model predicting this time traveling, to evaluate the bandwidth required for each macro-and-picocells users. Accordingly, the model helped the macrocell to better estimate the optimal value of the muting ratio. Additionally, our strategy lifted the traditional scheduling restriction and made the entire resource blocks available to all picocells users in the resource allocation process. The results obtained for this contribution showed that the proposed e-ICIC scheme provided an excellent trade-off between macro and picocells throughput, while outperforming the reference e-ICIC model.

As a conclusion, our evaluation studies have shown that our proposed technical models for dynamic inter-cell interference coordination mechanisms can significantly improve the cell-edge user's performance, since they are the most penalized users

when an interference occurs.

7.2 Future Work

The work presented in this thesis left multiple investigation lines open for the future work. In the following, we introduce short and medium term research directions that we are intending to purse in the near future:

1. **Comparison with centralized, decentralized methods;** the proposed solutions in this thesis adopted a MBS-assistance strategy, as this perspective offers an efficient means for coordinated optimizations. Nevertheless, it would be interesting to compare the performance of our schemes with the fully centralized and/or distributed solutions which were mentioned in the literature review. The most important parameters to quantify and to investigate are the throughput gains, the generated overhead, and the complexity introduced by each power allocation scheme with as part of the radio resource management procedure.

2. **Multi-Point transmission and reception (CoMP);** generally, the inter-cell interference coordination schemes are supported in LTE-A by means of coordinated exchanged messages among base stations via the standard S1 or X2 interfaces, however the delay of the exchanged messages depends mainly on the type of the interface, leading to the conclusion that the required latency cannot be always guaranteed. Making use of CoMP, several cells may coordinate their data transmissions to serve those users located in between cells and therefore suffering from low signal qualities. The cell-edge inter-cell interference could be significantly mitigated, because neighboring cells are turned from being interferer to become serving cells. In a similar way, macrocells and femtocells may also coordinate resource assignments utilizing CoMP principles to enhance network performance and mitigate user outages. Our future work can be represented by adapting our model with CoMP technique to enhance the proposed inter-cell interference.

3. Other high-level overview of the modern design challenges and perspectives are suggested and they can be possible solutions for interference mitigation such as

    - **Carrier aggregation**; with this feature, the system deployment allows operators to deliver a better user-experience to achieve high data rates by aggregating the scattered spectrum, as it also supports the interference management.
    - **Reference signal for enhanced multiple-antenna support**; the eNodeBs have different reasons for transmitting certain predefined reference signal for various purposes such as estimating and feeding back channel state indicator to neighboring eNodeBs, and the equalization of DL channel in the process of data demodulation; leading to a high density

of reference signals utilization. Normally, LTE-A introduced four non-overlapping reference signal patterns. However, one of the requirements in LTE-A is that, the system technology needs to support up to eight transmission ports. Toward this, the main change in the design of reference signals that should be increased from 8 to 10, is the separation between demodulation and the form of the channel state information reference signal. This would finally reduce a significant reference signaling overhead and could be a well subject to be investigated for comparison of the overhead in both cases.

List of Publications

Journal articles

- R. Kurda, L. Boukhatem and M. Kaneko, "Femtocell Power Control Methods based on Mobile-User Context Information in Two-Tier Heterogeneous Networks", EURASIP Journal on Wireless Communications and Networks, Sep. 2014, to appear.
- J. Pérez-Romero, A. Zalonis, L. Boukhatem, A. Kliks, K. Koutlia, N. Dimitriou and R. Kurda, "On the use of Radio Environment Maps for Interference Management in Heterogeneous Networks", IEEE Communications Magazine. Nov. 2014, (Submitted).

Conference articles

- R. Kurda, L. Boukhatem and T. A. Yahiya, "Interference Mitigation in Mobile Environment through Power Adjustment in Macro and Femto cell Systems", IEEE on Wireless Communications and Networking Systems (WCNC), April 2014.
- R. Kurda, L. Boukhatem, T. A. Yahia and M. Kaneko, "Power adjustment mechanism using context information for interference mitigation in two-tier heterogeneous networks", IEEE Symposium on Computers and Communications (ISCC), June 2014.
- R. Kurda, L. Boukhatem, M. Kaneko and T. A. Yahia, "Mobility-Aware Dynamic Inter-Cell Interference Coordination in HetNets with Cell Range Expansion", IEEE 24th Annual International Symposium on Personal Indoor and Mobile Radio Communications (PIMRC), Sept. 2014.

Bibliography

[1] ETSI, "GSM Technical Specifications (01–12 Series)."

[2] H. Chen, *The next generation CDMA technologies*. John Wiley & Sons, 2007.

[3] A. Eisenblätter, H. F. Geerdes, T. Koch, A. Martin, and R. Wessäly, "UMTS radio network evaluation and optimization beyond snapshots," *Mathematical Methods of Operations Research*, vol. 63, no. 1, pp. 1–29, 2006.

[4] A. Eisenblätter *et al.*, *Frequency assignment in GSM networks: Models, heuristics, and lower bounds*. Cuvillier, 2001.

[5] E. Dahlman, S. Parkvall, J. Skold, and P. Beming, *3G evolution: HSPA and LTE for mobile broadband*. Academic press, 2010.

[6] J. Wannstrom, "LTE-Advanced," *Third Generation Partnership Project (3GPP)*, Available at http://www.3gpp.org/, May 2012.

[7] Cisco Visual Networking Index(VNI), "Global mobile data traffic forecast update, 2010-2015," *White Paper, February*, 2011.

[8] A. Toskala, H. Holma, T. Kolding, F. Frederiksen, and P. Mogensen, "High-speed downlink packet access," *WCDMA for UMTS: Highspeed downlink Packet Access (HSPA) Evolution and LTE*, p. 353, 2010.

[9] G. Mansfield, "Femto cells in the us market-business drivers and femto cells in the us market," *business drivers and consumer propositions in FemtoCells Europe. AT&T*, 2008.

[10] M. Alouini and A. J. Goldsmith, "Area spectral efficiency of cellular mobile radio systems," *Vehicular Technology, IEEE Transactions on*, vol. 48, no. 4, pp. 1047–1066, 1999.

[11] R. Q. Hu, Y. Qian, S. Kota, and G. Giambene, "HetNets-a new paradigm for increasing cellular capacity and coverage [Guest Editorial]," *Wireless Communications, IEEE*, vol. 18, no. 3, pp. 8–9, 2011.

[12] A. Khandekar, N. Bhushan, J. Tingfang, and V. Vanghi, "LTE-Advanced: Heterogeneous networks," in *Wireless Conference (EW)*, pp. 978–982, IEEE, European, 2010.

[13] A. Damnjanovic, J. Montojo, Y. Wei, T. Ji, T. Luo, M. Vajapeyam, T. Yoo, O. Song, and D. Malladi, "A survey on 3GPP heterogeneous networks," *Wireless Communications, IEEE*, vol. 18, no. 3, pp. 10–21, 2011.

[14] E. Dahlman, S. Parkvall, and J. Skold, *4G: LTE/LTE-advanced for mobile broadband*. Academic press, 2013.

[15] J. Zhang, G. De la Roche, *et al.*, *Femtocells: technologies and deployment*. Wiley Online Library, 2010.

[16] *Available at http://www.smallcellforum.org/*. Academic press.

[17] D. Lopez-Perez, I. Guvenc, G. De La Roche, M. Kountouris, T. Q. Quek, and J. Zhang, "Enhanced intercell interference coordination challenges in heterogeneous networks," *Wireless Communications, IEEE*, vol. 18, no. 3, pp. 22–30, 2011.

[18] A. Golaup, M. Mustapha, and L. B. Patanapongpibul, "Femtocell access control strategy in UMTS and LTE," *Communications Magazine, IEEE*, vol. 47, no. 9, pp. 117–123, 2009.

[19] M. F. Khan *et al.*, "Femtocellular Aspects on UMTS Architecture Evolution," 2010.

[20] P. Bhat, S. Nagata, L. Campoy, I. Berberana, T. Derham, G. Liu, X. Shen, P. Zong, and J. Yang, "LTE-Advanced: an operator perspective," *Communications Magazine, IEEE*, vol. 50, no. 2, pp. 104–114, 2012.

[21] P. C. Lin and R. G. Cheng, "Dynamic two-threshold flow control scheme for 3GPP LTE-A relay networks," in *Personal Indoor and Mobile Radio Communications (PIMRC), 2013 IEEE 24th International Symposium on*, pp. 2649–2653, IEEE, 2013.

[22] Q. Ye, B. Rong, Y. Chen, M. Al-Shalash, C. Caramanis, and J. G. Andrews, "User association for load balancing in heterogeneous cellular networks," *Wireless Communications, IEEE Transactions on*, vol. 12, no. 6, pp. 2706–2716, 2013.

[23] C. Cox, *An introduction to LTE, LTE-Advanced, SAE and 4G mobile communications*. John Wiley & Sons, 2012.

[24] J. D. Hobby and H. Claussen, "Deployment options for femtocells and their impact on existing macrocellular networks," *Bell Labs Technical Journal*, vol. 13, no. 4, pp. 145–160, 2009.

[25] E. U. T. R. Access, "Further advancements for E-UTRA physical layer aspects," tech. rep., 3GPP TR 36.814, 2010.

[26] T. Ali-Yahiya, "LTE femtocell integration with wireless sensor/actuator networks and RFID technologies," in *Understanding LTE and its Performance*, pp. 225–244, Springer, 2011.

[27] G. Giambene and T. A. Yahiya, "LTE planning for soft frequency reuse," in *Wireless Days (WD), 2013 IFIP*, pp. 1–7, IEEE, 2013.

[28] A. S. Hamza, S. S. Khalifa, H. S. Hamza, and K. Elsayed, "A survey on inter-cell interference coordination techniques in OFDMA-based cellular networks," *Communications Surveys & Tutorials, IEEE*, vol. 15, no. 4, pp. 1642–1670, 2013.

[29] M. Beach, B. BELLOUL, Y. BIAN, S. MITCHELL, A. NIX, K. RICHARDSON, S. WALES, C. WILLIAMS, and M. WILLIS, "Study into the Application of Interference Cancellation Techniques," *rap. tech., Ofcom*, 2006.

[30] A. Carleial, "A case where interference does not reduce capacity (Corresp.)," *Information Theory & Tutorials, IEEE*, vol. 21, no. 5, pp. 569–570, 1975.

[31] K. Tachikawa, *W-CDMA mobile communications system*. John Wiley & Sons, 2003.

[32] J. G. Andrews, "Interference cancellation for cellular systems: a contemporary overview," *Wireless Communications, IEEE*, vol. 12, no. 2, pp. 19–29, 2005.

[33] C. Esli, M. Koca, and H. Deliç, "Iterative joint tone-interference cancellation and decoding for MIMO-OFDM," *Vehicular Technology, IEEE Transactions on*, vol. 57, no. 5, pp. 2843–2855, 2008.

[34] S. P. Weber, J. G. Andrews, X. Yang, and G. De Veciana, "Transmission capacity of wireless ad hoc networks with successive interference cancellation," *Information Theory, IEEE Transactions on*, vol. 53, no. 8, pp. 2799–2814, 2007.

[35] W. Webb, *Wireless communications: The future*. John Wiley & Sons, 2007.

[36] F. Capozzi, G. Piro, L. A. Grieco, G. Boggia, and P. Camarda, "Downlink packet scheduling in lte cellular networks: Key design issues and a survey," *Communications Surveys & Tutorials, IEEE*, vol. 15, no. 2, pp. 678–700, 2013.

[37] D. Stiliadis and A. Varma, "Rate-proportional servers: a design methodology for fair queueing algorithms," *IEEE/ACM Transactions on Networking (TON)*, vol. 6, no. 2, pp. 164–174, 1998.

[38] S. Elayoubi and B. Fourestié, "On frequency allocation in 3G LTE systems," in *Personal, Indoor and Mobile Radio Communications, 2006 IEEE 17th International Symposium on*, pp. 1–5, IEEE, 2006.

[39] S.-E. Elayoubi, O. Ben Haddada, and B. Fourestié, "Performance evaluation of frequency planning schemes in OFDMA-based networks," *Wireless Communications, IEEE Transactions on*, vol. 7, no. 5, pp. 1623–1633, 2008.

[40] V. H. Mac Donald, "Advanced mobile phone service: The cellular concept," *Bell System Technical Journal, The*, vol. 58, no. 1, pp. 15–41, 1979.

[41] H. Jia, Z. Zhang, G. Yu, P. Cheng, and S. Li, "On the performance of IEEE 802.16 OFDMA system under different frequency reuse and subcarrier permutation patterns," in *Communications, 2007. ICC'07. IEEE International Conference on*, pp. 5720–5725, IEEE, 2007.

[42] K. Begain, G. I. Rozsa, A. Pfening, and M. Telek, "Performance analysis of GSM networks with intelligent underlay-overlay," in *Computers and Communications, 2002. Proceedings. ISCC 2002. Seventh International Symposium on*, pp. 135–141, IEEE, 2002.

[43] R. Y. Chang, Z. Tao, J. Zhang, and C.-C. Kuo, "A graph approach to dynamic fractional frequency reuse (FFR) in multi-cell OFDMA networks," in *Communications, 2009. ICC'09. IEEE International Conference on*, pp. 1–6, IEEE, 2009.

[44] M. Shariat, A. U. Quddus, and R. Tafazolli, "On the efficiency of interference coordination schemes in emerging cellular wireless networks," in *Personal, Indoor and Mobile Radio Communications, 2008. PIMRC 2008. IEEE 19th International Symposium on*, pp. 1–5, IEEE, 2008.

[45] 3GPP Project Document R1-060 291, "OFDMA Downlink Inter-Cell Interference Mitigation," Available: http://www.3gpp.org., Feb. 2006.

[46] M. C. Necker, "Interference coordination in cellular OFDMA networks," *Network, IEEE*, vol. 22, no. 6, pp. 12–19, 2008.

[47] C. Kosta, B. Hunt, A. Quddus, and R. Tafazolli, "On interference avoidance through inter-cell interference coordination (ICIC) based on OFDMA mobile systems," *Communications Surveys & Tutorials, IEEE*, vol. 15, no. 3, pp. 973–995, 2013.

[48] T. Akbudak and A. Czylwik, "Distributed power control and scheduling for decentralized ofdma networks," in *Smart Antennas (WSA), 2010 International ITG Workshop on*, pp. 59–65, IEEE, 2010.

[49] G. De La Roche, A. Valcarce, D. López-Pérez, and J. Zhang, "Access control mechanisms for femtocells," *Communications Magazine, IEEE*, vol. 48, no. 1, pp. 33–39, 2010.

[50] I. Güvenç, M.-R. Jeong, F. Watanabe, and H. Inamura, "A hybrid frequency assignment for femtocells and coverage area analysis for co-channel operation," *IEEE Communications Letters*, vol. 12, no. 12, pp. 880–882, 2008.

[51] L.-P. David, V. Alvaro, L. Ákos, d. l. R. Guillaume, Z. Jie, *et al.*, "Intracell handover for interference and handover mitigation in OFDMA two-tier macrocell-femtocell networks," *EURASIP Journal on Wireless Communications and Networking*, vol. 2010, 2010.

[52] G. Gur, S. Bayhan, and F. Alagoz, "Cognitive femtocell networks: an overlay architecture for localized dynamic spectrum access [dynamic spectrum management]," *Wireless Communications, IEEE*, vol. 17, no. 4, pp. 62–70, 2010.

[53] J. Zhang, G. De la Roche, *et al.*, *Femtocells: technologies and deployment*. Wiley Online Library, 2010.

[54] A. Valcarce, D. López-Pérez, G. De La Roche, and J. Zhang, "Limited access to OFDMA femtocells," in *Personal, Indoor and Mobile Radio Communications, 2009 IEEE 20th International Symposium on*, pp. 1–5, IEEE, 2009.

[55] P. Xia, V. Chandrasekhar, and J. G. Andrews, "Open vs. closed access femtocells in the uplink," *Wireless Communications, IEEE Transactions on*, vol. 9, no. 12, pp. 3798–3809, 2010.

[56] D. Choi, P. Monajemi, S. Kang, and J. Villasenor, "Dealing with loud neighbors: The benefits and tradeoffs of adaptive femtocell access," in *Global Telecommunications Conference, 2008. IEEE GLOBECOM 2008. IEEE*, pp. 1–5, Nov 2008.

[57] H. B. Orange, "consideration and deployment scenarios for UMTS, 3GPP," *Kobe, Japan, 3GPP document reference R4-070825*, 2007.

[58] H. Claussen, "Performance of macro-and co-channel femtocells in a hierarchical cell structure," in *Personal, Indoor and Mobile Radio Communications, 2007. PIMRC 2007. IEEE 18th International Symposium on*, pp. 1–5, IEEE, 2007.

[59] C. Patel, V. Khaitan, S. Nagaraja, F. Meshkati, Y. Tokgoz, and M. Yavuz, "Downlink interference management techniques for residential femtocells," in *Personal Indoor and Mobile Radio Communications (PIMRC), 2011 IEEE 22nd International Symposium on*, pp. 117–121, IEEE, 2011.

[60] H. Claussen, L. T. Ho, and L. G. Samuel, "Self-optimization of coverage for femtocell deployments," in *Wireless Telecommunications Symposium, 2008. WTS 2008*, pp. 278–285, IEEE, 2008.

[61] M. Lin and T. La Porta, "Dynamic interference management in femtocells," in *Computer Communications and Networks (ICCCN), 2012 21st International Conference on*, pp. 1–9, IEEE, 2012.

[62] K. Han, Y. Choi, D. Kim, M. Na, S. Choi, and K. Han, "Optimization of femtocell network configuration under interference constraints," in *Modeling and Optimization in Mobile, Ad Hoc, and Wireless Networks, 2009. WiOPT 2009. 7th International Symposium on*, pp. 1–7, IEEE, 2009.

[63] D. López-Pérez, A. Valcarce, G. De La Roche, and J. Zhang, "OFDMA femtocells: A roadmap on interference avoidance," *Communications Magazine, IEEE*, vol. 47, no. 9, pp. 41–48, 2009.

[64] D. Gesbert, S. Hanly, H. Huang, S. Shamai Shitz, O. Simeone, and W. Yu, "Multi-cell MIMO cooperative networks: A new look at interference," *Selected Areas in Communications, IEEE Journal on*, vol. 28, no. 9, pp. 1380–1408, 2010.

[65] M. Bennis and D. Niyato, "A Q-learning based approach to interference avoidance in self-organized femtocell networks," in *GLOBECOM Workshops (GC Wkshps), 2010 IEEE*, pp. 706–710, IEEE, 2010.

[66] F. Bernardo, R. Agustí, J. Pérez-Romero, and O. Sallent, "Distributed spectrum management based on reinforcement learning," in *Cognitive Radio Oriented Wireless Networks and Communications, 2009. CROWNCOM'09. 4th International Conference on*, pp. 1–6, IEEE, 2009.

[67] M. Nazir, M. Bennis, K. Ghaboosi, A. B. MacKenzie, and M. Latva-aho, "Learning based mechanisms for interference mitigation in self-organized femtocell networks," in *Signals, Systems and Computers (ASILOMAR), 2010 Conference Record of the Forty Fourth Asilomar Conference on*, pp. 1886–1890, IEEE, 2010.

[68] H. Wang and R. Song, "Distributed Q-Learning for Interference Mitigation in Self-Organised Femtocell Networks: Synchronous or Asynchronous?," *Wireless personal communications*, vol. 71, no. 4, pp. 2491–2506, 2013.

[69] "BeFEMTO: Broadband Evolved FEMTO Networks," Available at http://www.ict-befemto.eu., 2012.

[70] M. Bennis, L. Giupponi, E. M. Diaz, M. Lalam, M. Maqbool, E. C. Strinati, A. De Domenico, and M. Latva-aho, "Interference management in self-organized femtocell networks: The befemto approach," in *Wireless Communication, Vehicular Technology, Information Theory and Aerospace & Electronic Systems Technology (Wireless VITAE), 2011 2nd International Conference on*, pp. 1–6, IEEE, 2011.

[71] E. U. T. R. Access, "Further advancements for E-UTRA physical layer aspects," tech. rep., 3GPP TR 36.814, 2010.

[72] M. S. Kim, H. Je, and F. A. Tobagi, "Cross-tier interference mitigation for two-tier OFDMA femtocell networks with limited macrocell information," in *Global Telecommunications Conference (GLOBECOM 2010), 2010 IEEE*, pp. 1–5, IEEE, 2010.

[73] S. Barbarossa, S. Sardellitti, A. Carfagna, and P. Vecchiarelli, "Decentralized interference management in femtocells: A game-theoretic approach," in *Cognitive Radio Oriented Wireless Networks & Communications (CROWNCOM), 2010 Proceedings of the Fifth International Conference on*, pp. 1–5, IEEE, 2010.

[74] P. Gao, D. Chen, M. Feng, D. Qu, and T. Jiang, "On the interference avoidance method in two-tier LTE networks with femtocells," in *Wireless Communications and Networking Conference (WCNC), 2013 IEEE*, pp. 3585–3590, IEEE, 2013.

[75] D. López-Pérez, A. Ladányi, A. Juttner, and J. Zhang, "OFDMA femtocells: A self-organizing approach for frequency assignment," in *Personal, Indoor and*

Mobile Radio Communications, 2009 IEEE 20th International Symposium on, pp. 2202–2207, IEEE, 2009.

[76] F. Bernardo, R. Agustí, J. Cordero, and C. Crespo, "Self-optimization of spectrum assignment and transmission power in OFDMA femtocells," in *Telecommunications (AICT), 2010 Sixth Advanced International Conference on*, pp. 404–409, IEEE, 2010.

[77] G. Cao, D. Yang, X. Ye, and X. Zhang, "A downlink joint power control and resource allocation scheme for co-channel macrocell-femtocell networks," in *Wireless Communications and Networking Conference (WCNC), 2011 IEEE*, pp. 281–286, IEEE, 2011.

[78] Z. Wang, W. Xiong, C. Dong, J. Wang, and S. Li, "A novel downlink power control scheme in LTE heterogeneous network," in *Computational Problem-Solving (ICCP), 2011 International Conference on*, pp. 241–245, IEEE, 2011.

[79] A. Zalonis, N. Dimitriou, A. Polydoros, J. Nasreddine, and P. Mahonen, "Femtocell downlink power control based on radio environment maps," in *Wireless Communications and Networking Conference (WCNC), 2012 IEEE*, pp. 1224–1228, IEEE, 2012.

[80] T. Nakano, M. Kaneko, K. Hayashi, and H. Sakai, "Downlink power allocation with CSI overhearing in an OFDMA macrocell/femtocell coexisting system," in *Personal Indoor and Mobile Radio Communications (PIMRC), 2012 IEEE 23rd International Symposium on*, pp. 454–459, IEEE, 2012.

[81] T. Nakano, M. Kaneko, K. Hayashi, and H. Sakai, "Interference Mitigation based on Partial CSI Feedback and Overhearing in an OFDMA Heterogeneous System," in *IEEE VTC-Spring 2013, Dresden, Germany*, IEEE, 2013.

[82] C. M. de Lima, M. Bennis, K. Ghaboosi, and M. Latva-aho, "Interference management for self-organized femtocells towards green networks," in *Personal, Indoor and Mobile Radio Communications Workshops (PIMRC Workshops), 2010 IEEE 21st International Symposium on*, pp. 352–356, IEEE, 2010.

[83] Y. Bai, J. Zhou, L. Liu, L. Chen, and H. Otsuka, "Resource coordination and interference mitigation between macrocell and femtocell," in *Personal, Indoor and Mobile Radio Communications, 2009 IEEE 20th International Symposium on*, pp. 1401–1405, IEEE, 2009.

[84] D. Lopez-Perez, X. Chu, and I. Guvenc, "On the expanded region of picocells in heterogeneous networks," *Selected Topics in Signal Processing, IEEE Journal of*, vol. 6, pp. 281–294, June 2012.

[85] B. A. Bjerke, "LTE-Advanced and the evolution of LTE deployments," *Wireless Communications, IEEE*, vol. 18, no. 5, pp. 4–5, 2011.

[86] D. López-Pérez, I. Guvenc, G. De La Roche, M. Kountouris, T. Q. Quek, and J. Zhang, "Enhanced intercell interference coordination challenges in heterogeneous networks," *Wireless Communications, IEEE*, vol. 18, no. 3, pp. 22–30, 2011.

[87] J. Oh and Y. Han, "Cell selection for range expansion with almost blank subframe in heterogeneous networks," in *Personal Indoor and Mobile Radio Communications (PIMRC), 2012 IEEE 23rd International Symposium on*, pp. 653–657, IEEE, 2012.

[88] M. Al-Rawi, "A dynamic approach for cell range expansion in interference coordinated LTE-Advanced heterogeneous networks," in *Communication Systems (ICCS), 2012 IEEE International Conference on*, pp. 533–537, IEEE, 2012.

[89] M. Vajapeyam, A. Damnjanovic, J. Montojo, T. Ji, Y. Wei, and D. Malladi, "Downlink FTP performance of heterogeneous networks for LTE-Advanced," in *Communications Workshops (ICC), 2011 IEEE International Conference on*, pp. 1–5, IEEE, 2011.

[90] C. Huang and C.-Y. Liao, "An interference management scheme for heterogeneous network with cell range extension," in *Network Operations and Management Symposium (APNOMS), 2011 13th Asia-Pacific*, pp. 1–5, IEEE, 2011.

[91] C. Chiu and C. Huang, "An interference coordination scheme for picocell range expansion in heterogeneous networks," in *Vehicular Technology Conference (VTC Spring), 2012 IEEE 75th*, pp. 1–6, IEEE, 2012.

[92] M. Simsek, M. Bennis, and A. Czylwik, "Dynamic inter-cell interference coordination in HetNets: A reinforcement learning approach," in *Global Communications Conference (GLOBECOM), 2012 IEEE*, pp. 5446–5450, IEEE, 2012.

[93] T. Kudo and T. Ohtsuki, "Cell range expansion using distributed Q-learning in heterogeneous networks," *EURASIP Journal on Wireless Communications and Networking*, vol. 2013, no. 1, pp. 1–10, 2013.

[94] S. Mukherjee and I. Guvenc, "Effects of range expansion and interference coordination on capacity and fairness in heterogeneous networks," in *Signals, Systems and Computers (ASILOMAR), 2011 Conference Record of the Forty Fifth Asilomar Conference on*, pp. 1855–1859, IEEE, 2011.

[95] J. Zhang, "Inter-cell interference control in heterogeneous access networks," in *UC4G Workshop, London*, 2011.

[96] J. Van De Beek, T. Cai, S. Grimoud, B. Sayrac, P. Mahonen, J. Nasreddine, and J. Riihijarvi, "How a layered rem architecture brings cognition to today's mobile networks," *Wireless Communications, IEEE*, vol. 19, no. 4, pp. 17–24, 2012.

[97] S. Assumptions, "Parameters for FDD HeNB RF Requirements," 2009.

[98] G. Piro, L. A. Grieco, G. Boggia, F. Capozzi, and P. Camarda, "Simulating LTE cellular systems: an open-source framework," *Vehicular Technology, IEEE Transactions on*, vol. 60, no. 2, pp. 498–513, 2011.

[99] M. Reisslein, "Video trace library," *Arizona State University,[online] Available: http://trace.eas.asu.edu*, 2012.

[100] C.-N. Chuah and R. H. Katz, "Characterizing packet audio streams from internet multimedia applications," in *Communications, 2002. ICC 2002. IEEE International Conference on*, vol. 2, pp. 1199–1203, IEEE, 2002.

[101] X. Li, L. Qian, and D. Kataria, "Downlink power control in co-channel macrocell femtocell overlay," in *Information Sciences and Systems, 2009. CISS 2009. 43rd Annual Conference on*, pp. 383–388, IEEE, 2009.

[102] G. Cao, D. Yang, X. Ye, and X. Zhang, "A downlink joint power control and resource allocation scheme for co-channel macrocell-femtocell networks," in *Wireless Communications and Networking Conference (WCNC), 2011 IEEE*, pp. 281–286, IEEE, 2011.

[103] Z. Wang, W. Xiong, C. Dong, J. Wang, and S. Li, "A novel downlink power control scheme in LTE heterogeneous network," in *Computational Problem-Solving (ICCP), 2011 International Conference on*, pp. 241–245, IEEE, 2011.

[104] R. Madan, J. Borran, A. Sampath, N. Bhushan, A. Khandekar, and T. Ji, "Cell association and interference coordination in heterogeneous LTE-A cellular networks," *IEEE Journal on Selected Areas in Communications*, vol. 28, no. 9, pp. 1479–1489, 2010.

[105] B. Sayrac, "D2.4: Final System Architecture," *Deliverable of FARAMIR project,[online] Available: http://www.ict-faramir.eu/*, 2014.

[106] L. Wang, Y. Zhang, and Z. Wei, "Mobility management schemes at radio network layer for LTE femtocells," in *Vehicular Technology Conference, 2009. VTC Spring 2009. IEEE 69th*, pp. 1–5, IEEE, 2009.

[107] Qualcomm, "Importance of Serving Cell Selection in Heterogeneous Networks," *3GPP R1-100701, 3GPP TSG RAN WG1 Meeting*, vol. 59, 2010.

[108] T. Hu, J. Pang, and H.-J. Su, "LTE-Advanced heterogeneous networks: Release 10 and beyond," in *Communications (ICC), 2012 IEEE International Conference on*, pp. 6999–7003, IEEE, 2012.

[109] M. R. Jeong and N. Miki, "A comparative study on scheduling restriction schemes for LTE-Advanced networks," in *Personal Indoor and Mobile Radio Communications (PIMRC), 2012 IEEE 23rd International Symposium on*, pp. 488–495, IEEE, 2012.

[110] W. Zhu and T. Lamarche, "Velocity estimation by using position and acceleration sensors," *Industrial Electronics, IEEE Transactions on*, vol. 54, no. 5, pp. 2706–2715, 2007.